

**ADVANCING SUSTAINABILITY ASSESSMENT TECHNIQUES:
MECHANISTIC BOTTOM UP APPROACHES TO MAP MATERIAL AND
THERMODYNAMIC FLOWS VIA PROCESS MODELING, INPUT-OUTPUT THEORY,
AND COMPUTATIONAL TOOLS**

by

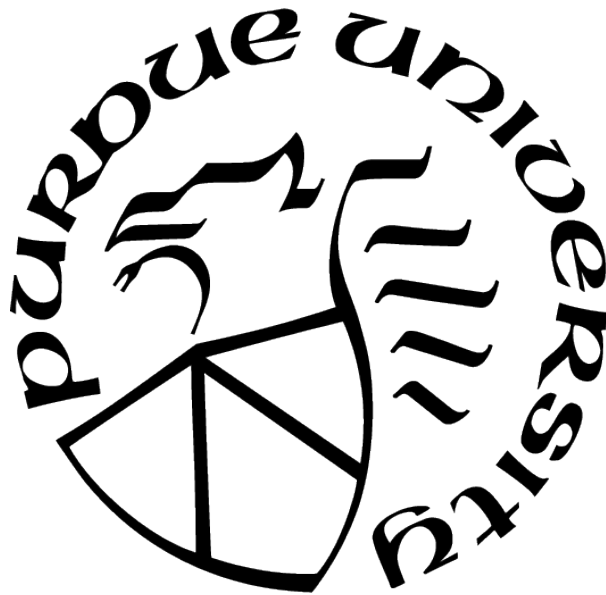
Venkata Sai Gargeya Vunnava

A Dissertation

Submitted to the Faculty of Purdue University

In Partial Fulfillment of the Requirements for the degree of

Doctor of Philosophy



Agricultural and Biological Engineering

West Lafayette, Indiana

December 2020

**THE PURDUE UNIVERSITY GRADUATE SCHOOL
STATEMENT OF COMMITTEE APPROVAL**

Dr. Shweta Singh, Chair

School of Agricultural and Biological Engineering
Division of Environmental and Ecological Engineering

Dr. Margaret Gitau

School of Agricultural and Biological Engineering

Dr. Rakesh Agrawal

Davidson School of Chemical Engineering

Dr. Riccardo Boero

Los Alamos National Laboratory

Approved by:

Dr. Nathan S. Mosier

Dedicated to everyone working towards making our planet sustainable for future generations of all life forms.

ACKNOWLEDGMENTS

I would like to thank my Ph.D. advisor Dr. Shweta Singh for giving me the opportunity to work with her on important environmental sustainability challenges. I was able to work on topics I deeply care about and my work under her guidance was highly fulfilling. I would also like to thank my colleagues Miriam, Nehika and Will for their support. I would to thank Dr. Riccardo Boero from Los Alamos National Laboratory for his research collaboration and for serving on my Ph.D. committee along with Dr. Rakesh Agrawal and Dr. Margeret Gitau from Purdue University. I thank them for all their guidance and feedback throughout my Ph.D. duration. I would also like to thank Dr. Manfred Lenzen and Dr. Futu Faturay from the University of Sydney for providing me access to the Industrial Ecology Virtual Laboratory, and Dr. Kevin Solomon for providing me access to his lab at Purdue Bindley Bioscience Center for conducting analytical experiments.

I would like to acknowledge the funding sources of my Ph.D. research, travel grants and conference fee waivers I received - National Science Foundation(CBET-1805741), Purdue Research Foundation, Purdue Climate Change Research Center, International Society for Industrial Ecology, and International Symposium for Sustainable Systems and Technology.

I thank my *Amma*, *Nanna* and my brother Yashaswi for all the sacrifices they have made to ensure that I get a great education and for being an incredible support system. I would like thank my girlfriend Tanmaye for being an amazing partner who constantly kept me motivated and without whom I might not have succeeded in completing my Ph.D. Finally, I would like to thank my friends Ganapathy, Vibhav, Neha, Shreya, Kaustabh, Sukirt, Sneha, and Kaustubh for all their support and for making my life at Purdue memorable.

TABLE OF CONTENTS

LIST OF TABLES	9
LIST OF FIGURES	11
ABSTRACT	13
1 INTRODUCTION	14
2 COMPUTATIONAL PROCESS MODELS TO QUANTIFY INDUSTRIAL MA- TERIAL FLOWS AT HIGH SPATIAL RESOLUTION TO PERFORM SPATIAL LIFE CYCLE ASSESSMENT	19
2.1 Chapter overview	19
2.2 Motivation and background	19
2.3 Methodology	22
2.3.1 System and System Boundary	22
2.3.2 Regional Life Cycle Inventory for Biodiesel from Soybean in Indiana . Soybean Farming	24 24
Soybean Biodiesel Production	24
Biodiesel Production Process Modeling	26
Transportation Life Cycle Stage	27
Upstream Life Cycle Inventory Data	28
2.3.3 Allocating Spatial Impacts at County Scale to Soybean Based Biodiesel Production	 29
2.4 Results	29
2.4.1 Northern Indiana	29
2.4.2 Central Indiana	30
2.5 Conclusions	32

3	COMPUTATIONAL BOTTOM-UP METHODS TO QUANTIFY ADVANCED THERMODYNAMIC FLOWS TO PERFORM THERMODYNAMIC SUSTAINABILITY ASSESSMENT	33
3.1	Chapter overview	33
3.2	Motivation and Background	34
3.3	Methodology	37
3.3.1	Entropy Generation Analysis (EGA) Methodology	37
3.3.2	Current P recovery technologies	38
3.3.3	EGA for Phosphorus (P) recovery from Waste Water Treatment Plant	39
	Entropy change calculation in Anaerobic Digester (AD)	42
	Entropy change calculation in Ion Exchange (IE)	44
	Entropy Flow Rates at various streams in the P recovery system	44
3.4	Results	45
3.5	Conclusion	47
4	MAPPING ECONOMY-WIDE MATERIAL FLOWS USING MECHANISTIC, BOTTOM-UP PHYSICAL SUPPLY USE TABLES AND PHYSICAL INPUT OUTPUT TABLES	49
4.1	Chapter overview	49
4.2	Motivation and background	50
4.3	Methodology	51
4.3.1	EM development process	52
	Identifying economic sectors	52
	Modeling the material transformation processes	52
	Scaling EMs to represent flows in the economy	53
4.3.2	Converting data from EMs into PSUTs and PIOTs	56
4.4	Case study	59
4.4.1	EMs for agro-based economy of Illinois	59
	Modeling field crops	59
	Modeling animal farming sectors	61

	Biomass processing and chemical manufacturing sectors	61
4.4.2	Validating EMs developed for Illinois agro-based economy	62
4.4.3	Reproducibility of EMs and their applications to other regions	62
4.4.4	Constructing the physical economy model	64
4.4.5	Identifying circular economy strategies	70
4.5	Conclusions	75
5	AUTOMATING THE PROCESS OF MATERIAL FLOW SIMULATION, EX- TRACTION, AND CHARACTERIZATION TO QUANTIFY PHYSICAL FLOWS AT HIGH SPATIAL, TEMPORAL, AND SECTORAL RESOLUTION	76
5.1	Chapter overview	76
5.2	Motivation and background	76
5.3	Overview of Existing Automation Tools in Industrial Ecology	77
5.4	Automating PIOT generation via MFDES tool : Architecture, Information flow and Data structures	81
5.4.1	Module 1: Simulation and Data Extraction	82
5.4.2	Module 2: Data processing for Material Flow Characterization	84
5.4.3	Module 3: Data reorganization and Partial PSUT Construction	86
5.4.4	Module 4: Balancing PSUT and External Data Integration	87
5.4.5	Module 5: PSUT to PIOT Construction	87
5.5	PIOT-Hub : A Cloud Based implementation of the MFDES tool for PIOT Generation	88
5.6	Automated PIOT Generation Demo on PIOT-Hub	90
5.7	Discussions and Potential Tool Applications	93
6	COMPUTATIONAL METHODS TO QUANTIFY MONETARY FLOWS AT HIGH SECTORAL RESOLUTION AND TO PERFORM SUSTAINABILITY ASSESS- MENT	97
6.1	Chapter overview	97
6.2	Motivation and background	98
6.3	Methodology	99

6.3.1	Method for collecting regionalized economic impacts of wind energy expansion	100
6.3.2	Method to quantify the multi-regional impacts using the US-MRIO table	103
6.3.3	Estimating manufacturing sector energy footprint due to wind energy expansion	104
6.4	Results	106
6.4.1	The US economic structure in the form of MRIO table	106
6.4.2	Multi-regional economic impacts of installing wind energy infrastructure	107
6.4.3	Manufacturing sector energy analysis	109
6.5	Conclusions	112
7	DISSERTATION SUMMARY AND FUTURE WORK	114
7.1	Research gaps addressed	114
7.1.1	Mapping material flows at spatial resolution for LCA	114
7.1.2	Quantifying advanced thermodynamic flows using EGA	115
7.1.3	Modeling the physical economy of a region using bottom-up approach	115
7.1.4	Automated tools and cloud platform for physical economy modeling .	116
7.1.5	Computational tools for disaggregating national level economic data for sustainability assessment	117
7.1.6	Conclusion of objectives	117
7.2	Future work	118
	REFERENCES	119
A	APPENDIX	133
A.1	Scaling PSCE models (Ch-4)	133
A.2	Scaling Aspen Plus models (Ch-4)	133
A.3	Aspen Plus property methods used (Ch-4)	134
A.4	NREL JEDI data (Ch-6)	134

LIST OF TABLES

1.1	Specific objectives and case studies	18
2.1	Biodiesel Production Capacity in Indiana. Data from Energy Information Agency (EIA), US Dept of Energy.	23
2.2	Aggregated inventory data for north and central biodiesel production life cycle stages (Source: USDA NASS and USDA NRCS report)	25
2.3	Aspen plus reactor blocks used in modeling	27
3.1	Phosphorus recovery technologies at Industrial Scale [58]	39
3.2	Biochemical reactions inside anaerobic digestion	45
3.3	Entropy generation at each operation of the P recovery process	47
4.1	Typical flows available as scaling variables in an EM	53
4.2	Structure of Physical Supply Table (PST) and Physical Use Table (PUT)	57
4.3	Description of variable used in PSUTs	57
4.4	PIOT constructed from the developed PSUTs (Z: intermediate demand, FD: Final demand, TI: Total of industry)	58
4.5	The agro-based sectors modeled in Illinois, USA	60
4.6	Scaling and validation data used for each model along with error of scaling	63
4.7	Physical supply table constructed for the agro-based Illinois economy from the EMs developed. Units: tons/oper-year (.csv file available in the supplementary material)	66
4.8	Physical use table constructed for the agro-based Illinois economy from the EMs developed. Units: tons/oper-year (.csv file available in the supplementary material)	67
4.9	Information derived from PSUTs and PIOTs	71
5.1	List of existing tools and methodologies for automation of model development in Industrial Ecology.	78
5.2	Physical supply use table format used by MFDES	86
6.1	Primary data used for US MRIO construction	100
6.2	Installed Wind energy capacity (MW) in top 10 States of the US (2016)	101
6.3	Type of JEDI data for each of the ten states.	102
6.4	Concordance matrix of sectors related to wind energy installation and US-MRIO sectors.	102
A.1	Aspen Plus properties used	134
A.2	State level data obtained from JEDI models	134

A.3 Energy intensity (Ω) calculated using EIA data [38]	135
--	-----

LIST OF FIGURES

2.1	(A) Cradle-to-Gate System boundary for northern Indiana biodiesel production; (B) Cradle-to-Gate System boundary for central Indiana biodiesel production	23
2.2	Stage 1 of soy diesel production process	26
2.3	Stage 2 of soy diesel production process	27
2.4	Farming life cycle stage impact assessment	30
2.5	Transportation and biodiesel production life cycle stage impact assessment	31
3.1	Sequential AD-IE P Recovery System (Dotted Line shows the CV for EGA)	41
3.2	Entropy flows in a control volume (CV)	41
3.3	EGA of P recovery method	42
3.4	Initial and final stages of AD for calculation of Entropy Change in AD.	43
3.5	Experimental Calibration Curve to calculate of ΔH° and ΔS° for Anion Exchange Unit	46
4.1	A typical engineering model (EM)	54
4.2	The heatmap representation of the PSUTs constructed	68
4.3	The heatmap representation of the carbon PSUTs constructed	69
4.4	The heatmap representation of the full material and carbon PIOT constructed	70
4.5	The heatmap of PIOT after implementing recycling	72
4.6	Structural changes induced in the physical economy	73
4.7	Percentage reduction in waste flows in the physical economy	73
4.8	Difference in change of physical throughputs (including commodities and waste flows) of industries before and after CE (tons)	74
5.1	Overview of the MFDES tool developed	83
5.2	Overview of PIOT-Hub Infrastructure	89
5.3	PIOTHub: Collaborative cloud implementation of the MFDES tool	91
5.4	Input tab of the PIOTHub	92
5.5	Output tab of the PIOTHub with PIOT view as a table.	92
5.6	Output tab of the PIOTHub with PIOT view as a heatmap.	93
6.1	Representative template for MRIO table generated by IE Lab. (RoE: rest of economy), Shaded Region shows the part of economy where shocks were introduced.	103
6.2	The 4-census regions of the US	105

6.3	Heat Map of the US-MRIO Table for 2017	107
6.4	Direct multi-regional economic impacts	109
6.5	Indirect multi-regional economic impacts	109
6.6	Total national economic impact by sector (log scale)	110
6.7	Top 6 Sector wise and state wise economic impacts in thousands of USD	111
6.8	4 census region-wise change in energy consumption (%) across the manufacturing sub-sectors .	112
A.1	YAML file contents	133
A.2	Scaling aspen plus models for other regions	133

ABSTRACT

For the first time in history, the world-wide material resource use by humanity has reached a record breaking 100 giga tons (gt) along with the release of 49.30 gt of greenhouse gases and 2.10 gt of solid waste. Such large-scale increases in anthropogenic emissions and waste flows could mean reaching catastrophic global temperatures and ecosystem destruction in the near future. In order to better manage resource usage and implement strategies to reduce waste flows and natural resource use intensity, a comprehensive environmental flow accounting is required, which proves to be a challenging task to accomplish. Hence, the current work aims at advancing the current techniques and reducing the efforts to map environmental flows by developing automated mechanistic and bottom-up approaches for material, thermodynamic and economic flow accounting. An integrative flow accounting framework based on process modeling, Input-Output theory and advanced thermodynamic principles is developed here that complements the existing top-down and empirical approaches. The developed techniques are demonstrated via multiple environmental sustainability assessments at high spatial, temporal, and sectoral resolutions ranging from accounting flows at a single process level to multi-regional economy-wide flows. Finally, the framework of material flow accounting was automated by building a Python based tool called - Material Flow Data Extraction and Simulator (MFDES), to reduce the time lead times of constructing material flow maps. MFDES was also implemented on a collaborative cloud platform called PIOT-Hub that generates material flow maps in the form of Physical Input-Output Tables (PIOTs). The potential applications of this research include performing environmental impact assessments of single/multiple supply chains, developing circular economy strategies, quantifying effects of renewable energy expansion, and assessing different types of sustainability policy implications. Further, the cloud-based automated tools built in this work make it possible for researchers from different areas of expertise to synergistically collaborate on large scale projects for sustainable design of emerging processes and technologies.

1. INTRODUCTION

For the first time in history, the world-wide material resource use by humanity has hit a record breaking 100 giga metric tonnes (Gt) in 2017 with only 8% of this total coming from recycling [1]. Of the 100 Gt consumed to build different types of infrastructures and products, 49.30 Gt of green house gases (GHGs) and 2.10 Gt of solid waste was sent back into the nature as emissions and waste flows [2][3]. These concerning numbers are projected to further go up by more than 52% for GHG emissions and 60% for solid wastes by the year 2050 [3][4]. Such large scale increases in anthropogenic emissions and waste flows could mean reaching potentially catastrophic global temperatures much before the predictions [5]. Recent studies have predicted that the 2050 projection of 1.5°C [6] rise in global temperature will now be attained by 2030 [7]. These alarming numbers indicate that there has never been a more critical time in human history to better manage our material resource usage, reduce destruction of natural ecosystems, and to keep the global temperatures under habitable limits for all life forms on our planet.

The first and foremost step in managing our material resource usage would be to comprehensively account/quantify all types of relevant flows from a sustainability standpoint. These flows could be both physical - material and thermodynamic flows, and economic - monetary flows. Although human activities influence and interact with nature only in terms of physical flows, there is a parallel need to track monetary flows to help in maintaining economic and social sustainability, and to further track economic changes induced by global climate changes and environmental policy implications. Comprehensive flow accounting creates ways to better understand how flows move from one human activity to another, and eventually back into the nature as physical flows. Such an understanding of flow movements enables development of sustainable resource use strategies ranging from increasing production efficiencies at a single process at an industry level to economy-wide circular economy implementations.

To achieve comprehensive flow accounting, advances have been made both in terms of metrics used for quantifying, and methodologies/frameworks to account different types of flows [8][9][10][11][12]. In most of the existing methods and metrics, two common themes can

be identified: top-down frameworks and their excessive reliance on empirical data. Top down approaches rely on using widely available empirical data-sets such as government records to feed into the methodology. Some of the commonly used top-down approaches include economic and physical input output (IO) analysis and material flow accounting (MFAs). The spatial, temporal and sectoral resolution of flow accounting through such methods is constrained by the available granularity in the data-sets used. To overcome granularity challenges, various allocation methods [13] [13] are used to disaggregate the flows to a finer scale. However, the allocation methods can only be used until meaningful interpretations can be made from disaggregation as the assumptions made for the aggregated flows may not necessarily hold true for the disaggregated flows. The heterogeneity in flow characteristics also tend to increase rapidly with disaggregation. For example, when allocating the US-wide fertilizer requirements of agriculture sector to its different sub-sectors, an averaged fertilizer input per unit output of agriculture sector may not be accurately representing the actual requirements of all the sub-sectors. The fertilizers required to grow different crops in the aggregated agriculture sector vary greatly in terms of quantities and fertilizer type used. This could lead to either overcounting or undercounting fertilizer requirements while allocation. Further, animal farming sub-sectors also fall under the agriculture sector and it makes no meaningful interpretation to use averaged fertilizer inputs as farm animal feeds. Allocation challenges are also prevalent in monetary flow disaggregations. For example, when spatially allocating the average economic throughput of the US agriculture sector to the agriculture sectors across different states, the average throughput may not be representative of a state's agriculture sector profile as the agriculture industry size varies greatly in the US (ex: California vs Alaska).

To overcome disaggregation challenges, bottom-up approaches such as process Life Cycle Assessment (LCA) can be used to quantify flows while maintaining high granularity. While process LCAs can provide high granular resolution in the form of highly detailed industry production recipes, they are generally based on empirical data-sets which may be aggregated spatially [14]. For example, the production recipe of biodiesel can be different in India when compared to Brazil [15] and a LCA based on average empirical data will not show spatial differences in environmental impact assessed. Also, the production technologies tend

to continuously evolve over time. Furthermore, LCA models scale linearly but the per-unit material requirements of production can change with economies of scale. For example, in the production of biodiesel from algae, the electricity required to operate a technical component called raceway paddle wheel (it ensures proper mixing of carbon dioxide and nutrients) is nearly independent of the algal growth rate [16]. An LCA of such a production processes will scale the electricity required linearly with algal production and will not be able to show the influence of economies of scale. To overcome some of these challenges, methods such as hybrid Input Output LCA (IO-LCA) approaches have also been established to utilize the advantages offered by both bottom-up and top-down approaches [17] [18], [19]. In such hybrid approaches, high sectoral resolution is maintained for the flows in focus for which physical data is available and the information of all other flows at an aggregated level is also retained. However, even the hybrid methods rely excessively on empirical data. While there are no inherent disadvantages of using empirical data in any of the flow accounting approaches, allocation could be an ubiquitous challenge at every step where empirical data is not available. Currently, there are no established bottom-up approaches that can mechanistically simulate (including economies of scale) missing flow information and, at the same time, be seamlessly compatible with top-down approaches. This results in lack of full accounting of waste flows, understanding interdependence between different industries in a region and a complete visibility into opportunities to improve material utilization and reduce emissions or wastes.

The research presented in this dissertation aims to address the challenges discussed above by proposing a new bottom-up flow accounting framework that uses computational and mechanistic models to account material, thermodynamic and monetary flows at high spatial, temporal and sectoral levels. While advancing the flow accounting research, the current work ensures that the technique developed is compatible and complements other established techniques. To this regard, it also attempts to advance the status quo of flow accounting research a step further by integrating existing bottom-up, top-down, empirical and mechanistic flow accounting methods through a novel cloud-based collaborative infrastructure. To successfully achieve these overall aims, the research work was divided into 5 specific research objectives which are discussed as individual chapters in this document (**table 1.1**). Each

specific objective addresses a unique research gap in the material flow accounting literature and the methodology developed is demonstrated via a case study. **Chapter 2** specifically attempts to address the research gaps in performing spatial Life Cycle Assessment. Currently, LCAs primarily rely on empirical data that scales linearly and is often available only at high regional aggregation levels. To tackle these challenges, computational process models were developed that are based on mechanistic principles and can simulate the required LCA inputs at high resolutions. In **chapter 3**, the research gap of a lack in established methods to quantify advanced thermodynamic flows for sustainability assessment of emerging technologies is addressed. An entropy generation assessment was performed at individual process levels of a technology for which empirical data was not available the quantified entropy flows were used in performing a thermodynamic sustainability assessment for opportunities in process improvement. **Chapter 4** broadens the scope of the methods established in the previous chapters by integrating the mechanistic models with the Input-Output (IO) framework to perform bottom-up economy-wide sustainability assessments by tracking material flows in a regional economy and quantifying waste along with identifying strategies to implement circular economy. While the first 3 chapters attempt to establish methodologies to quantify different types of physical flows, **chapter 5** attempts to bridge multiple bottom-up and top-down flow accounting frameworks through a collaborative cloud infrastructure where different researchers with varied modeling expertise can upload their models and data. The cloud infrastructure simultaneously simulates the different models, characterizes flows, and provides a compilation of flows from all the models in one standard format which can then be further used for sustainability assessment of material use.

Finally, **chapter 6** focuses on using economic analysis for impact of adoption of emerging technologies, particularly focusing on renewable energy expansion. This chapter further improves the existing allocation methods for monetary flow disaggregation. The methods developed in these five chapters together attempt to address multiple research gaps discussed above by establishing and standardizing bottom-up flow accounting methods, developing collaborative computational tools, and improving top-down allocation techniques.

The final **chapter 7** presents an overall conclusion by summarizing the contribution of this dissertation to achieve an advanced, reproducible and inclusive environmental flow ac-

Table 1.1. Specific objectives and case studies

Chapter	Objective	Approach	Case study
1	Quantifying material flows at high spatial disaggregation	LCA –	Spatial LCA of biodiesel production in North and Central Indiana, USA
2	Quantifying advanced thermodynamic flows for sustainability assessment	Entropy generation	Phosphorus recovery in a waste-water treatment system
3	Quantifying physical economy of a region at high sectoral disaggregation	IO theory –	Agro-based physical economy model for the state of Illinois, USA
4	Developing a collaborative tool to integrate multiple material flow modeling methods	IO theory –	Circular economy strategies for the agro-based economy of Illinois, USA
5	Computational Platform for spatially disaggregate economic impact analysis	IO theory –	Wind energy expansion in the US –

counting framework that can be used for sustainability assessment of emerging technologies, moving towards lower material wastes and implementing circular economy. Future possibilities of application and improvement for the work presented in this dissertation are also discussed in this chapter.

2. COMPUTATIONAL PROCESS MODELS TO QUANTIFY INDUSTRIAL MATERIAL FLOWS AT HIGH SPATIAL RESOLUTION TO PERFORM SPATIAL LIFE CYCLE ASSESSMENT

This chapter is based on the following published article: [20] V. S. G. Vunnava and S. Singh, “Spatial life cycle analysis of soybean-based biodiesel production in Indiana, USA using process modeling,” *Processes*, vol. 8, no. 4, p. 392, Mar. 2020. DOI: [10.3390/PR8040392](https://doi.org/10.3390/PR8040392)

2.1 Chapter overview

In this chapter (2), a computational approach of using chemical process models is used to achieve the first research objective (1.1) by simulating material flows at high spatial resolution representative of a region. To perform regionally specific environmental assessments, input data should be representative of the industries and material consumption patterns in the region being studied. Using spatially aggregated data-sets for impact assessment may not provide accurate quantification of impacts. To demonstrate how bottom-up computational approaches can be used in such situations, a case study of performing a spatial LCA of biodiesel production in Northern and Central Indiana is provided. Chemical process models were used to simulate material flows in soybean based biodiesel production systems in the two regions. Using material flow data from process models in conjunction with other available regional data-sets, the variations in environmental impacts of producing biodiesel were quantified for 61 counties in Indiana. The case study discussed in this chapter attempts to show how a standardized and reproducible technique such as process modeling can be used to get material flow information at high spatial disaggregation.

2.2 Motivation and background

Life cycle assessment (LCA) models are widely used to assess the sustainability of bio-based energy or material production. These models are developed to quantify the environ-

mental, societal, and/or economic impact of production systems [21]. While several LCA studies have highlighted the positive impacts of a shift to bio-based production, it has also been shown that a shift to bio-based energy or products leads to a “food vs. fuel” debate and also exacerbates the environmental challenges due to the Land Use and Land Use Change (LULUC) associated with bioenergy crops [22]. LCA studies have shown that bio-fuels from different cropping systems producing ethanol or biodiesel can reduce greenhouse gas emissions and non-renewable energy production, and increase other impacts such as eutrophication and acidification related to nitrogen release [23]. Thus, the choice of agricultural system and management has significant impact on the sustainability aspect of bio-based energy or products [24]. In their study, Qin et al. (2018), show that changing land management practices, such as reducing tillage intensity, can change the life cycle emissions for ethanol production significantly. Other studies have also shown similar results, highlighting how regional practices on agricultural systems result in significantly different life cycle emissions. Soybean-based biodiesel was shown to have 70% lower Green House Gas (GHG) emission if land use change impact in Argentina was not considered [25], highlighting the role of the regional sourcing of feedstock in accounting for true life cycle emissions. A 2018 study focused on the life cycle emissions of soybean-based biodiesel produced in the US, using a national average for farming practices and the pathway of soy-oil to biodiesel conversion through transesterification [26]. This study also found that soybean biodiesel significantly reduces GHG and nonrenewable energy consumption, however, accounting for LUC can result in additional GHG emissions. The comparison of sugarcane-based ethanol production in India and Brazil shows that Indian ethanol had lower impact, highlighting that the same product originating in different location can have different environmental impact [27]. Thus, it is important to account for regional variations and farm activities to improve the reliability of the life cycle environmental impacts of producing bioenergy. If the regional activity includes the clearing of tropical forests, the life cycle GHG can be worse than conventional diesel, as was the case for Brazilian soybean-based biodiesel production [28]. Further, whether the soybean is processed within a region to produce soybean biodiesel or imported as final product also has an impact on total life cycle impact, as was found in a study on soybean diesel being used in Europe from soybean grown in Brazil [29]. In this study, it was found

that cultivation and transportation played an important role. Through several studies, it has been established that regional cultivation practices [30] and processing pathways play an important role in truly estimating the sustainability of bio-based energy or products.

Following this lead of variations in impact from regional practices, there has been a growing interest in incorporating spatially explicit information in LCA studies. To incorporate regional information in the calculation of life cycle emissions for bio-based products, methods like GIS [31] and detailed mechanistic models [32], or spatial land use models [33] for capturing the variations, are being increasingly used. Utilizing mechanistic model of DNDC Tabatabaie et al [32], demonstrated the variations in life cycle emissions for biodiesel produced in Orgeon, USA as a result of temperature variation and soil organic carbon. Spatial models of LUC have been combined to show the impact on life cycle emissions from 1st generation biofuels in the European Union [33]. Another study focused on the Southwestern Michigan region and simulated the production of three different types of feedstock for corn-ethanol production in different watersheds using an EPIC model [34]. This study found the impact of feedstock type to be more prominent than the region where the second-generation feedstock was being cultivated.

While these studies have incorporated the impact of variations in feedstock growing stage, these studies have not accounted for the regional variations in the processing of the feedstock. Processing variations can have significant variation in life cycle emissions, as these form a significant step in the conversion to final product. Studies have shown that the size and capacity of power plants using biomass also impact the environmental impacts of products from these plants [35]. A critical review on integrating the spatial dimensions in LCA studies highlights that process recontextualization for a particular region should be adopted in order to develop regional life cycle inventories [36]. Hence, for spatial LCAs, utilizing process modeling for capturing the impact of variations in processing of biomass feedstock can contribute significantly to improving the representativeness of results for that region. However, such studies have not been widely done, mainly due to the lack of enough information about regional processing plants and for confidentiality reasons. In this work, this specific gap in the literature is addressed for soybean-based bio-diesel production. The focus of our work is on capturing the variation within a state. As it has been shown that

different parts of states can experience huge variations in agricultural practices owing to soil quality changes or farm size, etc., this causes variations in the processing of feedstock as well. Further, the size and type of processing plant can also result in variation in life cycle emissions. To capture this effect, soybean-based biodiesel production in northern and central Indiana was considered. A regionalized life cycle inventory is built on the farming, transportation and processing life cycle stages for the two regions. For capturing upstream life cycle stages, average data from SimaPro have been utilized. Results are presented for a functional unit of 1 liter of soybean biodiesel produced in north and central Indiana.

2.3 Methodology

A cradle-to-gate process LCA methodology has been followed here using standard International Organization for Standards (ISO) practices. The first step involved identifying the soybean-based biodiesel production system in Indiana. The cradle-to-gate boundary includes all upstream processes required for the production of biodiesel up to the point of biodiesel output. **Figure 2.1** shows the system boundary for the production of biodiesel in both north and central Indiana. Once the system boundary was selected, a regionalized life cycle inventory (LCI) was built. In this case, the regionalization accounted only for the life cycle stages of farming, transportation and biodiesel processing. Upstream processes were modeled using unit process information from LCA datasets such as ecoinvent and USLCI, hence the upstream processes represent average production. Final LCA results were obtained using the TRACI 2.1 (US version) Life Cycle Impact Assessment (LCIA) method and analyzed for global warming potential and eutrophication impact categories. The base year of analysis was 2013 and results have been normalized for per-liter biodiesel production for comparative analysis between the life cycle impacts of biodiesel from north vs. central Indiana.

2.3.1 System and System Boundary

Indiana is a major producer of soybean in US and ranks among the top five producers (about 7% of total soybean produced in the USA [37]. US Energy Information Agency (EIA) provides a detailed, state-level biodiesel production capacity information for several

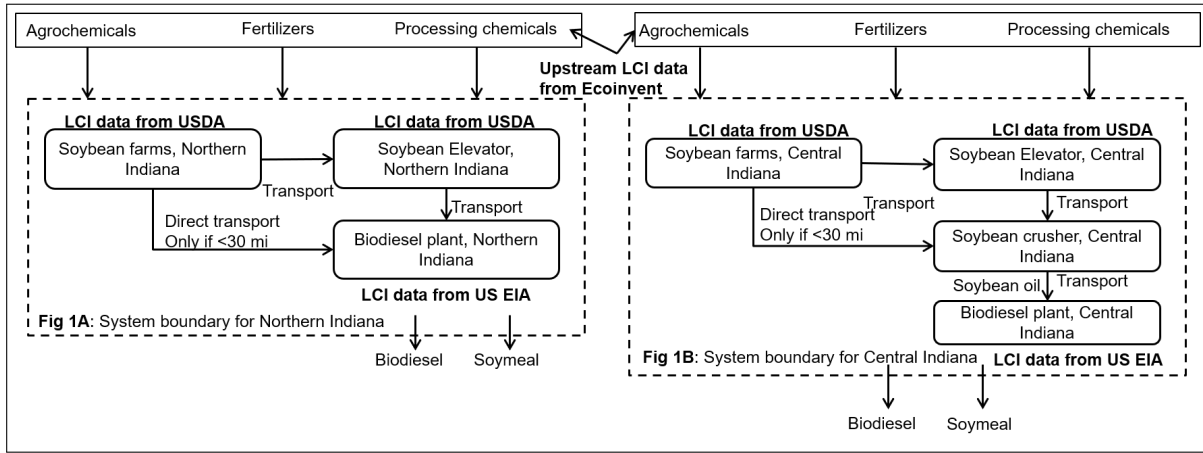


Figure 2.1. (A) Cradle-to-Gate System boundary for northern Indiana biodiesel production; (B) Cradle-to-Gate System boundary for central Indiana biodiesel production

years [38]. **Table 2.1** shows the production processes for biodiesel in Indiana along with the feedstock type. In 2013, two biodiesel plants were active. The plant in northern Indiana utilizes soybean as feedstock and the facility has full soybean-to-biodiesel production process infrastructure. The plant in central Indiana utilizes soy-oil from a dedicated soy-oil producer to make biodiesel. This difference in biodiesel production process from these plant location leads to different system boundaries in performing LCA for biodiesel obtained from different locations. Hence, to quantify these differences, two different system boundaries were selected for biodiesel production in Indiana. Figures 1A and 1B (in **figure 2.1**) show the cradle-to-gate system boundary for soybean-based biodiesel produced in northern and central Indiana.

Table 2.1. Biodiesel Production Capacity in Indiana. Data from Energy Information Agency (EIA), US Dept of Energy.

Location	Plant Capacity	Feedstock
Claypool, Kosciusko county, Indiana	99 Mega gallons per year	Soybean
Morrisontown, Shelby county, Indiana	5 Mega gallons per year	Soybean oil

2.3.2 Regional Life Cycle Inventory for Biodiesel from Soybean in Indiana

After identifying the system boundaries and pertinent life cycle stages for the life cycle of biodiesel production in northern and central Indiana, regional life cycle inventories were built as described below.

Soybean Farming

The life cycle stage of soybean farming for producing biodiesel in Northern and Central Indiana have differences in farm operations and resource consumption. Hence, the data for soybean yield, land used, water applied, and fertilizer applied to soybean fields in the 61 counties studied (2013 data) were collected from the United States Department of Agriculture (USDA) and National Agriculture Statistics Service (NASS) [37]. The emissions from the soybean farms were calculated based on the Conservation Effects Assessment Project by Natural Resources Conservation Service [39]. Spatial data for farming stage were collected/calculated (shown in supplementary material along with calculation methods) for each northern and central Indiana county that grows soybeans. This dataset includes spatial variation in land harvested, fertilizer usage, land irrigated, water usage based on irrigation practices, yield and production and nitrogen/phosphorus emissions. An aggregated overview of the data collected are shown in **table 2.2**.

Soybean Biodiesel Production

For the life cycle stage of soybean processing, the industry standard to produce soy diesel is crushing soybeans, extracting the soy oil, then using transesterification to convert the soy oil to soy diesel. In 2013, two facilities in Indiana were capable of producing biodiesel—the plants are located in Shelby and Kosciusko county [40]. The soy diesel production capacity of Indiana was 104 million gallons, with 99 million coming from the northern processing plant (Kosciusko county) and the balance was produced at a central Indiana plant (Shelby county) [40]. In Kosciusko county, the facility manufactures soybean oil and soy diesel on the same property. Hence, in the northern facility, the whole process from soybean to biodiesel production is done. The co-product from the facility is soybean meal. The producer in Shelby

Table 2.2. Aggregated inventory data for north and central biodiesel production life cycle stages (Source: USDA NASS and USDA NRCS report)

Life Cycle Stage	Material flow	North Indiana	Central Indiana
Soybean farming	Acres of soybean crop harvested - sq. m	5.530000e+09	308000000.0
-	Water applied - cubic m	6.750000e+08	37500000.0
-	Soybean - kg	1.800000e+09	91200000.0
-	Fertilizer applied - N (kg)	2.840000e+06	3420000.0
-	Bio fixation - N (kg)	1.510000e+08	192000000.0
-	Fertilizer applied - P2O5 (kg)	1.720000e+07	20800000.0
-	Fertilizer applied - K2O (kg)	4.620000e+07	55700000.0
-	N emissions air (kg)	1.170000e+07	14900000.0
-	N emissions soil (kg)	3.850000e+06	4910000.0
-	N emissions water (kg)	1.000000e+07	12800000.0
-	P emissions water (kg)	1.200000e+06	1530000.0
Soybean processing	Soybeans used (kg)	1.800000e+09	91200000.0
-	Sodium hydroxide (kg)	1.730000e+07	878000.0
-	Methanol (kg)	3.490000e+07	1760000.0
-	Hexane (kg)	3.680000e+08	18600000.0
-	Water (kg)	1.730000e+07	878000.0

county does not produce soybean oil onsite, and instead uses soybean oil from another facility in the same city of Morrisontown. Hence, in the central facility, the process involves buying soybean oil from the nearby soybean crusher. In this case, the co-product of soy meal is produced at the crusher unit, hence the impact was allocated using mass-based allocation to biodiesel production. As seen in **table 2.1**, the capacity of production in the northern facility is significantly larger than central facility production. This implies that one can assume almost all soy-biodiesel to come from the northern facility, however, for the purpose of demonstrating the impact of variations in processing pathways, a comparative LCA was performed here. The functional unit used for comparison in this study is per-liter biodiesel, which is being produced in both pathways. Mass-based allocation was used at the respective process units for the allocation of life cycle impacts to biodiesel and co-products. Process models were built for the conversion process in Aspen Plus (Version 8.8, Aspen Technologies) to obtain the unit process data that were fed into SimaPro (Version 9, PRé Consultants) for the life cycle stage of soybean processing to biodiesel.

Biodiesel Production Process Modeling

For soybean biodiesel production, a two-stage process was used.

Stage 1—Soybean to soybean oil conversion: In the first stage, soybeans are first cleaned to separate out any particulate contaminants before being cracked. After cracking open the beans, all the hulls are separated using blasts of air. Once hulls are separated, the beans are crushed into flakes and then processed to extract oil using a hexane extraction process. The soybeans were assumed to contain 19.2% oil in the form of three triglycerides: linoleic, oleic and palmitic fatty acids [40]. The various unit operational blocks used in Aspen plus are shown below in **figure 2.2**. Some of the assumptions about unit operations will result in variations from actual plant flows, however, most of the chemical processes were captured.

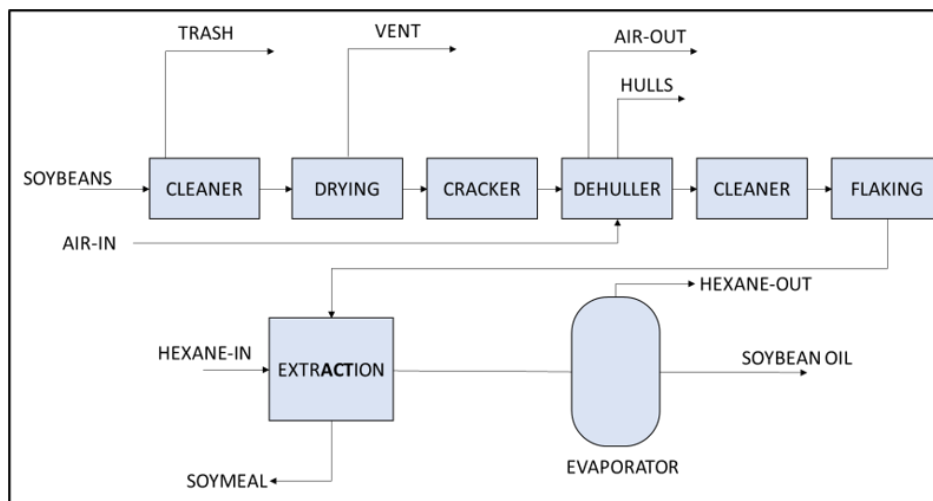


Figure 2.2. Stage 1 of soy diesel production process

Stage 2—Soybean oil to biodiesel conversion: Soybean oil was converted into biodiesel by a series of transesterification reactions in the presence NaOH. Soybean undergoes transesterification in a reaction tank and the outputs of the reaction are a mixture of methylated fatty acid molecules (biodiesel) (ex: CH₃-L, CH₃-O and CH₃-P), glycerol, and unreacted intermediate products, along with the catalyst NaOH. This mixture is then selectively distilled to separate out biodiesel. Reaction kinetics for soybean biodiesel production was obtained from literature [41]. As in stage 1, some of the modeling assumptions about unit operations will result in variations from actual plant flows, however most of the chemical processes are cap-

tured. The operational blocks modeled in Aspen plus are shown in **figure 2.3**. The northern facility combines both these stages in a single plant. Therefore, for northern biodiesel production, these two stages were combined as single plant data. The central Indiana uses the soybean oil from a soybean crushing facility nearby and is transported to the soybean biodiesel production facility by truck. The specific type of Aspen Plus reactors (or aspen blocks) that were used are shown in **table 2.3**.

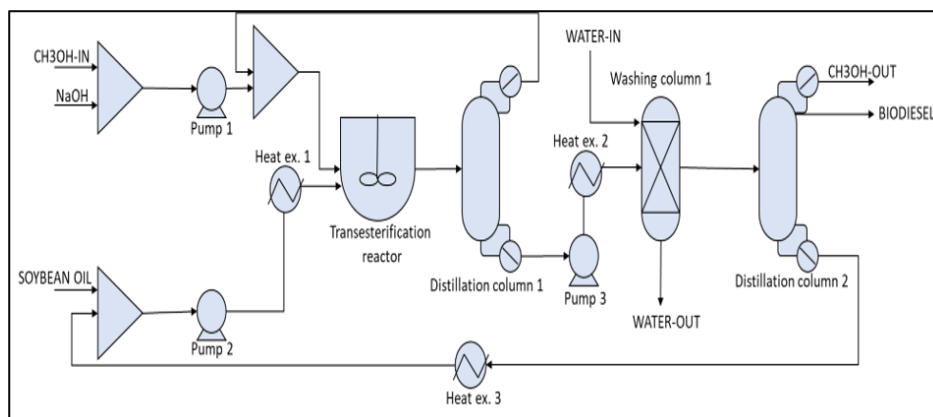


Figure 2.3. Stage 2 of soy diesel production process

Table 2.3. Aspen plus reactor blocks used in modeling

Unit operation	Aspen Plus Block	Block details
Transesterification	RCSTR	Rigorous simulation with kinetics reactions
Methanol Recovery	RadFrac	Rigorous multi-stage distillation model
Water Washing	Liquid-Liquid Extractor	Rigorous multi-stage liquid-liquid extractor model
–	–	–
Biodiesel Purification	RadFrac	Rigorous multi-stage liquid-liquid extractor model
–	–	–

Transportation Life Cycle Stage

The next important difference in biodiesel production in North and Central facility is the logistics involved in moving the feedstock between processes. As seen in the system boundary (**figure 2.1**), the transportation in north and central biodiesel production involves moving soybean first to the grain elevators, and then to either the grain crusher, as in the central

region, or to the biodiesel plant, as in the north region. The calculation of the transportation life cycle stage is described for both systems below.

Northern Biodiesel Production: In northern production system, soybeans were either directly transported to the facility (if the distance of the facility is less than 30 mi from the farm) [42] or transported to local grain elevator first, from which point the soybeans were then transferred to the processing facility. Since county elevator centers are present in almost all counties in Indiana [43], the distance between the production facility and all the northern county centers were calculated using Google maps (shortest driving time) and truck transportation was chosen as the mode of transport to ship the grains. The distances were used, along with the weight of the soybeans transported from each county to the biodiesel plant in SimaPro, to calculate the county-wise environmental impacts associated with transporting the soybeans.

Central Biodiesel Production: In the central facility, the feedstock is soybean oil which comes from a nearby crusher (Bunge North America) in Morrisontown. Once again, it is assumed that all central Indiana counties will ship their grains to the facility via grain elevators, with only one exception: the distance to facility is less than 30 mi, in which case the grains are directly shipped to the crushing facility. Similar to the northern counties, Google maps was used to calculate the distances and was used along with the weight transported in SimaPro to calculate the county-wise environmental impacts associated with transporting the soybeans.

Upstream Life Cycle Inventory Data

Additional inputs to the farming life cycle stage and processing stage for production of biodiesel were modeled using unit process information from Ecoinvent and US LCI datasets. These upstream data include inputs to the farming stage such as various types of fertilizers and chemical inputs in soybean diesel production (eg: Hexane for extraction process). Hence, the upstream process representation is an average representation that does not capture any regional variation in manufacturing impact for those products. The material flow mapping to SimaPro is shown in supplementary material.

2.3.3 Allocating Spatial Impacts at County Scale to Soybean Based Biodiesel Production

Spatial variations of assessed impacts occur due to variations in farming stage at county scale and associated transportation to the biodiesel plants. Since only one soybean biodiesel plant exists for each region studied, the final impacts due to farming required for supporting biodiesel production and transportation are allocated back to the county based on their contribution to biodiesel production. It was assumed that all counties in a region contribute towards the supply of soybeans for biodiesel production. The amount each county supplies to the biodiesel production was assumed to be equal to the county's soybean relative production within a region multiplied by the demand for soybean at the biodiesel plant. For example, if a county 'A' produces 'X'% of the soybeans in the northern Indiana region, then it was assumed that 'X'% of the total demand of soybeans by the biodiesel plant in the north was met by the county 'A' and 'X'% of all the impacts associated with producing a liter of biodiesel in the northern plant was allocated to the county 'A'. Similarly, impacts associated with transporting the 'X'% of soybean demand to the biodiesel plant was allocated to county 'A'. The same allocation technique was applied to impacts of biodiesel production in central Indiana. The percentage calculation for each county is provided in the supplementary material.

2.4 Results

2.4.1 Northern Indiana

Figures 2.4 and 2.5 (1st and 3rd columns) show the per-liter biodiesel environmental impacts of producing biodiesel at the northern plant in Claypool, Indiana. Among the impact of all the north counties studied, specific patterns of environmental impacts were found. Allen and White county were the top counties in the north that had the highest environmental impacts in terms of global warming potential, eutrophication, water consumed, and land used per liter of biodiesel produced. These results were consistent with the fertilizer and water application practices observed during the life cycle inventory collection. These counties tend to use some of the highest fertilizer and water per acre of soybean crop in the

entire state. On the other hand, Starke and Steuben counties in the north had the lowest environmental impacts in all the categories studied. When assessing transportation-related global warming and eutrophication impacts, it may initially seem trivial that the farther the soybeans must be transported, the larger the impacts. However, since different counties produce different amounts of soybeans, the results show the impacts considering not only distance travelled, but also the individual county's contribution to the total biodiesel plant's soybean demand. The highest environmental impacts related to this distance, coupled with soybean contribution, were seen in the counties of Benton and Jasper.

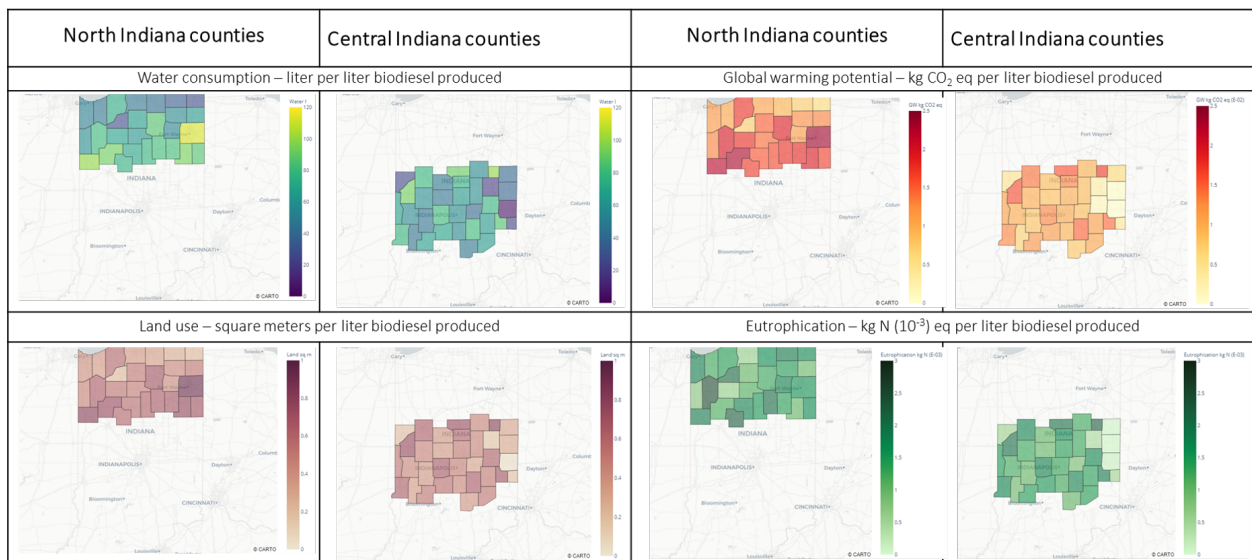


Figure 2.4. Farming life cycle stage impact assessment

2.4.2 Central Indiana

Figures 2.4 and 2.5 (2nd and 4th columns) show the per-liter biodiesel environmental impacts of producing biodiesel at the central soybean oil plant in Morrisontown, Indiana. Similar to the northern counties, some specific patterns were also observed in the central counties. Montgomery and Randolph counties had the highest environmental impacts related to water and land use, global warming potential, and eutrophication. Like the northern counties, this observation is consistent with the high fertilizer and water usage data observed in the life cycle inventory data collected. Of all the counties studied in the central region,

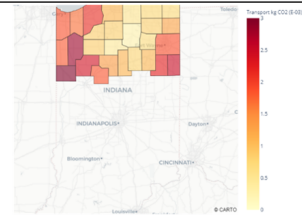
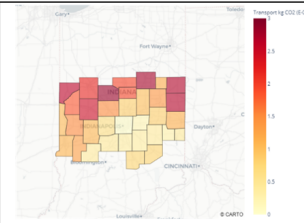
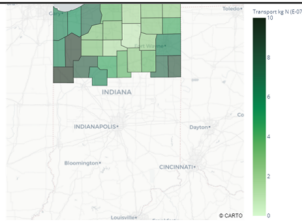
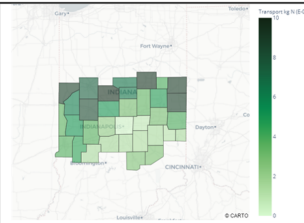
Transportation stage		Soybean processing stage	
North Indiana counties	Central Indiana counties	North Indiana counties	Central Indiana counties
Global warming potential – kg CO ₂ (10 ⁻³) eq per liter biodiesel produced			
		Soybean oil production Global warming potential – kg CO ₂ per liter biodiesel produced = 0.23 Eutrophication – kg N eq per liter biodiesel produced = 1.13E-03	
Eutrophication – kg N (10 ⁻⁷) eq per liter biodiesel produced			
		Soybean biodiesel production Global warming potential – kg CO ₂ per liter biodiesel produced = 0.39 Eutrophication – kg N eq per liter biodiesel produced = 1.16E-03	
		Soybean biodiesel production Global warming potential – kg CO ₂ per liter biodiesel produced = 0.17 Eutrophication – kg N eq per liter biodiesel produced = 2.54E-05	

Figure 2.5. Transportation and biodiesel production life cycle stage impact assessment

Vermillion and Marion counties had disproportionately low impacts per liter of biodiesel produced. This was again consistent with the very low fertilizer usage observed in the county based on the life cycle inventory data collection. When it comes to transporting the soybeans to Morrisontown, unlike the northern counties, the impacts were primarily related to distance transported and only slightly based on the contributions of the individual counties towards biodiesel production in the central plant. This can be explained by the disproportionately smaller biodiesel production capacity of the central plant coupled with a relatively uniform soybean production in the central counties. Since the soybeans were assumed to be first transported to the soybean oil processing center and then to the biodiesel plant (not directly to the biodiesel plant, as in the north counties), it is possible that the soybean oil processing center, which produces relatively generic commodities (oil and soymeal) compared to the biodiesel plant, sees a relatively uniform supply from the soybean farmers. Since the production facility is small, it may not be profitable in central Indiana for farmers to transport to biodiesel production, hence there is a lower impact from transportation in life cycle of biodiesel production in this part of state. Overall, at an aggregate level, both regions performed similarly in terms of global warming potential, but the northern region performed slightly better than the central in terms of eutrophication.

2.5 Conclusions

There were some commonalities between the studied environmental impacts of the northern and central Indiana counties. Irrespective of geographic region, the counties had higher environmental impacts if the fertilizer and water application was high. From the life cycle inventory data and the impacts studied, it appears that the farming practices vary greatly from county to county in both northern and central Indiana, hence sourcing soybean from different counties can result in a different overall impact for biodiesel production. However, based on the transportation model assumed in this study, it appears that the transportation-related environmental impacts are different in northern and central regions. While the central region was not sensitive to the contribution of individual counties towards biodiesel production, and was mainly sensitive to the distance travelled, the northern region was sensitive to both distance and the contributions of individual counties. This can be attributed to the volume of transportation based on capacity of the biodiesel production plant, which is much lower in the central plant.

Based on the environmental impacts calculated and patterns observed in this study, it can be concluded that the spatial distribution of environmental impacts of bio-based energy production depend on at least four factors: (1) fertilizer and water application rates for feedstock, (2) land usage, (3) distance to the processing plant, and (4) the available options for soybean farmers to sell their harvested soybeans. While the technology for biobased processing can be same, it can have different spatial impacts based on these factors. Hence, from a life cycle perspective, these sub-regional spatial variations can make the same product being produced in a different facility more favorable from an environmental perspective. Thus, these sub-regional impacts of a processing facility must also be considered while deciding on the environmental friendliness of products made using almost the same technology. Such spatial impact variations are not currently included in LCAs for bio-based energy and production, however, they must be included for decision making. Although not included in this study, it is also recommended that other factors, such as soil quality and percentage of cover crops in a county, along with energy inputs, be included in future studies, as these can also influence the spatial environmental impacts.

3. COMPUTATIONAL BOTTOM-UP METHODS TO QUANTIFY ADVANCED THERMODYNAMIC FLOWS TO PERFORM THERMODYNAMIC SUSTAINABILITY ASSESSMENT

This chapter is based on the following published article: [44] V. S. G. Vunnava and S. Singh, “Entropy generation analysis of sequential Anaerobic Digester Ion-Exchange technology for Phosphorus extraction from waste,” *Journal of Cleaner Production*, vol. 221, pp. 55–62, Jun. 2019. DOI: [10.1016/J.JCLEPRO.2019.02.020](https://doi.org/10.1016/J.JCLEPRO.2019.02.020)

3.1 Chapter overview

In the previous chapter (**ch-2**), bottom-up computational methods were established to quantify material flows at high spatial resolution when no regional empirical data was available to perform environmental impact assessment. In this chapter, bottom-up computational methods are proposed to quantify another type of physical flow: thermodynamic flow. In environmental sustainability research literature much emphasis has been given to material and monetary flows when compared to thermodynamic flows. This can be attributed to the focus of the research community on achieving better material resource use intensity with the help of existing mass-balance approaches to account material flows. The inherent thermodynamic irreversibilities in all the production systems and the abstract nature of the field make it challenging to quantify thermodynamic flows, especially more complex thermodynamic flows like entropy. However, thermodynamic efficiency is closely linked to material use intensity. Most of the energy used for human activities is produced by combustion of various natural material inputs and the per unit energy requirement of transforming materials could vary greatly based on the production process [45]. This means that if the thermodynamic efficiency of a production process is improved, it can lead to a reduction in overall material usage related to energy generation. Therefore, accounting thermodynamic flows could be equally important as accounting material flows for achieving reduction in global resource use intensity.

Several thermodynamic methods and metrics have been used in comparative analysis to select the technologies with minimal energy consumption. Simplest form of energy analysis involves assessment of total energy requirement by fuel or electricity consumption for running a system [46]. However, as the complexity of the systems increase, simple energy analysis does not provide in-depth insights into thermodynamic performance of the technology such as specific the design improvements needed to reduce the energy consumption and identifying the reasons behind energy inefficiencies. To overcome this deficit of energy analysis, exergy has been used as a metric which can provide insight into specific inefficient components of the system under study [47]. In a typical exergy analysis, the available energy consumption of various processes in the system under study are calculated and the processes that have highest exergy losses are identified. These selected processes are then put forward for improvement in design to improve energy utilization. Further, to include supporting upstream and downstream processes of a system, both energy and exergy analyses have been improvised on a life cycle scale to quantify cumulative consumption [48]. To achieve design optimization to improve efficiencies of identified sub-systems, more advanced methods such as exergy loss minimization and entropy generation analysis (EGA) have been used for system design optimization[47][49].

This chapter aims to demonstrate how entropy generation analysis can quantify the inefficiencies in a technical system and provide a starting point to improve thermodynamic efficiency via design optimization, which could consequently help reduce material use intensities. A case study of an emerging phosphorus recovery technology was used to demonstrate the application of bottom-up entropy generation analysis.

3.2 Motivation and Background

Phosphorus (P) is a critical resource as it is a major nutrient for food production and the availability of P is limited with irregular geographical distribution. Most of the commercial phosphate ores are disproportionately concentrated in a very few countries with the highest reserves being found in Morocco, China, Algeria, Syria, South Africa, Australia and the US [50]. Considering the recent supply and demand ratio, it is predicted that the world's demand for P will overrun supply by 2033 [51], i.e., the world may reach peak P production. However,

the demand of P will keep increasing as the demand of food production increases with increasing population. Despite the anticipated gaps in supply and demand of P, currently the available P in waste streams is not completely recovered. This leads to large amount of P being wasted as discharges of waste-water produced in agriculture, storm water [52] and livestock waste [53]. Along with the waste of valuable resource, this also leads to major environmental challenges such as eutrophication and oceanic dead zones [54]. It is estimated that it costs the US nearly 2.2 billion USD annually in damages due to P and nitrogen (N) water pollution [55]. A recent incident of toxic algal bloom was associated to P release in the Lake Erie causing water supply cut-off for the citizens [56]. Therefore, it is extremely important to recover P not only to meet the growing demand, but also to reduce the negative environmental impacts associated with P run-off along with reducing economic damage of infrastructure caused by struvite scaling in WWTPs [57].

The multiple benefits associated with P recovery from waste-water and treatment plants have motivated development of novel technologies [58], several of which are still at lab or pilot scale. While recovery of P can provide environmental and economic benefits, to avoid unintended consequences such as increased energy consumption, a thorough assessment of available options is necessary before large scale adoption of technologies under development. Since sustainability assessment of an emerging technology is a multidimensional problem, different metrics have been proposed to understand the trade-offs due to adoption on a new technology. For example, carbon footprint [59] focusing on GHG reduction, water footprint [60] improving water sustainability, ecological footprint [61] providing insights into land utilization etc. Due to the multidimensional nature, there is also emphasis on using multiple footprints together for decision making [62] to include the insights about trade-offs. Systems approach such as Life cycle assessment (LCA) methodologies have been used recently to evaluate such trade-offs [63]. While cumulative energy metrics used frequently in LCA provide an overall energy assessment, these do not provide a mechanistic understanding about opportunities to further improve technologies for reducing energy consumption. As reducing energy consumption is considered a key factor in reducing GHGs [12], understanding how to reduce energy intensity of nutrient recycling technologies will be critical to select and implement the most sustainable technology for P recovery. Hence, a first principle

thermodynamic assessment such as EGA will provide required mechanistic insight into energy consumption inefficiencies.

Approaches like EGA and entropy generation minimization (EGM) [47] will also prove useful to improve the design of waste treatment systems in order to achieve the goal of clean and sustainable technologies at large scale. However there are no studies of wastewater treatment plants using advanced thermodynamic methodologies such as EGA, that present a rigorous thermodynamic assessment for design improvement. Thermodynamics will play a crucial role in assessing sustainability of technologies for creating closed loop material cycles such as in P recovery by providing insights into energy requirement for the large scale adoption of technologies. Therefore, this case study is focused on implementing an advanced thermodynamic method of EGA for performing sustainability assessment of a modeled P recovery technology. First, the EGA methodology and its advantages as metric for energy sustainability assessment of recycling technologies is described. Second, a brief review of existing P recovery technologies is presented. Finally, EGA is implemented on the modeled sequential anaerobic digestion (AD) - ion exchange (IE) system (a system where AD is sequentially followed by IE) for P recovery from waste-water is presented. Selection of IE based technology was based on studies showing that IE systems provide good trade-off between P recovery rate, energy consumption and other environmental impacts [64]. The reason for choosing EGA over exergy analysis is that the current case study considers an anaerobic digester and no exergy data is available for all the biochemical reactions that take place inside the digester. Whereas entropy changes of the biochemical reactions that take place inside the digester can be calculated from online biochemical databases as explained in the next section (3.3) and entropy changes for ion-exchange can be calculated using batch experiments. Further, EGA provides insight into the mechanistic causes behind energy losses in each of the unit operations.

3.3 Methodology

3.3.1 Entropy Generation Analysis (EGA) Methodology

EGA and exergy analysis are closely related as both originate from second law of thermodynamics and account for losses in system. EGA focuses on quantifying entropy generation (\dot{S}_{gen}), which is a “residue” needed to complete the entropy balance. \dot{S}_{gen} is directly related to exergy analysis of the system as established by the Gouy-Stodola theorem (eq 3.1). In eq 3.1, T_0 is the temperature at which the system is functioning, \dot{W}_{rev} is the theoretical work that can be performed by a system in the absence of any irreversibilities and \dot{W} is the actual work that is performed by a system. The difference between these quantities is called exergy lost which is quantified in exergy destruction methods. The methods of EGA and EGM have mostly been used for industrial designs after the work done by Bejan. These methods also allow the selection of most thermodynamically efficient technologies for scaling up from several new technologies under development [65] for waste-water treatment and nutrient recovery. Considering the strength of EGA in informing design improvements, it is utilized in current work for performing thermodynamic sustainability analysis of nutrient recovery system. EGA approach is based on first principle estimation of energy losses using mechanisms behind entropy generation, so it allows for analyzing the system for improvement opportunities by relating the design to mechanisms of losses.

$$\dot{W}_{rev} - \dot{W} = T_0 \dot{S}_{gen} \quad (3.1)$$

It is evident from eq 3.1 that \dot{S}_{gen} is directly proportional to the exergy lost. This means that same conclusions about system efficiency can be made either by calculating exergy lost or \dot{S}_{gen} . In the current study \dot{S}_{gen} calculation approach is taken and \dot{S}_{gen} calculation opens up an opportunity for system design improvement. The equation for the second law of thermodynamics is shown in eq 3.2. In eq 3.2, S is the entropy of the control volume (CV); T_i is the temperature at which the heat transfer \dot{Q}_i enters the CV, $\dot{m}s_i$ is the entropy flow into or out of the system. The second law of thermodynamics states that the \dot{S}_{gen} term in eq 3.2 is always greater than or equal to zero. It can be zero in the hypothetical case where all

the changes in the system are reversible. Hence, a goal of designing sustainable technologies for minimum energy consumption is to minimize the entropy generation in the system to achieve the goal of reduction in energy wastage.

$$\dot{S}_{gen} = \frac{dS_{CV}}{dt} - \sum_i \frac{\dot{Q}_i}{T_i} + \sum_{out} \dot{m}s_i - \sum_{in} \dot{m}s_i, \quad (3.2)$$

with $\dot{S}_{gen} \geq 0$

Eq 3.2 provides an opportunity to improve the design as all the terms on the right side of the equation can be calculated based on chemical composition information for streams, mechanisms of entropy change in the unit operations in a system and heat flow information, thus allowing to quantify the net \dot{S}_{gen} for the given system. Each term on the right hand side of the equation can be further expanded as functions of mass/ heat transfer and design characteristics for each sub-process and unit operation in the system. With the knowledge of \dot{S}_{gen} as function of mass/heat and design characteristics, it becomes possible to create an objective function to minimize the \dot{S}_{gen} for the system and provides the starting point to do EGM. However, EGM is a complex task and computationally expensive, therefore it is usually preceded by EGA to identify the sub-processes where there are opportunities for improvement. In this work, the EGA approach on P recovery technology was demonstrated to pave the way for design improvements in upcoming technologies using EGA followed by EGM.

3.3.2 Current P recovery technologies

Several P recovery technologies are available today at various stage of development. **Table 3.1** lists some of the major P recovery technologies available at industrial scale. Most of the current P recovery technologies that are used commercially implement crystallization and precipitation processes to convert the water soluble phosphate molecules (usually orthophosphates) in waste-water into solid forms such as struvite. Since, these processes require flows rich in phosphate ions and such flows are usually located after biological treatment of waste-water, crystallization and precipitation is located at the end of waste-water

treatment. There are a number of industrial scale processes that are currently deployed to recover P from waste-water. Among these nutrient recovery processes, IE technology has also been put forth as a potential method if it can be made economically competitive. The benefit of IE method involves easier operation compared to fluidized bed reactors. REM NUT is one of the process that uses ion exchange technique and allows for a simultaneous removal of ammonium ions and phosphate ions from waste-water. IE technology is already being used in municipal waste-water treatment plants (WWTP) to remove/ recover nitrogen compounds like ammonium using zeolite resins [64]. IE takes place with the help of a resin, that can be an anion exchange or a cation exchange resin, which are loaded with charged functional groups. These contain “counter ions” that are exchanged with ions that are to be separated from the effluent. Hybrid anion exchange (HAIX) resins have also been developed to separate phosphate from waste-water [66]. HAIX resins work more like adsorbent resins than IE resins. These are loaded with particles with high affinity for phosphate ions and are embedded inside a polymeric anionic resin irreversibly. HAIX do not contain any counter ions but are loaded with charges that have very high selective affinity for phosphate ions and are also able to capture phosphate ions in the presence of high background concentrations of other anions like sulfate, chloride, and bicarbonate present in waste-water [66]. The authors reported 90% recovery of P entering the system in less than 10 bed volumes. This is one the main reasons that IE was selected in this study to demonstrate application of EGA in waste recovery system, since IE improves the recovery rate.

Table 3.1. Phosphorus recovery technologies at Industrial Scale [58]

Process	Developer	Feed	Method	Final product	Influent flow P conc. (mg/l) at installed sites
AirPrex	Berliner Wasserbetriebe	Digested sludge/ sludge liquor	Crystallization	Struvite	13.7
Crystalactor®	DVH Water BV	Liquid	Crystallization	Calcium phosphate	60 - 80
Ostara Pearl™	University of British Columbia / Ostara	Liquid	Crystallization	Struvite	60 - 150
Phosnix	Unitika Ltd.	Liquid	Crystallization	Struvite	100 - 150
Seaborne	Seaborne Environmental research laboratory	Digested sludge	Acid leaching, crystallization	Struvite	600

3.3.3 EGA for Phosphorus (P) recovery from Waste Water Treatment Plant

P recovery model in the current study is a side stream process associated with a waste-water treatment plant (WWTP). A side stream process is one which runs independently

alongside the main waste-water treatment process and uses some products from the main process as its inputs. The side stream for P recovery here (**figure 3.1**) uses the sludge liquor from the secondary sedimentation stage of WWTP as the starting input material. The sludge at this stage is rich in phosphates [58]. The system boundary in this work has two unit operations: Anaerobic Digester (AD) and Ion-Exchange (IE). The role of AD is to make the P present in sludge available for recovery while IE efficiently recovers the P generating clean water at the end. In anaerobic conditions, i.e., in the absence of oxygen, the organisms present in AD reactor make the P present in biomass available in a soluble form that can be separated in the IE stage of the recovery process. For this study, it was assumed that the sludge liquor from the anaerobic digester consists only of carbon (C), nitrogen (N) and P compounds. Carbon was assumed to exist only as acetate, N as ammonium and P as orthophosphate [67].

The AD contains P accumulating organisms (PAOs) which release P as ortho-phosphate under anaerobic digestion. The phosphate and ammonium rich solution is then sent to an anion exchange column followed by a cation exchange column. Both phosphate (PO_4^{-3}) and ammonium (NH_4^{+1}) ions get selectively exchanged at anion and cation exchanger respectively. Once the ion-exchange columns are saturated with phosphate and ammonium ions, brine solution is passed through the columns to regenerate the resins. The eluate from the ion exchange columns now contain NaCl, P as phosphate ions and N as ammonium ions. To this solution, $MgCl_2$ and NaOH are added to precipitate out struvite ($MgNH_4PO_4 \cdot 6H_2O$), similar to the chemical precipitation method but this time with much more P recovered as struvite. Thermodynamics of regeneration cycle and struvite precipitation method is not studied in this work as the focus is on demonstrating the applicability of EGA method and it is difficult to assume how regeneration cycle works with our hypothetical modeled system.

To calculate the total \dot{S}_{gen} in the modeled P recovery process, **eq 3.2** is used along with the relationship of terms to the control volume (CV) of system as shown in **fig 3.2**. The current study uses a control volume approach. In this approach, the internal properties are averaged throughout the control volume (ex. average heat flow, average mass flow, etc) and local in-equilibrium is not considered. Such a type of approach is also called as black-box approach [68]. A black-box approach is taken because it is not feasible (within the scope of

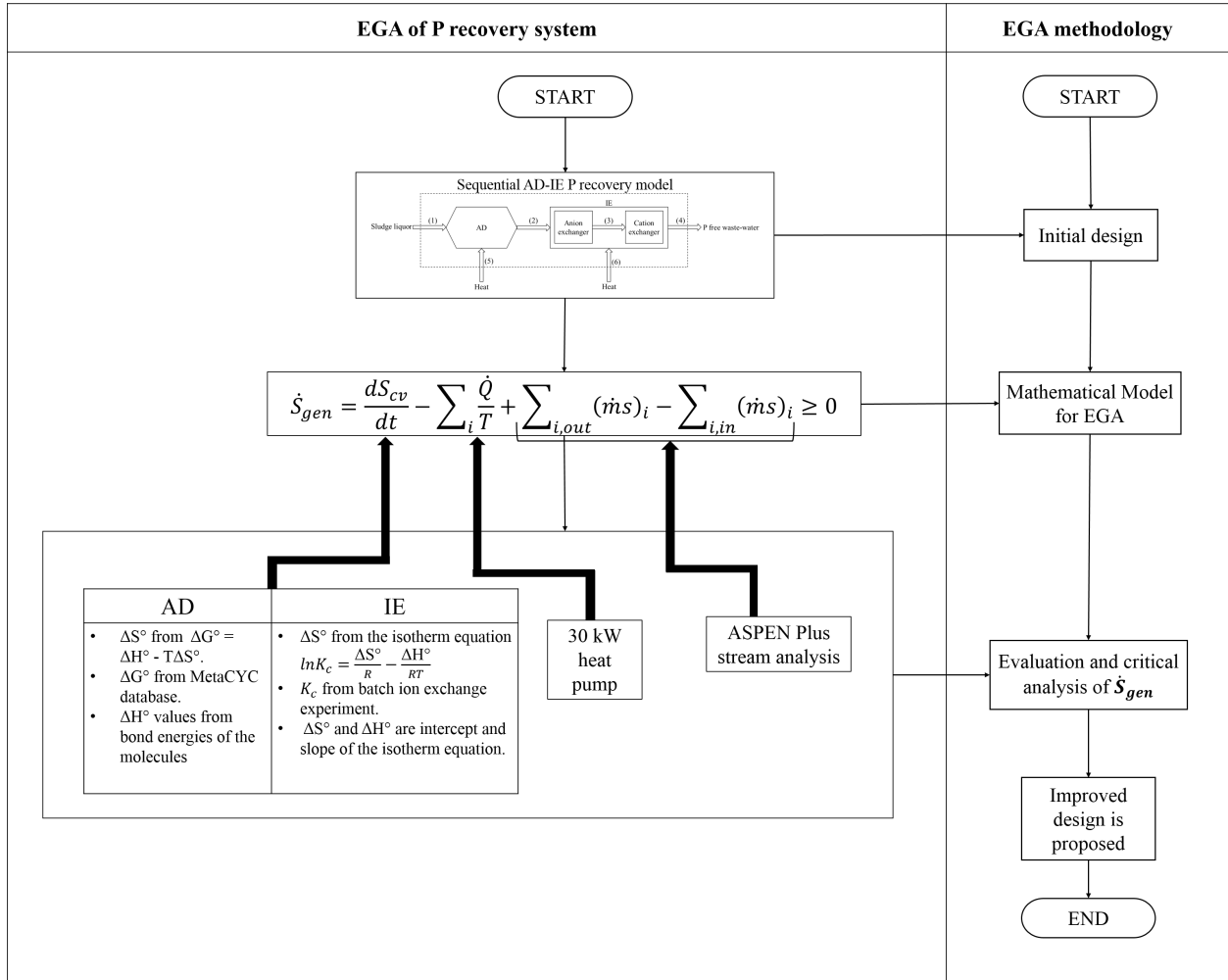


Figure 3.3. EGA of P recovery method

order to evaluate the total rate of change in entropy within the CV ($\frac{dS_{CV}}{dt}$). Results are evaluated to identify the mechanisms contributing the most to total (\dot{S}_{gen}), thus providing an opportunity for improving design to minimize (\dot{S}_{gen}). The details of calculations in each sub-system is provided in the following sections.

Entropy change calculation in Anaerobic Digester (AD)

For AD, the change in entropy of the whole CV is related to the chemical reactions that lead to change in the forms of existing chemical compounds. Since it is a black box approach and the flows are not steady during the chemical reactions, the term $\frac{dS_{CV}}{dt}$ for each unit operation is calculated as the product of the molar flow rate of the reacting species enter-

ing the unit process and the change in molar entropy (ΔS°) of the chemical reaction. The associated biochemical reactions happening in AD are shown in **table 3.2**. All the biochemical reactions inside the digester are part of a larger biological pathway called Ketogenesis [69]. The PAOs take in acetate molecules under anaerobic conditions and store them in the form of poly-hydroxy butyrate and in the process of ingesting acetate, they release P as orthophosphates. The initial and final states of CV used for calculation in anaerobic digestion are shown in **figure 3.4**. The entropy change associated with this state change is the mechanism leading to entropy change of control volume during anaerobic digestion process. Hence, calculating the contribution of these mechanisms (i.e. biochemical reactions) for total entropy generation in the system allows to identify the processes that can be optimized for reducing entropy generation.

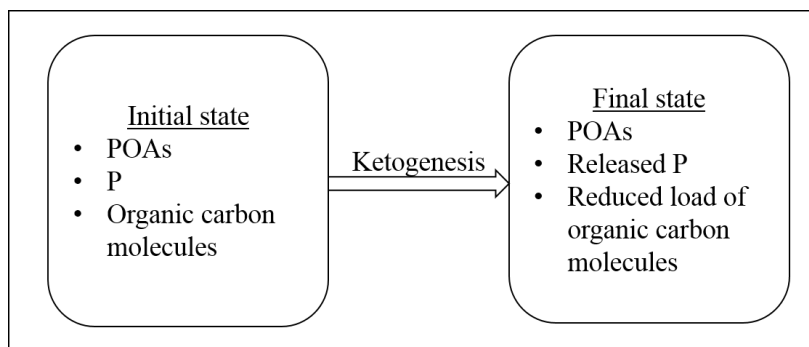


Figure 3.4. Initial and final stages of AD for calculation of Entropy Change in AD.

This entropy change for reactions was calculated with the help of the standard Gibbs energy equation, $\Delta G^\circ = \Delta H^\circ - T\Delta S^\circ$ (H-enthalpy, G-Gibbs free energy, S-entropy and T-Temperature). ΔG° values were found from the MetaCYC database [70] of biological pathways and ΔH° values were calculated based on bonds broken and formed during the reactions. Finally, ΔS° values were calculated using ΔG° , ΔH° and the temperature of 25°C [71] which was temperature of operation for AD. Other operating temperatures may lead to a different value, however the data was limited to perform calculations for other operating temperatures. Product of final value of ΔS° and molar flow rate was used as total entropy change in the control volume during the AD step.

Entropy change calculation in Ion Exchange (IE)

Similar to AD, initial and final states of the system were required to calculate total entropy change in CV associated with IE. For the IE, the initial and final states are related to the change in the form of ionic site which results in the overall entropy change of the system. In this case, the entropy change value for the cation exchange reaction was found in the literature and the entropy change of anion exchange reaction was calculated using the Langmuir isotherm **eq.(3.3)**. It relates standard entropy change ΔS° , equilibrium constant K_C , standard enthalpy change ΔH° , the universal gas constant R and the temperature T of the IE chemical reaction.

$$\ln K_C = \frac{\Delta S^\circ}{R} - \frac{\Delta H^\circ}{RT} \quad (3.3)$$

To calculate ΔS° , the unknown parameters K_C and ΔH° were found by performing batch ion exchange experiments at different temperatures using Purolite[®] MN500 (Hydrogen as counter ion) as the cation exchange resin and Purolite[®] FerrIX[™]A33E as the anion exchange resin. ΔS° was then calculated using the intercept of a linear plot of $1/T$ versus $\ln K_C$. Since, the entropy generation is dependent on the type of resin based on the isotherm characteristics, changing the type of resins can be a way of minimizing overall entropy generation for this system. The method shown here, can be used for different types of resin to understand such design changes.

Entropy Flow Rates at various streams in the P recovery system

Last two terms in **eq. 3.2** for calculation of total entropy generation in the overall system are related to flows streams. Six flow streams (see **figure 3.1**) were considered based on input and output of the unit operations. These streams are input stream to AD (ANAE-IN), output stream from AD (ANAE-OUT), input stream to anion exchanger (ANIX-IN), output stream from anion exchanger (ANIX-OUT), input to cation exchanger (CATIX-IN), and output from Cation exchanger (CATIX-OUT). To calculate the entropy of the chemical mixtures that go into each of these operations, ASPEN Plus-analysis module was used. ASPEN provides these standard relationships easily, so it used values from this

software. It was assumed that researchers interested in entropy calculation will either be able to use literature values, thermodynamic principle or will have access to standard databases such in ASPEN Plus. This allowed us to calculate the contribution of flow streams ($\dot{m}s_i$) in Equation 3.2. For entropy generation of the heat flow from the the heat pumps used to maintain temperature, a heat pump with a 30 kW capacity and an efficiency of 70% was assumed to calculate the contribution of heat source in entropy generation associated with the process.

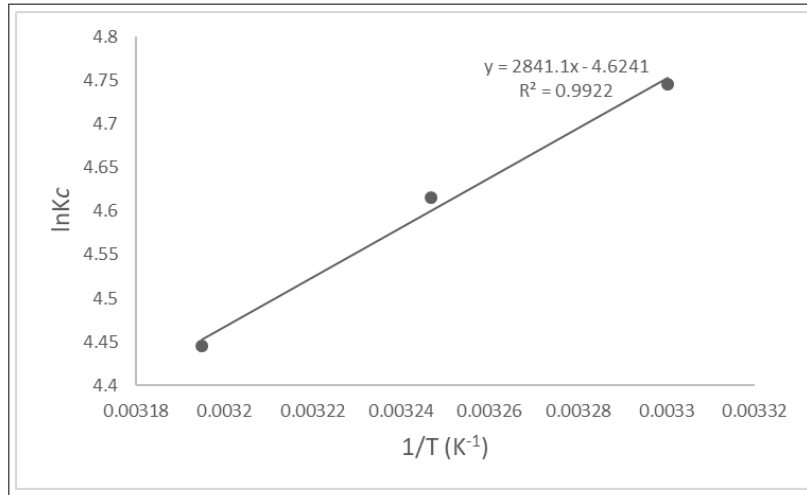
3.4 Results

Table 3.2 and figure 3.5 show the results of ΔS° calculations for AD biochemical reactions and ion exchange batch experiments respectively. Figure 3.5 is the graphical representation of the isotherm equation (eq 3.3) which is plotted from experimental values of K_c at various temperatures and the value of ΔS° is calculated from its intercept value.

Table 3.2. Biochemical reactions inside anaerobic digestion

No.	Reaction	ΔG° (kCal/mol)	ΔH° (kCal/mol)	ΔS° (kCal/mol-K)
1	Acetate + ATP + CoenzymeA \longrightarrow AcetylCoA + AMP + diphosphate	-11.19	-95.00	-0.28
2	AcetylCoA + AcetylCoA \longrightarrow AcetoacetylCoA + HCoA	7.06	4.00	-0.01
3	AcetoacetylCoA + AcetylCoA + H ₂ O \longrightarrow HMGC ₂ CoA + HCoA + H ⁺	-9.58	16.5	-0.087
4	HMGC ₂ CoA \longrightarrow Acetoacetate + AcetylCoA	-1.26	1.00	0.0076
5	Acetoacetate + NADH + H ⁺ \longrightarrow (R)-3-hydroxybutanoate	3.38	-82	-0.28

Table 3.3 shows \dot{S}_{gen} for the complete side stream process of P removal studied in this work. Since, the process requires a steady temperature of (25°C), the heat pump was continuously removing heat from the CV, thus leading to heat flow out from the system (-70.13 kJ/K-hr). At the given removal efficiency of the IE resins, the total \dot{S}_{gen} is 149.03 KJ/K-hr. As can be seen, the entropy change in AD is -ve which indicates a favorable process as contribution to entropy generation is negative. This is mainly because the organisms utilize the embodied energy of the waste organic compound for energy. Similarly, it can be seen that both anion exchange and cation exchange have -ve contribution to the entropy generation rate of the system which is because the ion-exchange process is driven by chemical potential and both reactions occur with a negative entropy change. There is a gradual reduction of



K_c as a function of temperature, See eq. (3.3)

Figure 3.5. Experimental Calibration Curve to calculate of ΔH° and ΔS° for Anion Exchange Unit

entropy of flow streams, the input stream has 43.84 KJ/K-hr while the final output stream from cation exchange is only 1.93 KJ/K-hr which can be attributed to relatively pure stream of water leaving the system and high retention of PO_4^{-3} and NH_4^{+1} in IE system which can be recovered with the regeneration cycle not studied here. Another important factor not discussed in the study is the cost and maintenance of ion exchange resins. Studies have shown that their maintenance can be costly at times [72], which will be focus of future study when full life cycle of the system maintenance can be included. From this analysis, it was concluded that the system can be made more efficient by improving the heat exchange system as it contributes the most to the total \dot{S}_{gen} . If the improvement in micro-organisms allow the biochemical reactions to operate at same efficiency but without the requirement of maintaining temperature at 25°C, it may reduce the requirement of heat removal, thus lowering the entropy generation. This is obvious from an energy sustainability perspective, however the method allows a quantification of how much reduction can be made when the technology is adopted at large scale.

Although EGM is not performed in this study, EGA followed by EGM will accomplish the task of design optimization. By using the \dot{S}_{gen} calculated for the P recovery system as the starting value, the right hand side of eq 3.2 can now be treated as an objective function for \dot{S}_{gen} minimization. The optimization can then be done utilizing various design variables

Table 3.3. Entropy generation at each operation of the P recovery process

Operation	$\frac{dS_{CV}}{dt}$ (kJ/K-hr)	$\sum \frac{Q}{T}$ (kJ/K-hr)	$\sum_{out} \dot{n}s$ (kJ/K-hr)	$\sum_{in} \dot{n}s$ (kJ/K-hr)	$\dot{S}_{gen} = \frac{dS_{CV}}{dt} - \sum \frac{Q}{T} + \sum_{out} \dot{n}s - \sum_{in} \dot{n}s$ (kJ/K-hr)
Anaerobic digestion	-17.00	-70.13	38.63	43.84	47.92
Anion Exchange	-0.15	-70.13	34.64	38.63	65.99
Cation Exchange	-2.30	-70.13	1.93	34.64	35.12
				Total	=149.03

that determine the overall design of P recovery the system. At the end of optimization, these variables are assigned new values given by the optimization algorithm which in turn effect the overall design of the system. A system design based on these optimized design parameters will be thermodynamically more efficient (reduced \dot{S}_{gen}) compared to the one optimization process was started with. Since, the quantification of entropy generation here is based on mechanistic approach, the values can easily be scaled up as the flow rates and hour of operation changes.

3.5 Conclusion

Second law based analyses are seldom performed on nutrient recovery systems involving different unit operations. In the current study, a second law based thermodynamic analysis was performed on a modeled side stream P recovery system. EGA is proposed to be a viable approach for comparison and selection of most sustainable nutrient recovery technology. The application of EGA on systems involving biological operations such as anaerobic digestion and chemical operations such as ion exchange was demonstrated. By performing EGA, critical inefficiencies in a system can be identified and these sub-processes can be improved or modified to improve the overall performance of the system. In the analysis presented here, the maximum entropy generation is related to the temperature maintenance of the system at 25°C which is related to the exothermic chemical reactions in both ketogenesis cycle and the ion-exchange process. If the design of these systems can be modified to improve heat dissipation there would be less energy requirement to maintain the desired isothermal conditions. Hence, with the additional insights of causal factors in the entropy generation found in this study, future studies can now utilize the mass/ heat transfer and design characteristics of targeted unit operation, to create an objective function to minimize

the total entropy generation rate for the complete process. This will involve identifying the role of mechanisms of flow patterns, mixing and reactor/column design for heat dissipation. The variables for optimization may come from the design characteristics of the heat exchanger used to maintain the temperature, from the parameters that go into selection of the reactor type used for anaerobic digestion and also from the type of ion exchange columns used in the ion exchange stage to selectively remove phosphate anions and ammonium cations. Optimizations such as these usually have a lot of variables and performing an analytic optimization is often difficult. Hence, optimizations that employ methods like evolutionary algorithms can be used. Therefore, this work concludes that EGA and EGM can give new insights into how designers can improve the performance of technologies for sustainable energy consumption before large scale adoption. EGA is suggested as a complementary first step to study thermodynamic sustainability of emerging technologies in conjunction with other metrics that have been widely used so far. An EGA based comparative study can also help in determining which of the systems studied have the highest potential for improvement and can be targeted for performing an EGM [73]. The formulations that come from performing an EGA can be applied to several different systems performing similar functions (in the current case, P recovery) and the relative significance of \dot{S}_{gen} from different sources among the systems under study can be discussed for performing a comparative study.

In terms of technology, the study here led to a conclusion that AD-IE systems can be a viable and sustainable technology with very less energy requirement if heat requirement can be reduced by design optimization as per our preliminary analysis. However, optimizing energy consumption during operations (which is a long term impact for technology adoption) needs to be complemented with a life cycle analysis (LCA) approach to include the upstream energy requirements to build the system, prepare resin etc, which will be part of a future study. In conclusion, EGA and EGM provide a very promising approach for design and optimization of waste recovery technologies before adoption at large scale to avoid the unintended consequence of increased energy demand. This will help to meet both resource and energy sustainability goals.

4. MAPPING ECONOMY-WIDE MATERIAL FLOWS USING MECHANISTIC, BOTTOM-UP PHYSICAL SUPPLY USE TABLES AND PHYSICAL INPUT OUTPUT TABLES

4.1 Chapter overview

The previous chapters (ch-2 & ch-3) established how bottom-up computational approaches can be used to quantify material flows for a specific region and thermodynamic flows in the absence of empirical data to perform sustainability assessment related to material and energy flows. This chapter focuses on scaling these established approaches to quantify flows at an economy level consisting of different sectors, thus achieving high sectoral resolution to perform sustainability assessments. Since the established bottom-up computational methods used in the previous chapters are reproducible spatially, temporally, and sectorally, these were employed to quantify material flows, across multiple economic sectors in a region. This chapter attempts to increase the scope of mechanistic bottom-up approaches from quantifying material flows in a single production technology to modeling detailed and accurate regional physical economies. Such an approach can finally overcome the challenges of both allocation in top-down approaches and linear flow scaling in empirical bottom-up approaches. To show how the mechanistic bottom-up approaches presented in this work can be used to model physical economies, a case study of agro-based economy of Illinois, USA is used. Different material flows of industries in the agro-based economy of Illinois are simulated and quantified using the methods discussed so far. The accounted flows are then used in conjunction with the Input-Output (IO) theory to account for the material flow interactions between industries and develop a physical economy model within the IO framework. The physical economy model was then used to implement system scale circular economy strategies in the agro-based economy modeled. In this chapter, before demonstrating the case study, a general methodology is presented first to establish a standardized approach for using bottom up approach to map regional physical economy using Physical Input-Output Tables (PIOTs) and then an approach to use the developed tables for circular economy strategies is given. Standardization of approach will contribute to reproducibility of results, thus contributing

to confidence in these systems scale transition strategies and can be used for wide range of studies by the research community.

4.2 Motivation and background

IO methods [74] have provided a robust framework for research in Industrial Ecology (IE) to map industrial and economic sector interconnections at multiple scales ranging from state [75] [76] [77], national [78] [79], and global scale [80] [81] [82]. The mapping of interconnections through input output theory makes it possible to study cascading impacts in economy due to change(s) in one sector(s) or industry along with evaluating total environmental impacts using the environmentally extended Input-Output (EEIO) approach. One such IO based modeling technique is Physical Input-Output Tables (PIOTs), which provides a comprehensive accounting framework for tracking material flows from one economic sector to another and to the final end users. By doing so, PIOTs can help perform detailed Economy Wide Material Flow Accounting (EW-MFA) which plays an important role in evaluating and improving our resource use efficiency. PIOTs record all the transactions in physical units, thus it also considers the flows such as emissions and wastes which are not reported in construction of purely monetary input output tables (MIOTs), but added in enhanced EEIO models.

As PIOTs can help track commodities used, produced, emissions and waste flows for each sector, it provides a framework to map all the material flows in an economic region and provide a physical economy model for the region being studied [83]. Moreover, PIOTs are compatible with national accounts of economic flows and can be used in conjunction with national level Material Flow Accounts (MFAs). Some of the PIOTs applications include understanding the physical metabolism and structure of an economy [84], water energy nexus at regional city levels [85], tracking elemental flows across a regional physical economy [75], and modeling solid waste recycling scenarios [86]. However, the true potential of PIOTs and their applications can be realized only if material flows are accounted at highly disaggregated economic sectors level. PIOTs developed using aggregated flows only provide minor improvements to conventional MFAs by allocating all the material flows in the economy to a few highly aggregated sectors. This aggregation gives rise to complications such as sector

aggregation bias during material flow allocation. The aggregation bias was demonstrated in a recent study using EEIO by highlighting overestimation of raw-materials requirement in an analysis using aggregated biomass sector [87]. Despite the known benefits of PIOTs, their development in a timely fashion for different regions of the world has been very slow. This has limited the use of PIOTs in solving relevant problems in IE such as material tracking over multiple years or at highly disaggregated regional scale. Specifically, sub-national level tracking of materials flows using PIOTs is very rare except for a few studies that only track one or a few type of materials [75] [76][85]. This is mainly because developing PIOTs at highly disaggregated economic sectors at regional levels has always been very challenging [83]. The primary hurdles to build disaggregated PIOTs include reliable data unavailability, data heterogeneity, validation, and continuity of data collection for long term updating. Additionally, compiling the regional data in the PIOT framework itself is very tedious even for a moderate size economic region [75]. Therefore, there is a critical need to improve the methodologies and tools for development of PIOTs at desired disaggregation level. This chapter aims at addressing these research gaps using mechanistic and bottom-up models to simulate material transformation processes across different industries in a region and use the material flow information extracted from them to model physical economies.

The chapter is organized as follows: section 4.3.1 details how mechanistic and bottom-up approaches can be used develop engineering models (EMs) that can simulate material flows associated with various economic sectors in a region, section 4.3.2 provides details on how the material flow information from the models can be used to construct the physical economy model in the form of Physical Supply Use Tables (PSUTs) and PIOTs. Finally, section 4.4 describes the application of the methodology using a case study to identify system scale circular economy transition strategies for the agro-based physical economy model of Illinois, USA.

4.3 Methodology

Computational models called “Engineering models” (EMs) form the core of the methodology presented in this chapter. EMs are scaled mechanistic models that mimic the material transformation processes in various economic sectors of a given region. They are based on

fundamental mass balance and physics based equations that mechanistically simulate production of various commodities and wastes without relying on any empirical data related to outputs of an economic sector during the modeling process. Empirical data were used only to validate the developed models. Once EMs were developed and validated for a specific production process, material flow information from them was used in construction of the physical economy model for the given region. The EM development process consists of three stages: identifying the economic sectors to be modeled, using physics based mechanistic approaches to model material transformation processes taking place in the identified economic sector, and to scale the developed EM to represent material flows of the region being studied. These three development stages are described in detail in the subsections below.

4.3.1 EM development process

Identifying economic sectors

The North American Industry Classification System (NAICS) [88] of economic sector classification was used to identify economic sectors. Specifically, all economic sectors were tagged with a 6-digit NAICS code, which is the most detailed economic sector classification system available in the NAICS (more the no of digits in the code, more detailed the classification is). The most detailed sector classification was selected to ensure the EMs developed accurately represent the production technology of economic sectors. As the level of economic sector aggregation goes higher, the underlying model of production technologies get more unrealistic and only represent an averaged material transformation process for all the sub-sectors in the aggregated sector. By selecting 6-digit level of disaggregation, the economic sectors can not only be well represented by EMs but can always be aggregated (by combining multiple EMs) to higher levels of classification if required.

Modeling the material transformation processes

A single EM type cannot be used to model the flows for all industries in the economy as the underlying material transformation processes are different for different industries. For example, agricultural industries involve growth of various biomass such as crops and

livestock, whereas chemical industries involve chemically transforming materials from one form to another, while a metal forming industry involves operations such as welding and machining. Hence, several types or categories of EMs will be needed to capture physical flows reliably for different sectors to capture all material flows. While the number of EM categories needed depends on the variations in production technologies of economic sectors being modeled, in this study three categories of EMs were used based on the scope and variations in production technologies of the economic sectors considered in the case study. All the industries that involve growing biomass were categorized as “Biomass” type and all the industries involving chemical transformation were categorized as “Process” type. Industries that do not perform any material transformation, but use joining/separating techniques such as in assembly were categorized as “operations” type. After categorizing the sectors by EM type needed, EM were developed using appropriate computational tools such as Python/Matlab code for biomass growth, ASPEN/ChemCad (process modeling software) models for process type and Python based model to simulate operations.

Scaling EMs to represent flows in the economy

After selecting the economic sectors to be modeled and developing the EMs using appropriate computational techniques, the EMs are scaled for a selected region, to accurately represent the material flows in the sector for a particular year using either input side or output side data. This scaling could be nonlinear (unlike LCA or similar approaches that always scale models linearly) based on the underlying mechanistic approach used to model material transformation. A typical EM is shown in **figure 4.1** along with possible scaling variables that can be used (**table 4.1**).

Table 4.1. Typical flows available as scaling variables in an EM

Model material flow feature	Type
Raw material	Input
Intermediate input	Input
Intermediate output	Output
Commodity production	Output
Waste and emissions	Output

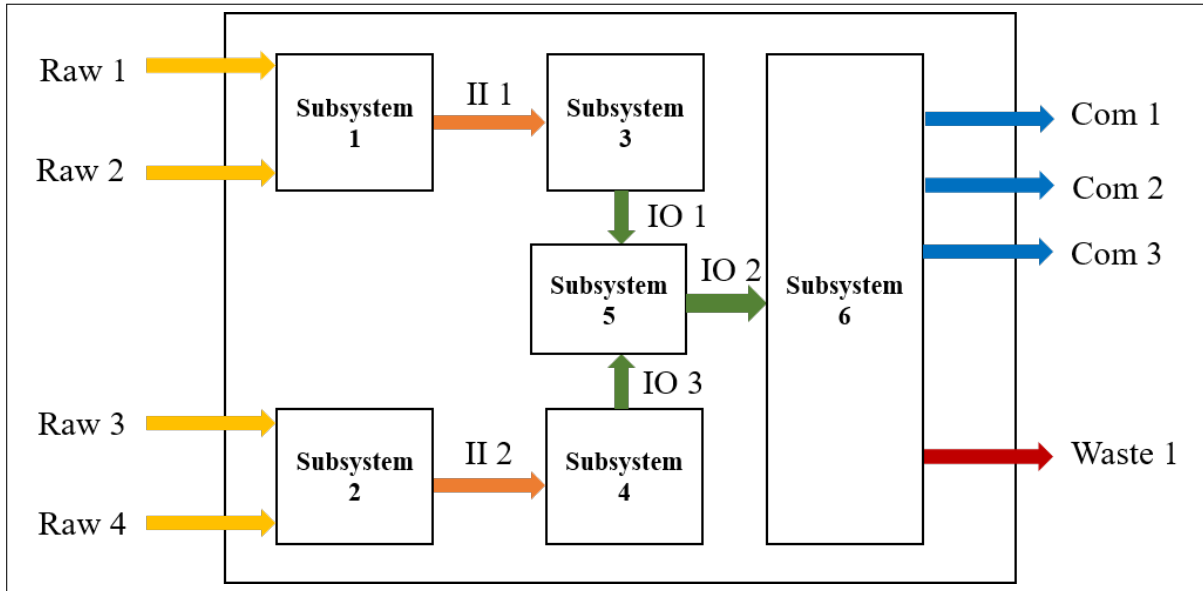


Figure 4.1. A typical engineering model (EM)

Raw: Raw materials, II: Intermediate Input, IO: Intermediate Output, Com: Commodity

The flows Raw 1 through Raw 4 are the raw material inputs to the model, II1 and II2 are intermediate inputs to the subsystems in the model, IO1 through IO3 are intermediate outputs from subsystems in the model, Com 1 through Com 3 are the commodity outputs of the model, and Waste 1 is the waste flow from the model. Since EMs are mechanistic in nature, each of these flows can be used for scaling an EM, which will scale all the flows to follow the mass balance and material transformation constraints. These constraints are inbuilt in the EMs and can be enhanced when additional knowledge about the technology or transformation of material flows in a sector becomes available. The scaling data can be highly heterogeneous and certain assumptions could be needed when required. For example, consider an EM modeled for the soybean processing industry. A mass-based allocation assumption is required to assign the reported soybean production in a region to different industries that consume soybeans. Such information may not be available in any standard data-sets and requires industry specific data available in a region (ex: soy bean association in Illinois, USA. [89]). Wherever possible, standard scaling data sets from sources such as USDA [90], USGS [91], and USEIA [38] which provide county/state level information were used to maintain the reproducibility of the approach to other regions in the US. In **table**

4.1, two types of flows are shown that can be used for scaling – input and output. The input side scaling is simpler than output side scaling. Whenever input scaling data in the form of commodity consumption (as raw material or intermediate input) was available, the material flow input data for all possible input commodities was used to scale EMs. Since EMs are based on underlying production or operation methodology, it scales as defined by the method encoded into it. Input side data can be usually obtained from state level commodities information which are either published by local public agencies or industry associations. In some cases, university extension offices and not-profit organizations also release regional data, especially for primary sector industries like agriculture. For example, going back to the soybean processing example, the input side scaling data could be the total quantity of soybeans crushed in a region provided by agricultural department statistics or state soybean industry association.

If only the commodity production data was available (output scaling), it is not as straightforward as using the input side commodity consumption data. This is due to the inherent “input driven” nature of the EMs. The encoded methods used to build EMs rely on a series of input data (material flow in this study) which is further used as input parameters in multiple simulating functions defined in source code of EMs. Therefore, EMs usually are run in forward direction, i.e. generating outputs for given inputs. Thus, it is not feasible to simulate these models backwards, i.e., provide outputs and return inputs which makes it a “one-way process”. In order to sidestep this ‘one-way process’, in our approach, the EMs were run using multiple input estimates till the outputs of the model match the available commodity production data for scaling. Since this could involve trying with a large set of inputs, the process is automated for testing different range of inputs. The EMs are given a range of inputs as an automated program using which EMs simulate the model for each input given and return a series of outputs. The input flow range can be estimated approximately using the order of the output number (ex: 10^6 or 10^8 kg) and using mass balances and stoichiometry information from the documented process methodology used for the engineering model. Although it is challenging to deduce the inputs based on multiple simulations till desired output is matched, it is a one-time process for each sector being scaled and automation provides faster search of valid inputs that follows the mass balances. Finally, once the

models are scaled, they are validated on a case-by-case basis as demonstrated in the case study.

While validating scaled EMs, it is important to validate both inputs and outputs of an EM. A highly accurate validation of material outputs of an EM could be of no use if the input side validation is not accurate (a model can be realistic only when both inputs and outputs are accurate). While developing EMs, care has to be taken to make sure that each material flow (input or output) associated with an EM should be realistically close to the material flow information available in validation data. The data used for scaling, in most cases, can also be used for validating the model. For example, if regional level material flow information is available for inputs and outputs of a particular industry for which an EM was modeled, the input information can be used to scale the model and the output information can be used to validate the model. Since the EMs are mechanistic in nature, if they are correctly modeled and scaled, their outputs should be close to the output material flow information available. If both inputs and outputs are not available, then a decision must be made about how to use the only available input/output data. If any missing information can be approximately deduced, it can be used in either scaling or validation based on a case by case basis.

4.3.2 Converting data from EMs into PSUTs and PIOTs

After modeling, scaling, and validating the developed EMs, the input and output material flow information from them can then be used to construct PSUTs and PIOTs. Based on the EM developed, different material flow information can be arranged to occupy various placeholders such as natural inputs, commodities, and wastes in a PSUT as shown in **table 4.2**. The description of the variables used is provided in **table 4.3**.

After populating all the variables in both the **table 4.2**, they are then converted into an industry by industry PIOT using an adaptation of the conversion model D described in Eurostat manual (Fixed product consumption structure assumption where each product has its own consumption/sales patterns, irrespective of where it is produced) [20]. The adapted conversion is described here using the equations **eq 4.1** through **eq 4.3**. First a transformation matrix \mathbf{T} (industry by commodity matrix) is defined (**eq 4.1**) which will be

Table 4.2. Structure of Physical Supply Table (PST) and Physical Use Table (PUT)

Supply	Case Study Industries	Imports	–	Total
Natural inputs	–	–	–	–
Commodities	SC	IC	–	TSC
Waste flows	SW	–	–	–
Use	Case Study Industries	Exports	Final demand	Total
Natural inputs	UN	–	–	–
Commodities	UC	EC	FC	TUC
Waste flows	–	–	–	–

Table 4.3. Description of variable used in PSUTs

Variable notation	Variable type	Variable detail
SC	Matrix	Commodity by industry supply
SW	Matrix	Waste flows by Industry supply
IC	Column vector	Import of commodities
UN	Matrix	Natural resource flows by Industry use
UC	Matrix	Commodity by industry use
FC	Column vector	Final demand of commodity
EC	Column vector	Export of commodities

All the variables starting with “T” represent column or row sums and are column/row vectors

used to multiply and transform all the asymmetric matrices in the PSUT into a symmetric PIOT. \mathbf{T} matrix can be interpreted as the record of the contribution of each industry to the supply of each commodity. The calculated \mathbf{Z} and FD matrices can then be used to construct a PIOT as shown in **table 4.4**.

$$\mathbf{T} = \mathbf{SC}^T \cdot \text{diag}(TSC)^{-1} \quad (4.1)$$

The asymmetric \mathbf{UC} and \mathbf{FC} can then be transformed into symmetric industry by industry intermediate demand matrix \mathbf{Z} and final demand FD matrices respectively by multiplying them with the \mathbf{T} matrix (**eq 4.2 and 4.3**).

$$\mathbf{Z} = \mathbf{T} \cdot \mathbf{UC} \quad (4.2)$$

$$FD = \mathbf{T} \cdot FC \quad (4.3)$$

Table 4.4. PIOT constructed from the developed PSUTs (Z: intermediate demand, FD: Final demand, TI: Total of industry)

PIOT	Industries	Final demand	Waste flows	Total
Industries	Z	FD	$(TSW)^T$	TI
Natural resources	TUN	–	–	–
Total	TI	–	–	–

The **tables 4.2** and **4.4** can now quantitatively represent the physical economy of a region. In the next section (4.4), a case study to model the physical agro-based economy of Illinois is presented which follows the same template of methodology described in this section. The resulting tables may be unbalanced as not all the available physical commodities are included in the developed EMs. The imbalances can be handled by using external data such as trade, imports/exports, and consumer final demand. Since the entire process of extracting material flow information from the simulated EMs, constructing PSUTs and then transforming them into PIOTs can become very tedious and time consuming (especially when multiple EM types are involved), a Python based automated tool called Material Flow Data Extractor and Simulator (MFDES) was developed that can drastically reduce the time and effort to construct PSUTs/PIOTs from any number of developed EMs (presented in the next chapter 5).

It has to be noted that while PSUTs provide highly detailed and useful information at a specific commodity level, only PIOTs can quantify inter-industry dependencies. Further, since PIOTs are symmetric matrices, they can be used to perform standard IO analysis using Leontief’s inverse matrix \mathbf{L} (eq 4.4) [74]. In eq 4.4, \mathbf{A} is called the technical coefficient matrix which is derived using information from the \mathbf{Z} matrix and the FD column vector. The \mathbf{L} matrix can be used to calculate the changes in economic throughput of all industries being studied with respect to final demand changes of specific industries by the end user.

Further, as seen in **table 4.4**, PIOTs can also capture the dependencies of various industries on natural resources.

$$\mathbf{L} = (\mathbf{I} - \mathbf{A})^{-1} \quad (4.4)$$

In **eq 4.4**, each element of the technical coefficient matrix \mathbf{A} is calculated using **eq 4.5**. Where $z_{i,j}$ represents each element of \mathbf{Z} matrix and X_j represents each element of the column sum vector TI (see **table 4.4**)

$$a_{i,j} = z_{i,j}/X_j \quad (4.5)$$

$$\Delta\mathbf{X} = \mathbf{L} \cdot \Delta\mathbf{FD} \quad (4.6)$$

4.4 Case study

Illinois is one of the major agricultural state in the US producing some of the highest percentages corn and soybean grains in the country [37]. It also houses a big biofuel industry based on corn and soybean [92]. This case study section attempts to capture a highly detailed physical economy model for the major economic sectors that constitute this agro-based economy in Illinois. To this regard, the physical economy model was developed using the methodology discussed in the previous section (4.2).

4.4.1 EMs for agro-based economy of Illinois

The major agro-based sectors in Illinois were first identified and tagged with a 6-digit NAICS code as shown in **table 4.5** and the EM type was given to each sector based on the type of material transformation processes. The different computational techniques used to develop the EMs in **table 4.5** and their validation is discussed in the following subsections.

Modeling field crops

Field crops (EMs 1-5 in **table 4.5**) were modeled using Python Crop Simulation Environment (PCSE) PCSE is a Python package for building crop simulation models [93]. PCSE

Table 4.5. The agro-based sectors modeled in Illinois, USA

EM No	Sector name	NAICS code	EM type
1	Soybean farming	111110	Plant growth model – Python
2	Bean farming	111130	Plant growth model – Python
3	Wheat farming	111140	Plant growth model – Python
4	Corn farming	111150	Plant growth model – Python
5	Potato farming	111211	Plant growth model – Python
6	Hog farming	112210	Animal growth model – Python
7	Urea manufacturing	325311	Chemical process model – Aspen plus
8	Soybean crushing	311224	Chemical process model – Aspen plus
9	Soybean biodiesel	324199	Chemical process model – Aspen plus
10	Corn alcohol manufacturing	325193	Chemical process model – Aspen plus
11	Ammonia manufacturing	325311	Chemical process model – Aspen plus

provides the environment to implement crop simulation models which give crop yield information and much more. Since only the crop yield data was used in this study, other outputs such as plant phenology, respiration and evapotranspiration parameters that PCSE models produce are not discussed. The PCSE simulation engine produces outputs for daily time steps and requires four primary inputs:

1. Weather data: The PCSE NASA weather data provider Python module was used to collect weather data. The historical weather data for a location can be accessed by using the latitude and longitude values in the Python module.
2. Model parameters: Three model parameters - crop, soil and site parameters are encapsulated as a single parameter which is used by the PCSE simulation engine to set the characteristics of the crop being modeled. An example parameter is the atmospheric CO₂ concentration at the crop site.
3. Agromanagement information: This includes all the schedule of all the farming activities such as date of sowing, date of harvesting, amounts of fertilizer and water applied.
4. Configuration file: This file specifies what components should the simulation engine use and store as final and intermediate output.

For each of the four inputs, PCSE provides a range of data provider options. For example, NASA power API [94] was used in this study as the primary weather data provider. However, PCSE supports other data providers such as excel files containing weather data. Complete information on all the data providers are available at the PCSE documentation website [95]. PCSE reports the crop yield in terms of mass per unit area (kg per hectare). This yield data was multiplied with the field crop area cultivated from USDA [37] to get the total crop yield for each field crop modeled in Illinois.

Modeling animal farming sectors

Animal farming sectors (EM No. 6 in **table 4.5**) were modeled using custom Python programs that were built to simulate the animal farming practices for the state of Illinois, USA. The models built were based on animal biomass growth rate, feed consumption, and overall mass balance equations. The animal farming models take 3 primary inputs:

1. Feed composition: Since different farm animals have different nutrition requirements, the models consider the feed composition (ex: 60% soymeal, 20% DDGS and 20% corn) as an input.
2. Feed intake: The amount of feed that each farm animal intakes.
3. Model parameters: These parameters include details on the exact animal type, farm age distribution, and average daily mass gain rates for each age group.

The three types of input information were obtained for each of the animal farming model from sources such as USDA NASS [37].

Biomass processing and chemical manufacturing sectors

The sectors with conventional chemical processing (EMs 7-11 in **table 4.5**) were modeled using Aspen Plus process modeling software. Aspen Plus is an industry standard software for developing process models for various chemical processes in chemical manufacturing industries. A typical process model developed using Aspen plus involves rigorous application of mass and thermodynamic first principles that determine how different chemicals are

transformed from one form to another. Process modeling allows the development of highly accurate process models when all the relevant modeling data is available. For example, if the chemical reaction kinetics are known for each reaction taking place in the soybean oil to biodiesel conversion process, an EM can be developed that takes in soybean oil input data and accurately calculates the amount of biodiesel produced. However, information such as chemical kinetics may not be available for all processes being modeled. In such cases, pure mass balance and stoichiometric equations can also be used to specify the exact amounts of input being transformed into an output. This becomes highly useful when dealing with nonconventional chemical material flows such as animal feed, soybean, and corn meal, etc. Once a process model was developed for an industry in Aspen Plus, it was scaled to match the material flows of the representing industry in Illinois.

4.4.2 Validating EMs developed for Illinois agro-based economy

The scaling variables and variable used for validation for each EM is shown in **table 4.6**. As seen in the table, the scaling and validation data is highly heterogeneous as it is challenging to find a single Illinois regional level material flow information for all the sectors being modeled. However, similar type of scaling datasets were available for models developed using similar modeling methods. For example, for all the farming sectors modeled, fertilizer and area fertilized was available from the USDA NASS online tool [37]. These crop farming models were then validated using the crop yield data again from the USDA NASS. Standard datasets from agencies such as USDA NASS and Energy Information Agency [92] were used wherever possible to make the scaling and validation methodology as reproducible as possible for other regions too.

4.4.3 Reproducibility of EMs and their applications to other regions

The development process of the EMs ensured that they can be reproducible to other regions. While the underlying mechanistic processes of EMs are industry or production recipe specific, their scaling is completely controlled by the EM developers to make EMs representative of the regional industry being modeled. Two types of standardized scaling

Table 4.6. Scaling and validation data used for each model along with error of scaling

NAICS Code	Sector name	Scaling variables	Output variables	Model value	Unit	Validation notes
111110.0	Soybean farming	Fertilizers used	Soybean yield	5.74E+01	bu/ac	State level USDA data - total production
111130.0	Bean farming	Fertilizers used	Bean yield	1.18E+08	kg	State level USDA data - total production
111140.0	Wheat farming	Fertilizers used	Wheat yield	8.03E+01	bu/ac	State level USDA data - total production
111150.0	Corn farming	Fertilizers used	Corn yield	1.72E+02	bu/ac	State level USDA data - total production
111211.0	Potato farming	Fertilizers used	Potato yield	9.12E+03	kg/ha	State level USDA data - total production
112210.0	Hog farming	Feed consumed	Hog mass	1.23E+09	lb	USDA data - total slaughtered hog mass
325311.0	Urea manufacturing	Ammonia used	Urea produced	4.99E+05	tonne	Urea industry in very small in Illinois
311224.0	Soybean crushing	Soybeans crushed	Soybean oil	1.55E+06	tonne	USDA AMS dataset
-	-	-	Soybean meal	3.13E+06	tonne	-
324199.0	Soybean biodiesel	Soybean oil used	Soybean biodiesel	1.53E+02	Mgal	US EIA data
325193.0	Ethyl alcohol manufacturing	Corn crushed	Ethanol produced	1.75E+03	Mgal	US EIA data
325311.0	Ammonia manufacturing	Natural gas consumed	Ammonia produced	5.24E+05	tonne	Average of national data to Illinois

were employed in this chapter. For the PCSE models, regionally specific data such as weather and fertilizer management are fed to the models independent of the main mechanistic process code block/program file. Such auxiliary scaling/region specific information were stored in “.yaml” files. Yaml files are human readable programs with very minimal syntax. An example of yaml file code block containing scaling information for soybean farming in Illinois is shown in appendix (A.1). The information in yaml files can be changed accordingly to make the EM representative of another regions. For Aspen Plus models models, since manipulating different models through the Aspen Plus software can be time taking, models were accessed remotely through a Python code that can scale specific flows in an EM to make it representative of a given region. The example code to access the soybean oil production Aspen Plus model remotely to scale flows is shown in appendix (A.2). Further, standard Aspen plus methods such as NRTL (Non-Random Two-Liquid), Ideal, and Redlich-Kwong-Soave were used during EM development to ensure that EMs can be easily used by other researchers familiar with process modeling techniques. The property methods used for the EMs in this study are shown in appendix (table A.1)

4.4.4 Constructing the physical economy model

After validating all the EMs for the agro-based sectors developed, the material flow information was extracted from them to construct PSUTs. The various material inputs and outputs of each EM were tabulated as individual columns following the structure shown in table 4.2. While this process of extraction can be done manually, an automated tool (chapter 5) was used to reduce the time and effort in constructing the tables. The PSUTs constructed for the agro-based economy of Illinois are shown in tables 4.7 and 4.8. A heatmap version of the tables is provided in figure 4.2 for a better qualitative understanding. In order to handle imbalances, a closed economy was assumed and all the imbalances were assigned to a “Rest of Economy” (ROE) sectors. Each of these tables quantify material flows in the form of commodities and waste being supplied or used by the industries modeled. Since the EMs developed are bottom-up and mechanistic in nature, information such as any available elemental chemical composition of different flows is retained throughout the process.

This means that the granularity can be taken a step further by constructing elemental PSUTs. The heatmaps of carbon PSUTs are shown in **figures 4.3**.

Table 4.8. Physical use table constructed for the agro-based Illinois economy from the EMs developed. Units: tons/oper-year
 (.csv file available in the supplementary material)

Commodity	ammonia_production	dry_corn_milling	soy_diesel	soy_oil	Beam_farm	Corn_farm	Potato_farm	Soybean_farm	Wheat_farm	Urea_manufacturing	Hog_farming	RoE
AIR	0.00E+00	0.00E+00	0.00E+00	1.10E+01	0.00E+00	0.00E+00	0.00E+00	0.00E+00	0.00E+00	0.00E+00	0.00E+00	0.00E+00
AIR_MIX_01	7.11E+03	0.00E+00	0.00E+00	0.00E+00	0.00E+00	0.00E+00	0.00E+00	0.00E+00	0.00E+00	0.00E+00	0.00E+00	0.00E+00
AIR_MIX_02	2.89E+06	0.00E+00	0.00E+00	0.00E+00	0.00E+00	0.00E+00	0.00E+00	0.00E+00	0.00E+00	0.00E+00	0.00E+00	0.00E+00
AMMONIA_LIQ_99PCT	0.00E+00	0.00E+00	0.00E+00	0.00E+00	0.00E+00	0.00E+00	0.00E+00	0.00E+00	0.00E+00	2.33E+05	0.00E+00	2.87E+05
AMMONIA_VAP_MIX_01	0.00E+00	0.00E+00	0.00E+00	0.00E+00	0.00E+00	0.00E+00	0.00E+00	0.00E+00	0.00E+00	0.00E+00	0.00E+00	2.36E+03
CO2	0.00E+00	0.00E+00	0.00E+00	0.00E+00	0.00E+00	0.00E+00	0.00E+00	0.00E+00	0.00E+00	3.18E+05	0.00E+00	0.00E+00
CORN	0.00E+00	1.91E+07	0.00E+00	0.00E+00	0.00E+00	0.00E+00	0.00E+00	0.00E+00	0.00E+00	0.00E+00	1.68E+06	2.97E+08
DDGS	0.00E+00	0.00E+00	0.00E+00	0.00E+00	0.00E+00	0.00E+00	0.00E+00	0.00E+00	0.00E+00	0.00E+00	6.91E+05	5.60E+06
COMMODITY_CO24	0.00E+00	0.00E+00	0.00E+00	0.00E+00	0.00E+00	0.00E+00	0.00E+00	0.00E+00	0.00E+00	0.00E+00	0.00E+00	3.07E+06
COMMODITY_CO2WAT	0.00E+00	0.00E+00	0.00E+00	0.00E+00	0.00E+00	0.00E+00	0.00E+00	0.00E+00	0.00E+00	0.00E+00	0.00E+00	2.65E+04
COMMODITY_COOL4	0.00E+00	0.00E+00	0.00E+00	0.00E+00	0.00E+00	0.00E+00	0.00E+00	0.00E+00	0.00E+00	0.00E+00	0.00E+00	1.95E+08
COMMODITY_EXTRAPC	0.00E+00	0.00E+00	0.00E+00	0.00E+00	0.00E+00	0.00E+00	0.00E+00	0.00E+00	0.00E+00	0.00E+00	0.00E+00	0.00E+00
COMMODITY_HPC2	0.00E+00	0.00E+00	0.00E+00	0.00E+00	0.00E+00	0.00E+00	0.00E+00	0.00E+00	0.00E+00	0.00E+00	0.00E+00	0.00E+00
ETHANOL	0.00E+00	0.00E+00	0.00E+00	0.00E+00	0.00E+00	0.00E+00	0.00E+00	0.00E+00	0.00E+00	0.00E+00	0.00E+00	2.58E+06
GLYCERINE_WASTE	0.00E+00	0.00E+00	0.00E+00	0.00E+00	0.00E+00	0.00E+00	0.00E+00	0.00E+00	0.00E+00	0.00E+00	0.00E+00	5.91E+06
HEXANE	0.00E+00	0.00E+00	0.00E+00	0.00E+00	0.00E+00	0.00E+00	0.00E+00	0.00E+00	0.00E+00	0.00E+00	0.00E+00	0.00E+00
H2_NH3_MIX_WASTE	0.00E+00	0.00E+00	0.00E+00	2.34E+06	0.00E+00	0.00E+00	0.00E+00	0.00E+00	0.00E+00	0.00E+00	0.00E+00	0.00E+00
HYDROGEN_MIX_01	5.26E+04	0.00E+00	0.00E+00	0.00E+00	0.00E+00	0.00E+00	0.00E+00	0.00E+00	0.00E+00	0.00E+00	0.00E+00	0.00E+00
HYDROGEN_MIX_WASTE	0.00E+00	0.00E+00	0.00E+00	0.00E+00	0.00E+00	0.00E+00	0.00E+00	0.00E+00	0.00E+00	0.00E+00	0.00E+00	0.00E+00
METHANOL	0.00E+00	0.00E+00	5.46E+04	0.00E+00	0.00E+00	0.00E+00	0.00E+00	0.00E+00	0.00E+00	0.00E+00	0.00E+00	0.00E+00
METHANOL_WASTE	0.00E+00	0.00E+00	0.00E+00	0.00E+00	0.00E+00	0.00E+00	0.00E+00	0.00E+00	0.00E+00	0.00E+00	0.00E+00	0.00E+00
NATURAL_GAS_01	3.47E+05	0.00E+00	0.00E+00	0.00E+00	0.00E+00	0.00E+00	0.00E+00	0.00E+00	0.00E+00	0.00E+00	0.00E+00	0.00E+00
NFDS	0.00E+00	9.84E+04	0.00E+00	0.00E+00	0.00E+00	0.00E+00	0.00E+00	0.00E+00	0.00E+00	0.00E+00	0.00E+00	0.00E+00
NFDS_MIX_01	0.00E+00	9.52E+05	0.00E+00	0.00E+00	0.00E+00	0.00E+00	0.00E+00	0.00E+00	0.00E+00	0.00E+00	0.00E+00	0.00E+00
SOYBEAN	0.00E+00	0.00E+00	0.00E+00	7.00E+06	0.00E+00	0.00E+00	0.00E+00	0.00E+00	0.00E+00	0.00E+00	0.00E+00	1.03E+08
SOYBEAN_BIODIESEL	0.00E+00	0.00E+00	0.00E+00	0.00E+00	0.00E+00	0.00E+00	0.00E+00	0.00E+00	0.00E+00	0.00E+00	0.00E+00	4.63E+05
SOYBEAN_HULLS	0.00E+00	0.00E+00	0.00E+00	0.00E+00	0.00E+00	0.00E+00	0.00E+00	0.00E+00	0.00E+00	0.00E+00	0.00E+00	1.33E+06
SOYBEAN_MEAL	0.00E+00	0.00E+00	0.00E+00	0.00E+00	0.00E+00	0.00E+00	0.00E+00	0.00E+00	0.00E+00	0.00E+00	0.00E+00	6.31E+05
SOYBEAN_OIL	0.00E+00	0.00E+00	5.58E+05	0.00E+00	0.00E+00	0.00E+00	0.00E+00	0.00E+00	0.00E+00	0.00E+00	0.00E+00	1.00E+06
WATER	5.57E+06	6.20E+05	5.31E+04	0.00E+00	0.00E+00	0.00E+00	0.00E+00	0.00E+00	0.00E+00	0.00E+00	0.00E+00	0.00E+00
N_FERTILIZER	0.00E+00	0.00E+00	0.00E+00	0.00E+00	1.61E+03	5.67E+06	0.00E+00	0.00E+00	0.00E+00	0.00E+00	0.00E+00	0.00E+00
P_FERTILIZER	0.00E+00	0.00E+00	0.00E+00	0.00E+00	8.06E+02	3.56E+06	0.00E+00	0.00E+00	0.00E+00	0.00E+00	0.00E+00	0.00E+00
K_FERTILIZER	0.00E+00	0.00E+00	0.00E+00	0.00E+00	1.48E+03	4.45E+06	0.00E+00	0.00E+00	0.00E+00	0.00E+00	0.00E+00	0.00E+00
BEANS	0.00E+00	0.00E+00	0.00E+00	0.00E+00	0.00E+00	0.00E+00	0.00E+00	0.00E+00	0.00E+00	0.00E+00	0.00E+00	0.00E+00
PEAS	0.00E+00	0.00E+00	0.00E+00	0.00E+00	0.00E+00	0.00E+00	0.00E+00	0.00E+00	0.00E+00	0.00E+00	0.00E+00	0.00E+00
POTATO	0.00E+00	0.00E+00	0.00E+00	0.00E+00	0.00E+00	0.00E+00	0.00E+00	0.00E+00	0.00E+00	0.00E+00	0.00E+00	0.00E+00
HOGS	0.00E+00	0.00E+00	0.00E+00	0.00E+00	0.00E+00	0.00E+00	0.00E+00	0.00E+00	0.00E+00	0.00E+00	0.00E+00	1.30E+05
MANURE_WASTE	0.00E+00	0.00E+00	0.00E+00	0.00E+00	0.00E+00	0.00E+00	0.00E+00	0.00E+00	0.00E+00	0.00E+00	0.00E+00	3.14E+03
WHEAT	0.00E+00	0.00E+00	0.00E+00	0.00E+00	0.00E+00	0.00E+00	0.00E+00	0.00E+00	0.00E+00	0.00E+00	0.00E+00	1.65E+05
MANURE_WASTE	0.00E+00	0.00E+00	0.00E+00	0.00E+00	0.00E+00	0.00E+00	0.00E+00	0.00E+00	0.00E+00	0.00E+00	0.00E+00	1.50E+06
CO2_WASTE_01	0.00E+00	0.00E+00	0.00E+00	0.00E+00	0.00E+00	0.00E+00	0.00E+00	0.00E+00	0.00E+00	0.00E+00	0.00E+00	5.63E+06
CO2_WASTE_02	0.00E+00	0.00E+00	0.00E+00	0.00E+00	0.00E+00	0.00E+00	0.00E+00	0.00E+00	0.00E+00	0.00E+00	0.00E+00	8.24E+06
NITROGEN_MIX_WASTE_02	0.00E+00	0.00E+00	0.00E+00	0.00E+00	0.00E+00	0.00E+00	0.00E+00	0.00E+00	0.00E+00	0.00E+00	0.00E+00	0.00E+00
NITROGEN_MIX_WASTE_03	0.00E+00	0.00E+00	0.00E+00	0.00E+00	0.00E+00	0.00E+00	0.00E+00	0.00E+00	0.00E+00	0.00E+00	0.00E+00	6.05E+06
STARCH_WASTE_01	0.00E+00	0.00E+00	0.00E+00	0.00E+00	0.00E+00	0.00E+00	0.00E+00	0.00E+00	0.00E+00	0.00E+00	0.00E+00	2.07E+06
WATER_WASTE_08	0.00E+00	0.00E+00	0.00E+00	0.00E+00	0.00E+00	0.00E+00	0.00E+00	0.00E+00	0.00E+00	0.00E+00	0.00E+00	1.55E+04
												0.00E+00
												0.00E+00
												0.00E+00
												7.84E+06

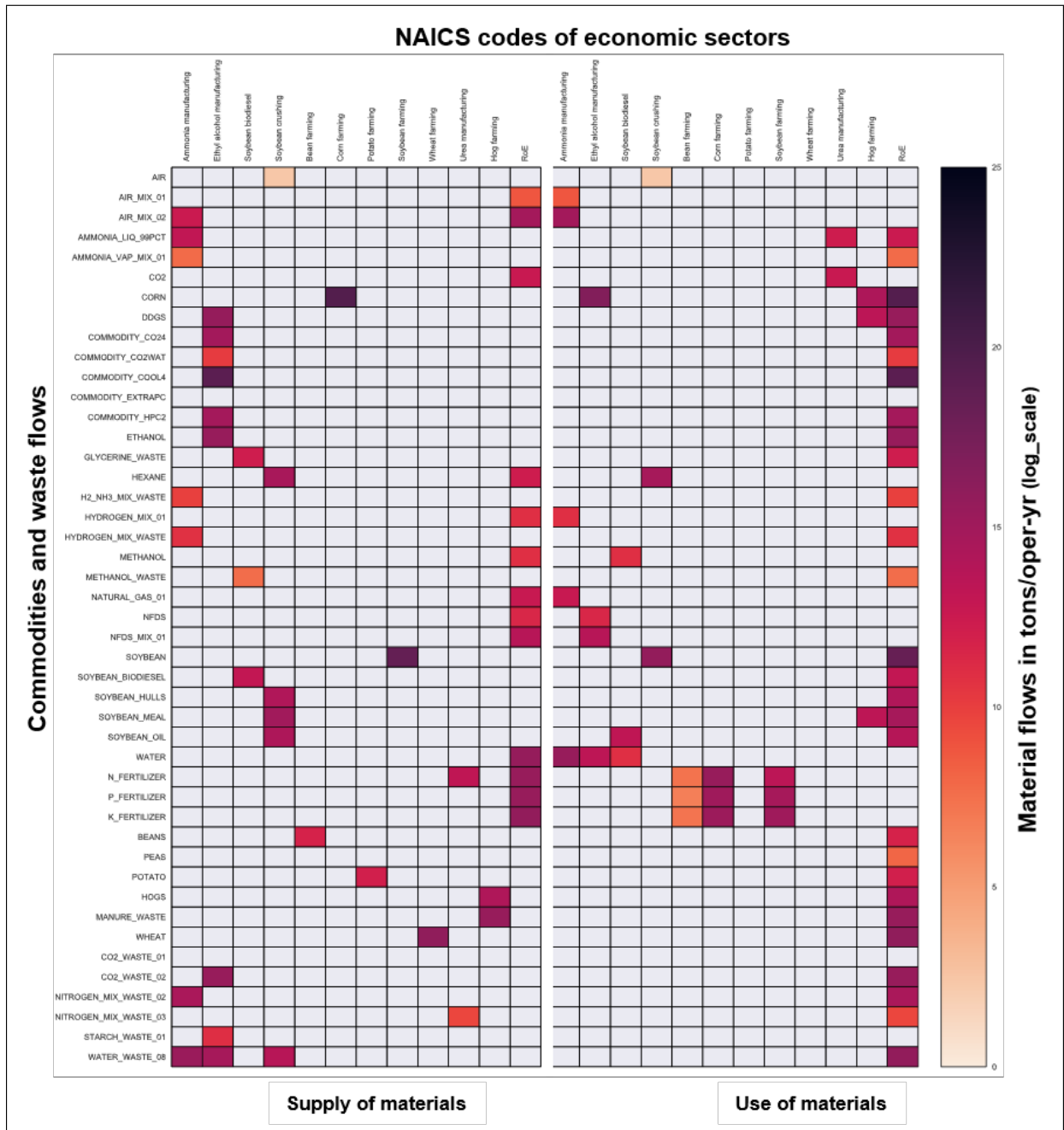


Figure 4.2. The heatmap representation of the PSUTs constructed

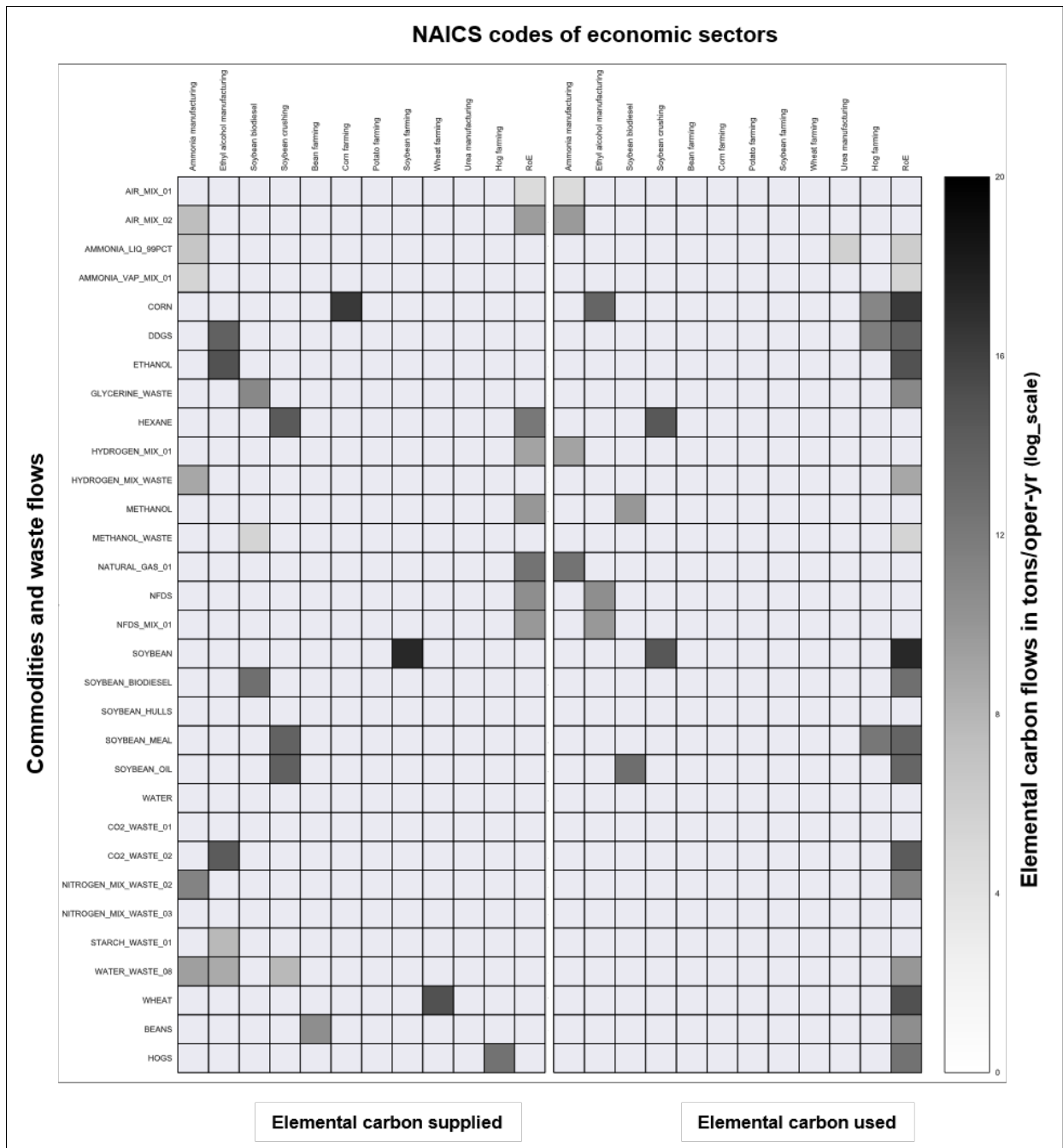


Figure 4.3. The heatmap representation of the carbon PSUTs constructed

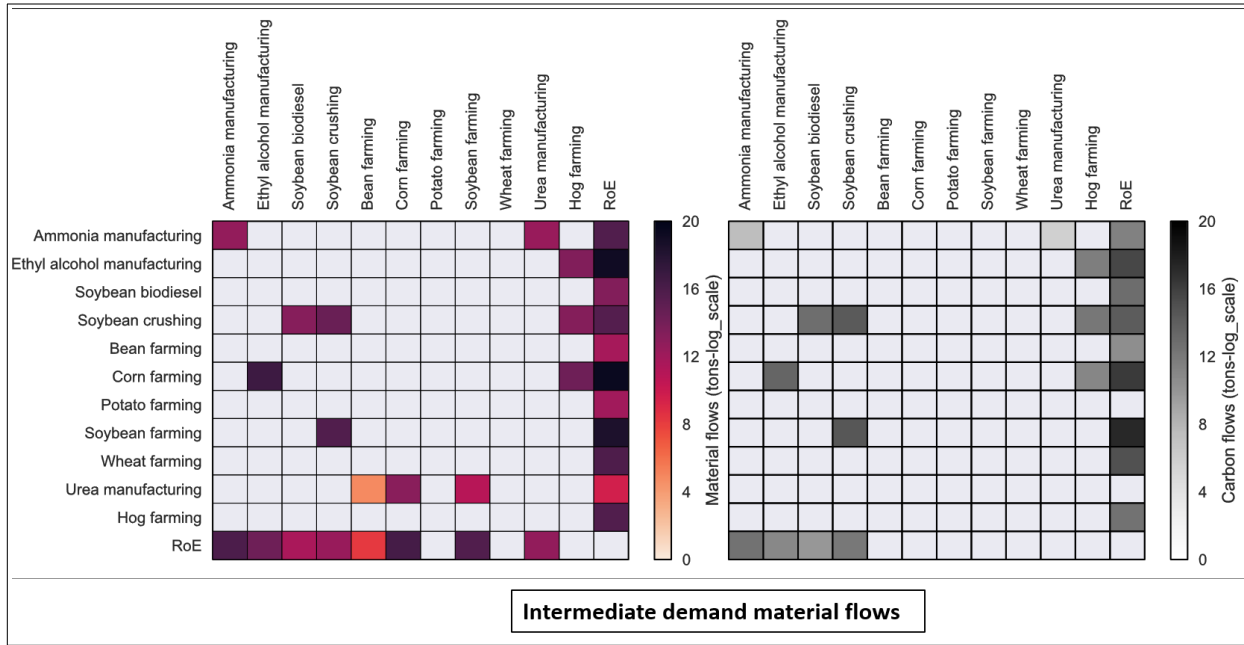


Figure 4.4. The heatmap representation of the full material and carbon PIOT constructed

The various matrices of the PSUTs developed were then assigned to the variables in PSUT table structure to construct a PIOT that quantifies the physical economy model in an industry by industry table format. Using [eq 4.1](#) and [4.3](#), the PSUTs were transformed to a full material PIOT and carbon PIOT as shown in [tables 4.4](#). All the tables and heatmaps presented here provide a highly detailed physical map of materials flowing from one agro-based industry to another in Illinois, while barely relying on any empirical data or the LCA data-sets. Such physical economy models can be critically useful to better manage regional resource usage and to track elemental use efficiencies of different industries. Together, the two tables provide a highly disaggregate material flow information at detailed economic sector and commodity level. For example, highly useful information shown in [table 4.9](#) can be derived from the PSUTs constructed for the agro-based economy of Illinois.

4.4.5 Identifying circular economy strategies

Since it was possible to capture highly detailed chemical characteristic information of individual material flows across the physical economy model, they can be used to determine the recycling potential of various waste flows. The identified waste flows can then be recycled

Table 4.9. Information derived from PSUTs and PIOTs

Industry Information	Name	Value	Units
Highest mass output	Corn farming	3.20E+08	tons/oper-yr
Least mass output	Bean farming	1.30E+05	tons/oper-yr
Highest mass input	Corn ethanol manufacturing	2.10E+07	tons/oper-yr
Least mass input	Bean farming	3.90E+03	tons/oper-yr
Highest known elemental C output	Corn farming	3.40E+07	tons/oper-yr
Least known elemental C output	Bean farming	3.90E+04	tons/oper-yr
Highest known elemental C input	Soybean crushing	4.10E+06	tons/oper-yr
Least known elemental C input	Corn ethanol manufacturing	3.50E+02	tons/oper-yr
Highest commodity use intensity	Ammonia manufacturing	1.20E+00	tons/ton
Least commodity use intensity	Bean farming	3.00E-02	tons/ton

to implement a circular economy strategy. It has to be noted that some waste flows may have very high concentrations of a valuable chemicals, but the required recycling/extraction technology may not be available. The available recycling technologies could constrain the real potential of recycling. If the technology is available, the waste flows can be supplied as an input to the recycling industry where it transforms them into valuable commodities. New EMs can be developed for the new recycling stage and can then be included in the PSUT construction to reflect the recycling of materials. In this case study, the manure flow from hog farming and industrial waste water from ammonia manufacturing, corn ethanol manufacturing, and soybean crushing were identified as flows which can be potentially recyclable. A new recycling industry was included in the economy to process them and the entire process of constructing PSUTs and PIOTs was repeated as in the previous section. The revised PIOT constructed is shown in **figure 4.5**.

It can be observed from the heatmap that the recycling sector is taking inputs (last column) from hog farming, ammonia and corn ethanol manufacturing sectors, and supplying recycled materials (last row) to all other sectors, thus reducing the demand for virgin input material flows. This means that the demand for materials from other sectors in the modeled physical economy may go down. For example, the demand for nitrogen fertilizer by all the crop farming sectors is now partially met by recycled hog manure. This leads to a decrease in demand for urea coming from the urea manufacturing sector. Such a reorganization in material flows across the sectors will lead to structural changes in the physical economy and

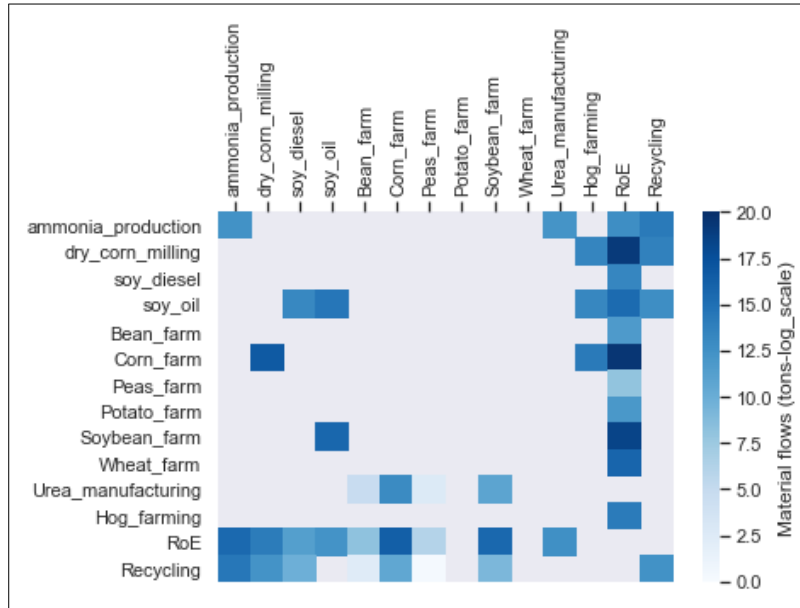


Figure 4.5. The heatmap of PIOT after implementing recycling

these changes are shown in a heatmap (**figure 4.6**) as changes in intermediate material use intensities (contribution of each industry per unit intermediate output). It can be interpreted from the heatmap that most industries such as crop farming sectors and ammonia manufacturing now use less materials from other sectors per unit output as their requirements are now partially met by the recycling sector. While such conclusions may seem intuitive, there can be counter intuitive structural changes too. For example, it can be seen that the material requirements per unit output of urea manufacturing has increased slightly. This can be attributed to the non linear nature of economies of scale. This is a reflection of the fact that material requirements for urea production is non linear and depends on the amount of urea produced. Such a conclusion can never be made from other approaches that use empirical LCA data sets to linearly scale material flows. These structural changes and increase in recycling can provide a comprehensive pathway to enable system wide transition into a circular economy with reduced overall waste flows coming out of the physical economy (**figure 4.7**).

Further, to demonstrate how the symmetric PIOTs can be used, final demand changes (ΔFD) were simulated for the outputs of three industries: Corn farming (100 tons), dry corn milling (200 tons), and urea manufacturing (50 tons). The Leontief inverses (\mathbf{L}) were

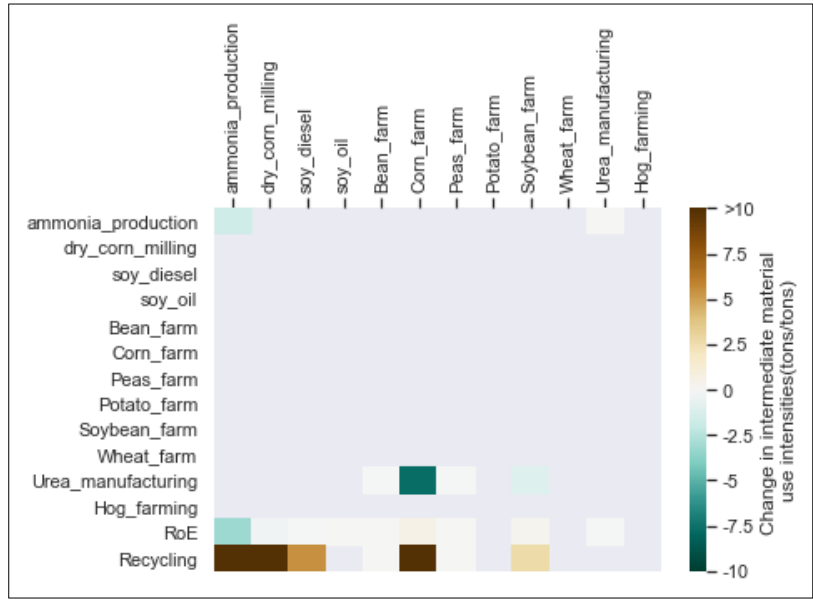


Figure 4.6. Structural changes induced in the physical economy

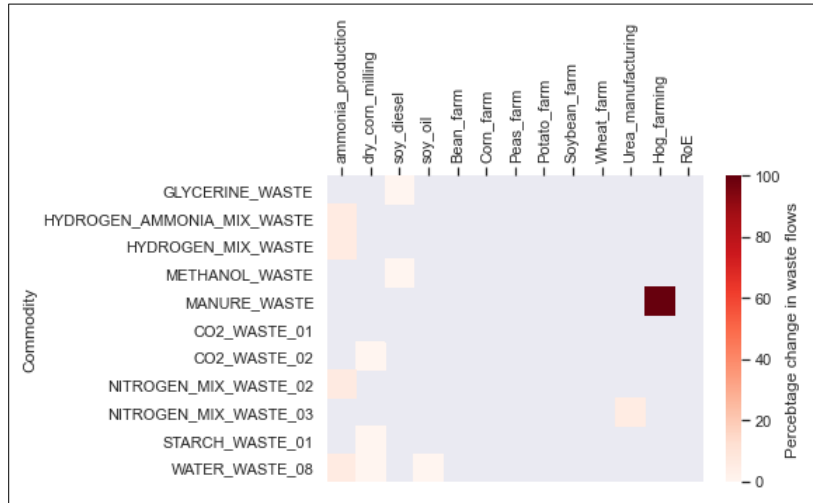


Figure 4.7. Percentage reduction in waste flows in the physical economy

calculated (using eq 4.4) for both the baseline scenario and after implementing circular economy. Then, using eq 4.7 from the previous section (also shown below), changes in physical throughput (ΔX) of all the industries were calculated. The difference in change of throughputs (CE scenario - Baseline scenario) is shown in the bar chart figure 4.8. It has to be noted that the total flow throughput changes include both the commodity flows and waste flows. Several useful information can be extracted from this demonstrative bar

chart to understand how the physical economy responds to demand fluctuations in both the scenarios. The negative values in the bar chart indicate that the total throughput change of an industry was smaller in magnitude when compared to the baseline scenario. For example, for the given final demand fluctuations, some industries such as soybean oil manufacturing will be producing relatively smaller quantities compared to baseline scenario. The introduction of the recycling industry has restructured the physical dependencies of the industries and the overall physical economy modeled responds accordingly based on the different final demand changes induced.

$$\Delta X = L \cdot \Delta FD \tag{4.7}$$

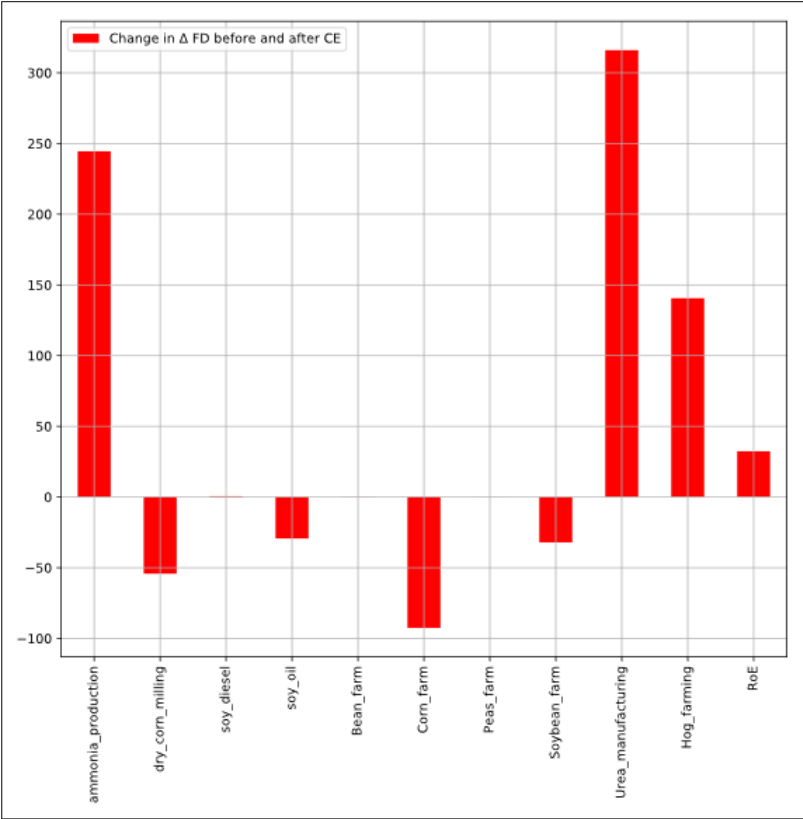


Figure 4.8. Difference in change of physical throughputs (including commodities and waste flows) of industries before and after CE (tons)

4.5 Conclusions

The mechanistic and bottom-up approach of developing EMs to simulate material transformations and using the data from them to construct PSUTs and PIOTs proved to be a comprehensive technique to account economy-wide material flows without overly relying on empirical data. The only empirical data used was in validating and scaling the models, but not in modeling the mechanisms of material transformations. Once validated, the same EMs can now be used for other regions or to find material flows in consequential scenario assessments, thus making this approach highly reproducible. Since the final output of the approach is in the form of PSUTs and PIOTs, it can also be highly compatible with other existing top-down and hybrid flow accounting techniques. Finally, as demonstrated in the case study, the established approach can have wide ranging applications by providing novel insights on material flows and their environmental impacts. However, since the overall approach presented here can be very tedious and time consuming, the next chapter (**ch-5**) aims at providing ways to automate much of the approach to reduce lead times in modeling highly detailed physical economies and further increase the scope of applications.

5. AUTOMATING THE PROCESS OF MATERIAL FLOW SIMULATION, EXTRACTION, AND CHARACTERIZATION TO QUANTIFY PHYSICAL FLOWS AT HIGH SPATIAL, TEMPORAL, AND SECTORAL RESOLUTION

5.1 Chapter overview

The last three chapters ([ch-2](#),[ch-3](#),[ch-4](#)) established mechanistic and bottom-up modeling methods that can accurately quantify physical flows at both single process levels and at an economy wide level with multiple economic sectors. Since the implementation of the methodology presented so far can be tedious and time taking, this chapter focuses on providing automated tools that can significantly reduce the efforts required to implement the methodology. The chapter also discusses how the developed tools were implemented on a cloud-based collaborative environment to help researchers with different modeling expertise and backgrounds to synergistically collaborate on large scale sustainability projects.

5.2 Motivation and background

The primary hurdles to build disaggregated PIOTs include reliable data availability, data heterogeneity, validation, and continuity of data collection for long term updating. Additionally, compiling regionalized empirical data for PIOT construction can be very tedious even for a moderate level economic size and region [75]. Therefore, there is a critical need to improve the methodologies and tools for development of PIOTs at desired disaggregation level through automation that can also reduce the over dependency on empirical data and manual PIOT construction. In this chapter, this need for an automated tool for constructing PIOTs is addressed. The tool developed is called Material Flow Data Extractor and Simulator (MFDES) and it was developed using Python programming language. The rest of the chapter is structured as follows. Advancement in Industrial Ecology (IE) related tools that have overcome significant challenges in modeling through automation (Section 5.3) are discussed first. In Section 5.4, a detailed description is given for the MFDES tool developed that extracts data from EMs and converts them into PSUTs and PIOTs via data integration

and standardized back-end data infrastructure. Next, in Section 5.5, details are provided on the cloud infrastructure for implementation of MFDES in a collaborative environment for automation of PIOT generation. This cloud infrastructure developed is called PIOT-Hub and was developed using Purdue’s MyGeo Hub infrastructure that provides an easy to use Graphical User Interface (GUI) for generating PIOTs. Finally, in section 5.7, potential future applications are discussed along with additional development for future functionalities on PIOT-Hub and possibilities of integration of the PIOT-Hub with other existing IE tools.

5.3 Overview of Existing Automation Tools in Industrial Ecology

In recent years there has been a growing interest in the IE community regarding automation and collaborative model development because of the tedious nature of model development along with lack of reproducibility and transparency. Reproducibility of results is an important criteria in most established scientific disciplines for design. As IE moves towards redesigning our economy and industrial systems towards the goal of sustainability, reproducibility will become essential to identify the most robust pathway. IE community is making gradual progress in this direction to enable large scale collaborations and reproducible model development. In **table 5.1**, some of the existing IE tools and methods are listed which address the need of automation in developing MIOT [78] and hybrid tables [19], that are widely used to identify the scenarios for sustainable growth, transition to low carbon economy and circular economy. The most commonly found methods in tool and method development in IE focus on using top-down approaches. Top down approaches rely on using available empirical data data such as large survey data sets and government records to feed into the IO models. One application of the top-down approach is focused on hybrid tables which are a combination of PIOTs and Monetary Input-Output Tables (MIOTs). Hybrid tables can be very useful when parts of the economy can be difficult to represent in physical units (such as service sectors) but the relevant monetary flow data could be widely available. This also highlights the data heterogeneity issue in modeling the full physical economy. Hence, to overcome the problem of data heterogeneity, researchers have proposed an computational methods to develop hybrid supply-use tables (HSUTs) [96]. In the work by Merciai and Schmidt, the authors describe a method that relies on an existing database

Table 5.1. List of existing tools and methodologies for automation of model development in Industrial Ecology.

	Name	Features	Scale	Sectoral scope	Primary data inputs	Unit	Source
1	EXIOBASE	Builds hybrid supply use and input-output tables	Global	All sectors	International trade data	Monetary Physical	[96]
2	FABIO	Builds physical supply, use, and multi-regional input-output tables	Global	Agriculture		Physical	[97]
3	IELab	Builds highly disaggregated multi-regional input-output tables	Global National Regional	All sectors	International trade, National and regional economic statistics, National and regional employment	Monetary	[98]
4	MFI	Process level information on physical flows	Set by case study	Manufacturing	Process level data	Physical	[99]
5	Pymrio	High level abstraction tool to analyze global MRIO databases like EXIOBASE, WIOD and EORA26	Set by database being analyzed	Set by database being analyzed	EXIOBASE, WIOD, EORA26 databases	Set by database being analyzed	[100]
6	PyIO	Python functions for performing a variety of mathematical tasks involved in input output analysis			Input output tables		[101]
7	PySUT	Python classes for efficiently handling supply use tables and transforming them into input output tables			Supply use tables		[102]
8	USIO	Python scripts for creating an US input-output database for the use in hybrid LCA	USA	US NAICS classification	US Bureau of Economic Analysis supply and se tables	Monetary	[103]

called the EXIOBASE for the construction of multi-regional HSUTs [96]. In their work, hybrid tables use both monetary and physical data to generate the supply and use tables for 43 countries and 5 rest of the world regions. The developed algorithm is automated to process the physical flow data available from the Food and Agriculture Organization statistics, United Nations Comtrade data [104], energy supply use tables and data from the supply use tables from the previous studies by the authors' institute [105]. Since most of the data is from international-level data sets, the built hybrid tables are aggregated at national or multi-national levels.

Another significant advancement has been provided by development of Industrial Ecology Virtual Laboratory (IELab) [98], to overcome the challenge of data unavailability and tedious nature of multi-regional input-output (MRIO) model generation. The IELab is an automated collaborative platform that has been used to develop multi regional supply-use tables and MRIO tables for multiple countries [78], [98], [106], [107]. The automated platform utilizes international, national, and sub-national monetary data available generally from agencies such as US Bureau of Economic Analysis [108] or other survey agencies to construct supply use tables. Since there are many non-survey approaches [74] (ex: Simple Location Quotient, Flegg Location Quotient, etc.) to disaggregate a national level input-output table, the IELab automates the process of disaggregation based on the non-survey approach selected by users. To create the multi-regional tables the algorithm relies on regional proxy data (such as state GDP, employment, personal consumption expenditure, etc.) and follows an optimization approach to transform the national supply use tables to regional supply use tables. The IELab can theoretically generate monetary supply use tables at very high levels of disaggregation provided corresponding constraining data sets (ex: regional GDP, personal consumption and expenditure, etc. at detailed sectoral classifications level) are also available at equally high disaggregation levels [78]. However, since the algorithm utilizes an optimization approach, if the data quality that forms basis of disaggregation is not good or is at highly aggregated level, the reliability of tables generated can be doubtful. Hence, IE lab provides a significant advancement to generation of MRIO tables using computational power, however relies on availability of national level data and supplementary data to generate MRIO models. This is not limiting for generation of MRIOs as national level IO and supporting data are avail-

able for many countries even though lagged, but such information for physical flows are not available, hence IELab currently does not provide automated generation of PIOTs.

In another recent work [97], the focus was on agricultural commodities in order to document the complex flows of agriculture and food commodities in the global economy. Agriculture being one of the primary sectors, usually has a better level of disaggregated data available at an international level from agencies such as the Food and Agriculture Organization. Capitalizing on this, the authors developed a model called Food and Agriculture Biomass Input- Output (FABIO) model, which is a set of multi-regional supply, use and input-output tables in physical units [97]. The model brings together multiple data sources related to trade, crop production, and utilization in physical units along with supplementary technical data to build consistent and balanced supply use tables. FABIO uses data sources such as FAOSTAT [109], UN Comtrade [104], and Energy Information Agency (EIA) [92], and also fills/estimates any missing data manually. FABIO covers 191 countries and 130 agriculture, food and forestry products from 1986 to 2013. Although FABIO has a standardized methodology for building physical supply use tables from large public datasets, it relies on FAOSTAT data which is at national level so does not produce tables at sub-national/regional levels. Further, the reliance on FAOSTAT data puts this method in top-down approach category.

Another approach to create these models is the bottom-up approach that builds from fine scale to coarse scale, instead of the top-down approach where the super-structure is already known to create detailed models. In a study by Hanes and Carpenter [99], a detailed MFA/supply-chain work was performed that falls in bottom-up approach category. In this work, a tool called material Flow through Industry (MFI) is used to provide lists of production recipes and uses them to model the physical supply chain of the product of interest. MFI tool focuses on mapping the material flow through selected product, instead of mapping the whole economy as per the IO framework. Hence, it provides useful analysis related to a particular supply chain, however does not provide insights into overall economy wide material flow accounting.

Other tool developments in the IE domain have focused on making tasks such as data transformation and data visualization easy. A tool called Pymrio [100] was developed to

break down large data sets and perform high level abstraction to analyze global MRIO databases like EXIOBASE, WIOD and EORA26. To make the calculations involved in converting supply use tables to input-output tables easy, tools such as [102] and PyIO [101] were developed. In another work, to make data extraction from online sources easy and to convert data in formats usable in hybrid Life Cycle Assessment, a tool called USIO was also developed [103]. The specific features and input requirements for all the tools discussed in this section are shown in **table 5.1**

So far, most of the methodologies, algorithms and tool developed in the literature have mainly followed a top-down approach of processing the available national and regional level physical/monetary databases to build physical/monetary supply use tables, and in a few cases, use some form of optimization approach for sectoral disaggregation. Few bottom-up based tools such as MFI are not standardized to create IO models, hence creating large scale economy wide models using bottom-up approach is not feasible currently. The work in this chapter aims to complement these tools based on top-down approaches with a bottom-up approach based tool called *Material Flow Data Extractor and Simulator* (MFDES) that aims to utilize mechanistic knowledge of our physical systems in automating the development of PSUTs and PIOTs. MFDES was also implemented on a collaborative cloud platform, PIOT-Hub to advance PIOT generation collaboratively. Next, the structure and functionality of MFDES tool (Section 5.4) and the implementation of it tool in a collaborative cloud platform, PIOT-Hub (Section 5.5) is described.

5.4 Automating PIOT generation via MFDES tool : Architecture, Information flow and Data structures

The Material Flow Data Extractor and Simulator (MFDES) tool is built following a bottom-up approach that automatically extracts data from the fundamental bottom-up physics based engineering models (EMs) to account for material flows that are then converted to PSUTs and PIOTs. At the core of MFDES, computationally developed EMs are used to simulate each economic sector through Python implementation. These EMs are developed to simulate material transformation operations for different industries in the economy and are based on fundamental mass, energy balance and chemical kinetics equations.

When EMs are simulated at the scale at which an industry operates in a region, it enables the extraction of all relevant material flow information of that industry. Since the material flow data is extracted from computational models representing material flows and material transformations for an industry, the data reliability is high. Mass balances are automatically maintained and uncertainty around input and output flows are reduced. The material flow information about resource use, products and emissions, completes the requirements to build a PSUT for the regional industry being simulated. The data from all the EMs representing different industries in a regional economy can then be used to develop a highly accurate PSUT and PIOT. Similar to the approach discussed previously (**ch-4**), MFDES maps each industry to the corresponding NAICS sector classification (US specific) [88] to maintain the IO sectoral framework. After mapping NAICS codes, MFDES automates the process of simulating individual EMs, extracting the relevant data from simulation results, characterize the flow based on chemical composition, and finally, constructs a PSUT and PIOT along with their heatmaps. The key novelty of MFDES is in providing this functionality of automating the mapping of stream information from bottom up EMs of industries to respective supply and use tables.

The MFDES tool implementation has been divided into 5 modules (see **figure 5.1**). The main architecture of MFDES is built in Python with different modules with functions to simulate models and extract data from models (module 1); process heterogeneous data from EM simulation for material flow characterization (module 2); data mapping to generate PSUTs (module 3); balancing using additional data (module 4) and finally conversion of PSUTs to PIOTs (module 5). The approach used by MFDES functionalities in modules 4 and 5 overlap with other tools that generate IO based models as it relies on standard methods for transforming PSUTs to PIOTs, however, modules 1 through 3 are unique in approach and capability to automate data acquisition through bottom-up approach that provides the link from EMs to PIOT. The different functional modules of MFDES are discussed below.

5.4.1 Module 1: Simulation and Data Extraction

Module 1 in MFDES tool consists of a Python based script that takes in heterogeneous EMs built using different modeling techniques and simulates them to extract the material

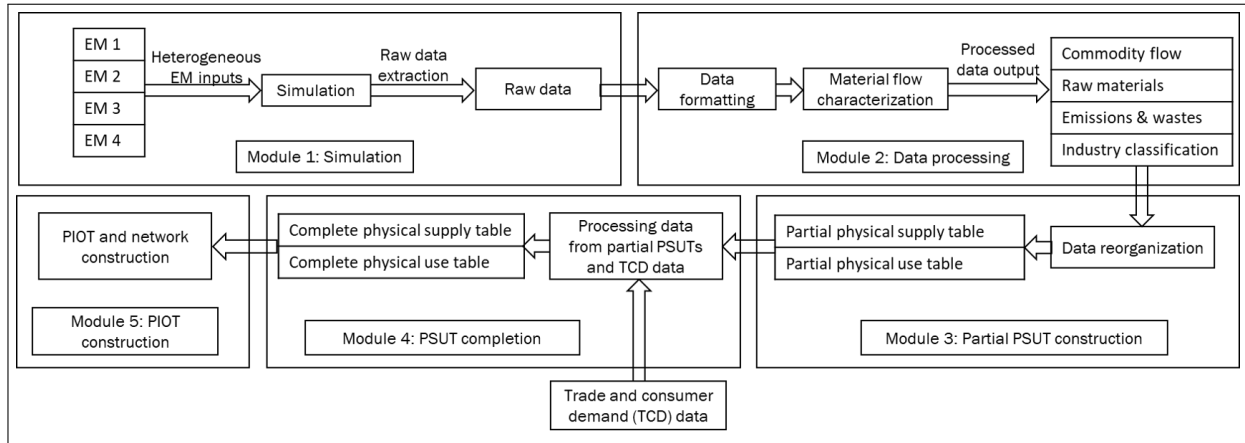


Figure 5.1. Overview of the MFDES tool developed

flow data for the corresponding economic sector. Each of the EMs that are input to module 1 represent different economic sectors in a region. In order to ensure that these models represent the physical flows in the economic region and MFDES can extract the relevant flows, EMs must be first scaled and primed into a format that MFDES can simulate. Scaling of EMs is independent of MFDES tool, so that users can simulate any regional economy. Priming is done as part of the MFDES tool for standardization of extracting data from EMs to be mapped to PSUTs.

Scaling the EMs: Although EMs are very good at representing the material transformation processes of various industries, they need to be scaled appropriately so that they are also representative of the scale at which an industry operates in a region. Hence, the scaling process is tightly linked to the EM development and user dependent. The users would be required to upload scaled models as appropriate for their region of interest. MFDES will not perform any scaling operations to allow the users to select specific year and size of regional operations for which PIOTs are desired. There are different approaches that the users can adopt for scaling based on industrial information or survey based data sets.

Priming the EMs: Priming involves modification steps to make an EM compatible with MFDES. These modifications usually involve simple tweaking of the variable names used in an EM so that they can be parsed and passed on as a MFDES object or as a .csv file in case a black-box like model (model with just in/out material flow information) is used. These name tweaking is part of standardization approach like other simulation engines for enabling

automation of material tracking. For example, if an EM represents the biofuel industry and is built in Aspen Plus software, then there will be a series of variable names in the EM representing different flows and sub-systems in the process of producing biofuel. Now, to prime this EM, some of the variable names containing relevant material flows have to be changed/edited to make it compatible with MFDES. MFDES then processes this information to keep track of the relevant flows picked during the simulation process. This process of priming must be done by the user by modifying the variable names in the EMs using the priming manual that will be provided for PIOT-Hub model uploads or leave to MFDES to do it automatically by specifying the variable names used via upload meta information option in the GUI. An example of priming process is provided in the supplementary material.

Data Extraction and Storage: Once EMs are primed, MFDES invokes different simulation infrastructures to simulate different EMs based on their types (ex: Aspen plus, Python, MATLAB, etc.) and extracts raw data from the EMs. Raw data extracted contains information about mass flows for each relevant stream, that is model specific. Each EM is simulated using a relevant EM simulator based on the file extension type. For example, if EM1 is a python file, then MFDES recognizes the .py extension of the file and invokes a Python compiler to simulate the material flows for the industrial sector represented by EM1. The functionality of invoking different EM simulators and extracting the outputs of the simulated EMs for building PSUT/PIOT is novel and unique to the MFDES tool. While it may be obvious to automatically simulate a series of single file types (say .py files) that represent different sectors, it is not a straightforward approach to simulate different model file types, and simultaneously process material flows from all model types to develop PSUTs and PIOTs. MFDES provides standardization for extraction of the data and compilation to generate the PSUTs and PIOTs. MFDES provides the required infrastructure that can run a variety of model types used for simulating a physical economy and maintain compatibility during material flow extraction from different model types.

5.4.2 Module 2: Data processing for Material Flow Characterization

The raw data from the previous module cannot be directly used as it will still be in the format compatible with different simulators invoked. In the data processing stage, MFDES

is equipped to automatically clean the raw data by stripping any simulator specific non-material flow information so that data flows can be characterized. The automatic process of stripping non-material flow information from EMs and categorizing them is novel and unique to MFDES. MFDES stores all the recorded information from the EMs in temporary memory files and interprets the internal nomenclature used by the EMs to identify different flows and selectively pick only the essential material flow information. For example, if an EM is developed using Aspen Plus process modeling software, then MFDES looks for the nomenclature used for identifying flows in the variable explorer section (input flows are tagged by '#0' character and outputs are tagged by '#1' character in Aspen Plus) of the model and picks only the input and output material flows and leaves out any intermediate flows in the model. After stripping and cleaning raw data from Aspen Plus models, MFDES looks for individual chemical constituents in each flow extracted and matches them with existing information in its database. Similarly, if Python based models are uploaded, MFDES looks for variable tags used to mark input/output material flows in the priming stage and extracts material flow information from the tagged variables after simulating them. For classification of materials into products or wastes, MFDES maintains a database that contains the chemical composition of all commodities in the form of individual component and mass fractions. This database will be provided as default to users, however as new models for additional materials are added to the system, this database will be updated. MFDES then calculates the mass fractions of all the material flows it extracts from the EMs and compares them with the available mass fraction combinations. If there is a match, it assigns the database name for the extracted material flow. If not, it will create a new material in the the database and store the new mass fraction combinations.

Once mapping material flow information to the information in database is complete, MFDES identifies the flows based on priming information as either a "commodity", "raw material", "emission" or "waste". These are the datatypes defined in the MFDES tool for final organization to build PSUTs and PIOTs. "Commodity" flows simply identify the different commodities that are supplied and used by industries, raw materials identify the material inputs from the nature to industries, emissions and wastes identify the material flows from industries to nature.

Table 5.2. Physical supply use table format used by MFDES

Use table	Industry codes			Export	Final demand
	Code 1	Code 2	Code 3		
Commodity 1	-	-	-	-	-
Commodity 2	-	-	-	-	-
Commodity 3	-	-	-	-	-
Commodity 4	-	-	-	-	-
Natural resource 1	-	-	-	-	-
Natural resource 2	-	-	-	-	-
Total	-	-	-	-	-
Supply table	Industry codes			Import	
	Code 1	Code 2	Code 3		
Commodity 1	-	-	-	-	
Commodity 2	-	-	-	-	
Commodity 3	-	-	-	-	
Commodity 4	-	-	-	-	
Emission 1	-	-	-	-	
Waste 1	-	-	-	-	
Total	-	-	-	-	

5.4.3 Module 3: Data reorganization and Partial PSUT Construction

MFDES takes all the data stored in the four flow types (commodity, raw material, emission or waste) from the flow characterization step and reorganizes these in the form of a PSUT first. This is another innovative feature that connects the engineering model outputs to the macroeconomic framework of PSUTs and PIOTs. The standard PSUT format used by the MFDES is same as shown in the previous chapter (**table 4.2**). Although this step involves only reorganization of data simulated through EM engines and classified in step 2, it is normally time consuming if done manually for a large economy with all the commodities, waste and emissions data. Hence, another key strength of MFDES is in automating the whole process of simulating (i.e. generating reliable data), classifying and finally organizing it in an easy to interpret user-friendly format. At this stage, MFDES has all the data required to build PSUTs except for the columns and rows relating to exports, imports and final consumer demand. Hence, at this stage the PSUTs are only partially completed with information of supply and use of commodities by various sectors in the economy.

5.4.4 Module 4: Balancing PSUT and External Data Integration

The PSUTs generated by module 3 are generally unbalanced as supply and use in an economy will not balance without inclusion of imports, exports and consumer use. These partially completed PSUTs will need to be balanced with trade and consumer demand (TCD) data that cannot be obtained from engineering models alone. However, from this step, the tables can be used with the standard IO theory to generate balanced tables and perform further analysis. Many balancing approaches already exist in the literature [110] [111] [112]. MFDES combines the partially completed PSUT with any available user specific trade (ex: state level import/export data) and consumer demand (TCD) data to build a complete PSUT. In this stage, all the missing information in the partially completed PSUTs can be filled by uploading .csv files containing missing information. These .csv files can be uploaded to the MFDES tool just like any other EMs. But on recognizing the .csv file type, MFDES will not invoke any simulator for these file. It simply parses through the missing information and extracts the required information to complete the PSUT. If all the data is filled correctly, the PSUTs will be mostly balanced except for places where external balancing information is unavailable, or the confidence intervals of data reported are too high . Finally, once PSUT balancing and construction is complete the results can be rendered to user and also passed on to module 5 for PIOT construction.

5.4.5 Module 5: PSUT to PIOT Construction

Module 5 uses custom built Python libraries to convert PSUTs to PIOTs. The PSUTs from module 4 are provided as input to the Python libraries in module 5 which transforms PSUTs to PIOTs using a modified version of the Model D approach from the Eurostat [113] manual (eq 4.1 to 4.3). This final module also provides multiple ways of visualizing the constructed PIOTs: 1) raw PSUT and PIOT in .csv table format, and 2) heatmap of the PIOT. All the visualization forms are based on the raw PIOT constructed. MFDES uses the data from this raw PIOT and applies the data to different visualization program libraries encoded with the MFDES infrastructure.

5.5 PIOT-Hub : A Cloud Based implementation of the MFDES tool for PIOT Generation

PIOT-Hub has been developed on a collaborative cloud platform to make building PSUTs and PIOTs easily accessible and more collaborative by implementing the MFDES tool on a cloud based service. Deployed on a production quality HUBzero [114] based science gateway called MyGeoHub [115], PIOT-Hub builds upon the open source HUBzero science gateway framework and directly leverages HUBzero's support for online collaboration, scientific data management, hosting of dynamic online simulation tools, as well as common functions including federated authentication and user management, connection and job submission mechanism to high performance computing (HPC) systems on the Purdue campus and national resources such as XSEDE. In addition, MyGeoHub provides the capabilities to interoperate with remote data repositories and cyberinfrastructures with synergistic functions and social networking tools such as group, wiki, blog, ticket, and forum, making it an ideal platform for the development, publication, and dissemination of PIOT-Hub to the user community.

The beta version of PIOT-Hub has been released for early testing by a small group of selected users. It will be released to the public once all the underlying cyberinfrastructure and workflow for the collaborative environment has been established and tested.

There are several challenges in implementing the PIOT-Hub to map full economy. First, the system needs to support several types of input models commonly used by the community, including open source python models, Aspen Plus models, and CSV files. Second, the Aspen Plus software runs on Windows while the rest of the system are Linux based. In addition, the Aspen Plus software is proprietary with complex installation and set-up process. Third, users upload python or Aspen Plus modeling code as input for MFDES jobs. However, it poses a security risk to execute user-provided code on the server side, leading to system vulnerability to malicious attacks. Finally, when the size of the PIOT table grows, it could become data and computationally intensive, making it harder to scale to a large number of users or support a large number of industry segments. Hence, a cloud based modular PIOT modeling system to address these challenges was developed. Implemented as a Jupyter Notebook (JN) [116] application, PIOT-Hub provides an easy to use web based user interface that collects user inputs in a flexible format and presents PIOT, PST and PUT outputs in

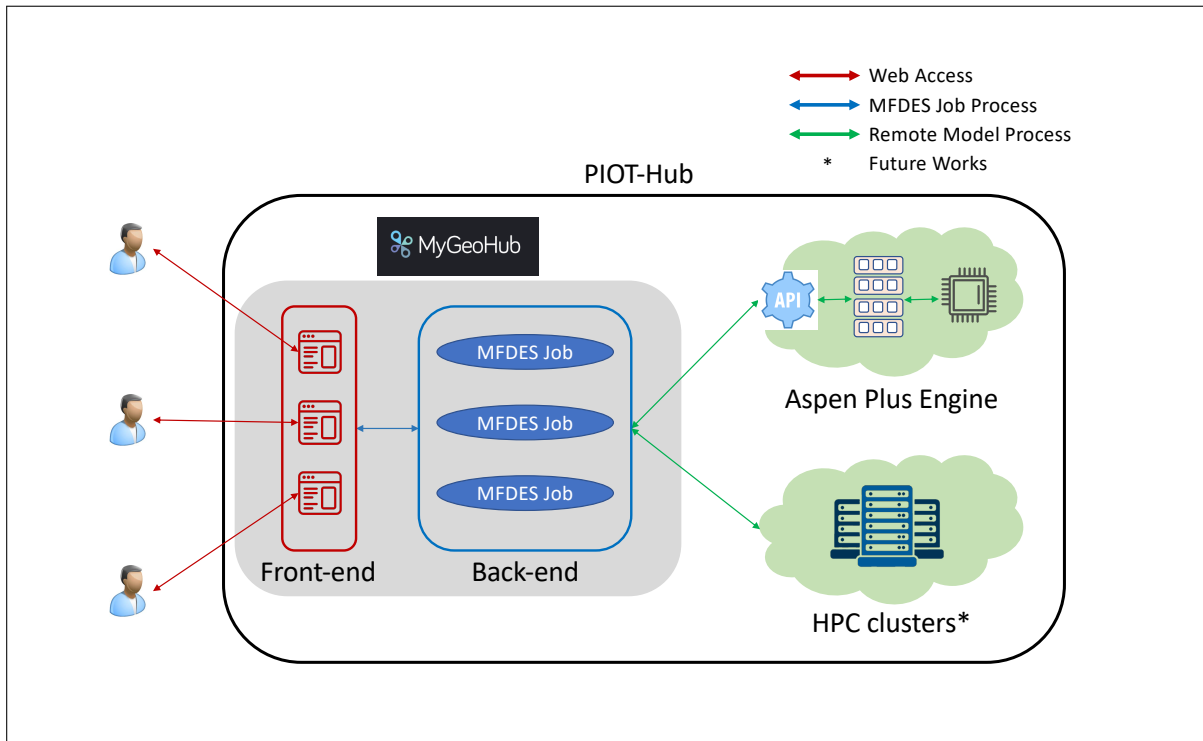


Figure 5.2. Overview of PIOT-Hub Infrastructure

multiple ways. As shown in **figure 5.2**, the functionality of PIOT-Hub includes an easy to use GUI front-end built on the JN that is integrated with back-end simulation services. Users can launch the JN instance in a virtual container on MyGeoHub to set input parameters or get results through a web browser. Once users set all of the required input parameters on the web, the information is submitted to the back-end services. The back-end PIOT services consist of four modules: (1) a python model engine that is responsible for executing python input models; (2) an Aspen Plus model engine that runs on a remote Aspen Plus server with a service API that accepts Aspen Plus model input and returns output after execution; (3) a controller that runs on MyGeoHub and is responsible for preprocessing user requests, creating MFDES jobs, dispatching the jobs to either the python engine or Aspen Plus engine, getting the results back, and merging the results in the MFDES job instances once all simulations are done; and (4) a visualization module for converting the outputs to tables or network diagrams.

The PIOT-Hub front-end user interface and most of the back-end services including the controller and python model engine are built in Python using open source python pack-

ages such as Jupyter Widgets for GUI, Matplotlib/NetworkX for result visualization, and Numpy/Pandas for data processing. The service API on the Aspen Plus server is built using Javascript with Node.js, which provides an access point to the controller running on MyGeoHub for receiving simulation requests and sending the simulation results back. The Aspen Plus simulation engine manages the user requests through Docker containers and RabbitMQ for scalable and efficient data processing.

The PIOT-Hub tool is designed to be a usable, scalable, and secure online modeling environment. The system automatically detects the input model type and dispatches it to the corresponding back-end processing engine. Priming manual will be made available to help users prepare their models so that they comply with the format expectation of the tool. The PIOT-Hub tool currently runs python models on the hub server and Aspen Plus models on a remote Aspen Plus server. Aspen Plus backend services will be migrated in future to Linux server using windows VM support. Validation code is added to prevent malicious attack as well as to provide feedback to the user if the model fails to run. Furthermore, in each user session, the PIOT-Hub tool runs in a secure virtual container on the HUBzero platform which helps mitigate the security risk as well.

The flowchart for the cloud implementation process, called PIOT-Hub is shown in **figure 5.3**. When a user uploads a model, PIOT-Hub will attempt to parse it and check if the model is primed and compatible with MFDES. The model will proceed to next stage if primed, if not, PIOT-Hub will notify users that the model is not primed. A primed model will be handled by MFDES following all the steps in section 5.4 to generate PSTs, PUTs and PIOTs.

5.6 Automated PIOT Generation Demo on PIOT-Hub

In this section, the tool functionalities and step by step information on using the tool is presented. The same agro-based industries of Illinois from previous chapter (ch-4) were used as an example to automate extraction of the physical flows using PIOT-Hub and develop a PIOT and a heatmap of the PIOT. Users begin the process by uploading different EMs that are developed and primed to the PIOT-Hub using the GUI. The screenshot of input GUI of PIOT-Hub is shown in **figure 5.4**. In **figure 5.4**, the drop-down list **a** and **b** allow users

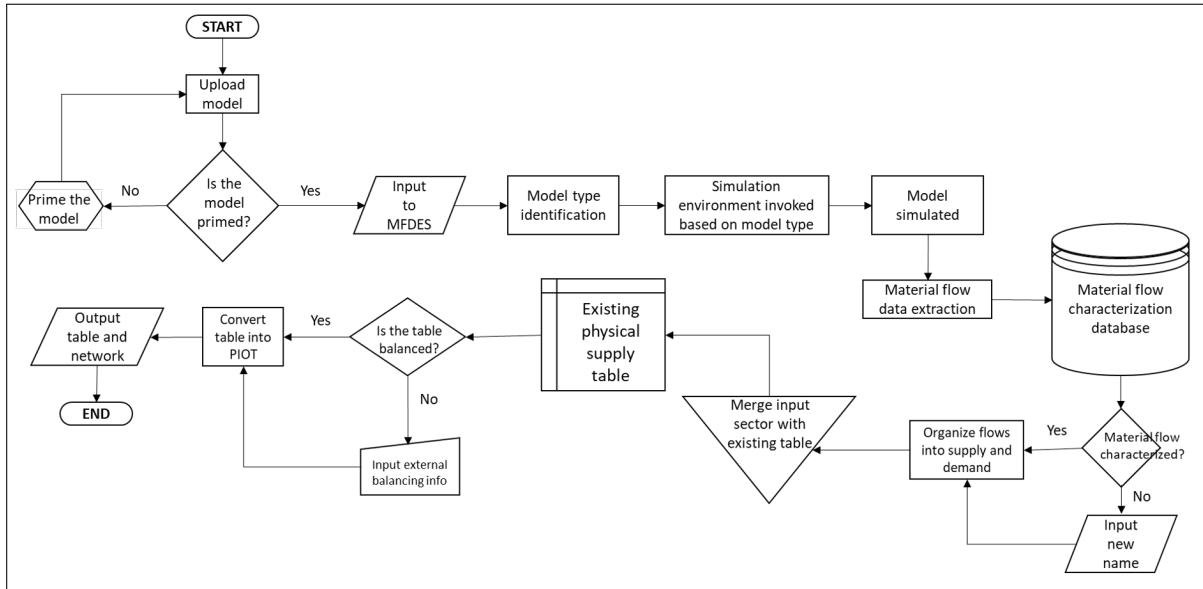


Figure 5.3. PIOTHub: Collaborative cloud implementation of the MFDES tool

to select the region and the year associated with the uploaded EM. The text field **c** allows users to name the corresponding industry represented by EM. PIOT-Hub is also capable of dealing with NAICS classification codes for EMs representing industrial sectors. Users can directly select the relevant preloaded NAICS code using the drop-down list **d** prompted while entering the sector name. As discussed in Section 5.5, users can utilize the default models on PIOT-Hub in the drop-down list in **e** or upload/change EMs **f**. However, the current selection of EMs are limited by the models developed in our group, which will be expanded. The red and green buttons (**g** and **h**) enable removing uploaded EMs and uploading new EMs respectively. Since EMs could also have many supporting files as per priming needs, the users are required to upload all files associated with an EM as a zip file. File types such as .csv, .py, .mat, and aspen plus .bkg files are currently accepted). For each EM upload, PIOTHub creates a directory in the user’s home on MyGeoHub and unpacks all the files in the directory to be accessed by the MFDES job instance. Once all the EMs are uploaded and data input is complete, users submit the job using ‘Run’ button to start the simulations.

After submitting the job using ‘Run’ button, MFDES initiates different simulating environments based on EM file extensions and proceeds with all the steps shown in **figure 5.3**. Once simulation is complete, the GUI takes the user to the output tab. All the results

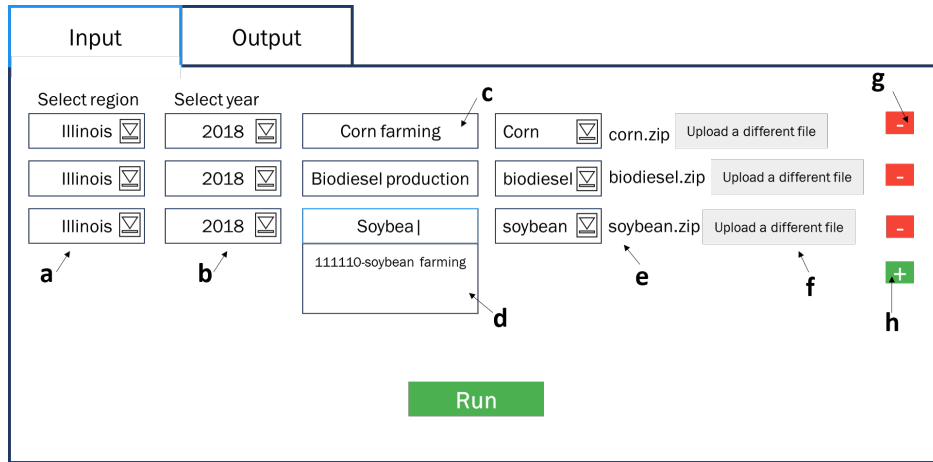


Figure 5.4. Input tab of the PIOTHub

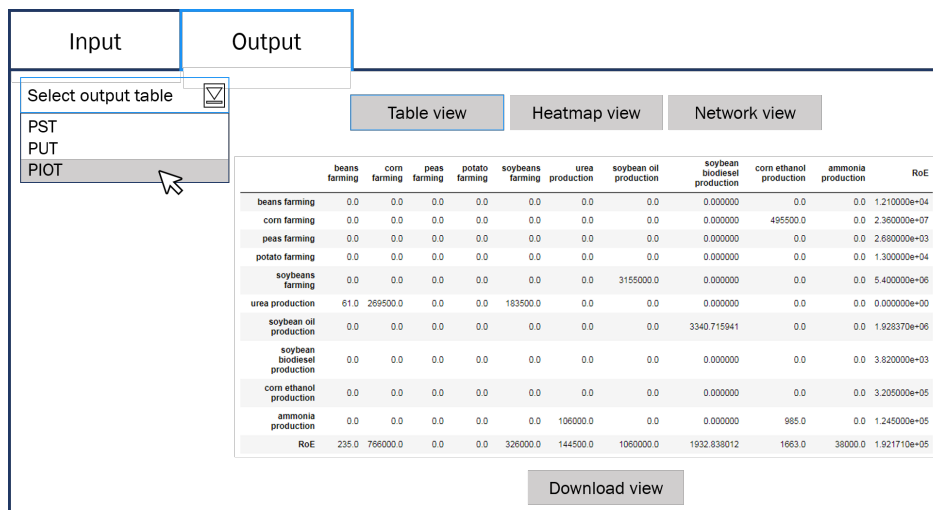


Figure 5.5. Output tab of the PIOTHub with PIOT view as a table.

generated by the PIOT-Hub can be directly viewed within the GUI as PST, PUT or PIOT. It also provides users with options to view and download the heatmap of PIOT and material flow network of PIOT. **Figure 5.5** shows a PIOT for Illinois generated using the simulation of EMs.

The tables such as the one shown in **figure 5.5** can be downloaded as .csv files using the “Download view” button at the bottom of the output window. The heatmap view (**figure 5.6**) can also be downloaded as high-resolution images. The default units shown across all output tables is metric tons. Unless external information related to final demand, imports and exports is given, MFDES assigns all the unbalanced material flows to the rest of economy

sector (RoE). If users also upload these information as a .csv model file in the input window, MFDES will use that data to fill in respective columns and rows in the tables and the table format will be updated.

The tool and GUI features will be further advanced as per initial beta tester’s feedback.

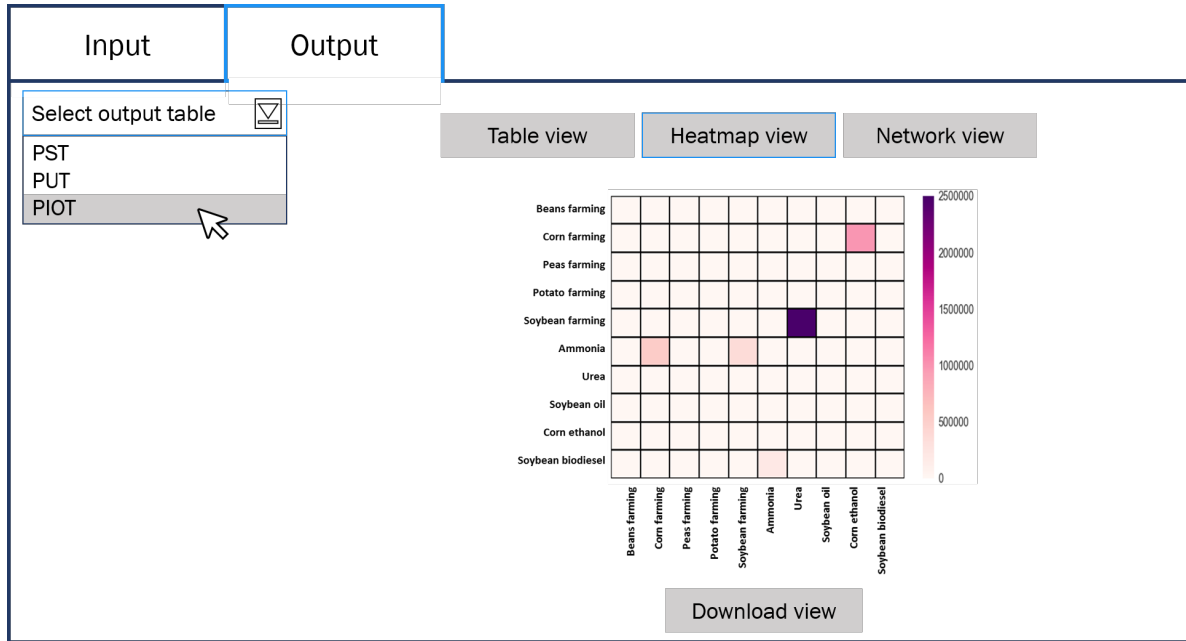


Figure 5.6. Output tab of the PIOTHub with PIOT view as a heatmap.

5.7 Discussions and Potential Tool Applications

Mapping our physical economy continuously as the technologies, industrial design and consumption patterns change is a significant challenge. This tool is being developed with a vision to provide the much needed automation in generating the material flow map using the power of mechanistic engineering models and advances in cyberinfrastructure. The cloud based PIOT-Hub provides a novel platform that enables a faster generation of PIOTs using bottom-up approach implemented via MFDES that generates PSUTs and PIOTs for a region and converts it into a network map of material flows in the modeled region. Hence, PIOT-Hub can be a place where industries, academics and stakeholders can collaborate to understand material flows and their dependency with other industries in the region. The key novelty of this platform is that it allows integration of mechanistic EMs for physical econ-

omy modeling using a bottom-up approach with the macroeconomic view of economy. The mechanistic approach also allows visualizing the material flow network changes in real time. The automation of bringing such large-scale complex information together to build the PIOT models is another key novelty and unique strength of this tool, along with the adaptability and scalability for any region and any emerging technology that can be modeled using first principle knowledge. While, the current implementation is focused on regional scale where homogeneous technology was assumed for each sector, the method and tool can be expanded to include multiple technologies being used in same sector as percentage share of production. A significant advantage of the MFDES tool is that it can overcome the basic limitations of complete dependence on survey-based databases that form the foundation of modeling in IE and time lag that arises due to reliance on survey data. It also serves a larger goal of enabling collaborations between engineering modeling community and Industrial ecologists. While this tool goes a step further and integrates EMs to generation of PIOTs, it remains compatible to be integrated in future with other methodologies and build on the progress made so far, especially the constrained optimization approaches to fill data gaps such as in MRIO construction. It can also be used in utilizing the survey databases to reconcile results and perform comparative analysis of survey-based vs model-based results, while not demonstrated in the demo presented here. Finally, some potential applications envisioned for the tool that can support mapping physical economy and decision making are presented below :

1. Material Flow Maps to Identify Vulnerability in Production Systems due to Risks to a particular Industry: Once the physical economy of a region is modeled, it can be used to study the material intensities of different supply chains in the economy and trace everything back to unit process levels as MFDES uses a bottom-up approach. This can be used to identify the vulnerabilities for production in a region which can be used by plant managers and engineers to anticipate material supply challenges.
2. Material Flow Dynamics for Future Planning of Material Supplies: Since, EMs are capable of simulating scenarios, such scenarios can be executed fast on PIOT-Hub

to generate time series of material flow networks, providing insights into potential dynamic changes.

3. Evaluating Impact of recycling technologies on Material Flow Networks : Another important application using PIOT-Hub can be in the area of identifying the impact of implementing circular economy on material flow intensities. Using EMs, it is possible to identify co-products/ waste flows in one industry that can be used as potential feedstocks in another industry. Using this information, an EM for a new recycling technologies can be added to waste processing sector and PIOTs updated to evaluate material intensities in new economy.
4. Identifying the best Emerging Technology for Scale Up: The integration of EMs to update PIOTs, allow to test scale up of any emerging technology such as recycling systems etc for it's impact on material flows, which can help in selection of best technology.

PIOT-Hub eliminates the need to install or set up any software by end users. However, for Aspen Plus a license agreement needs to be provided currently, which can be overcome by moving to open source process modeling softwares. The system is scalable to multiple simultaneous users as well as to large computation needs by leveraging the high performance computation (HPC) resources provided by campus clusters or national cyberinfrastructure such as XSEDE. Its modular architecture makes it easy to expand the tool to support models of different types in the future. However, the cloud implementation and capacity of PIOT-Hub is at an early stage of development, mainly limited in large scale PIOT generation, multiple user access and implementation of potential applications discussed above. Our future work entails scaling up the capability for wider IE audience, adding features for industrial stakeholders and academic research use. Further, integration of this tool with open source tools such as US-IO may also be pursued for hybrid model creation or for comparison of economic structure presented by MIOTs vs PIOTs. Through this tool, a faster, reproducible and collaborative mapping of the physical economy using PIOT framework was envisioned. Model and data sharing between users will be enabled in the future to facilitate online collaboration. Provenance information will be automatically recorded and associated with each MFDES job, making it easy to reproduce the results when needed. This automation

tool and cloud infrastructure developed will also be helpful in validating the reproducibility of PIOTs being generated in one group by other researchers, thus enabling open science approach to material tracking and collaboration. Reproducibility of material tracking models in the economy has been challenging due to the significant effort and propriety nature of data being used to create such models in the past.

6. COMPUTATIONAL METHODS TO QUANTIFY MONETARY FLOWS AT HIGH SECTORAL RESOLUTION AND TO PERFORM SUSTAINABILITY ASSESSMENT

This chapter is based on the following published article:

[78] F. Faturay, V. S. G. Vunna, M. Lenzen, *et al.*, “Using a new USA multi-region input output (MRIO) model for assessing economic and energy impacts of wind energy expansion in USA,” *Applied Energy*, vol. 261, no. 3, p. 114141, Mar. 2020. DOI: [10.1016/j.apenergy.2019.114141](https://doi.org/10.1016/j.apenergy.2019.114141)

6.1 Chapter overview

This final chapter of the dissertation attempts to further advance the research of top-down approaches by using methods to quantify monetary flows at high spatial, temporal, and sectoral levels. While the previous chapters focused on advancing mechanistic bottom-up approaches, it is equally important to continue advancements in the capabilities of existing top-down approaches. To achieve a comprehensive flow accounting framework, the advantages offered by all existing approaches have to be embraced as no single approach (bottom-up nor top-down) can account all flow types at all levels of spatial, temporal, and sectoral disaggregation. Therefore, in this chapter, new computational methods are discussed that can disaggregate monetary flows at a national level to sub-regional levels while maintaining high sectoral resolution. A case study of disaggregating the US national IO table into a 52 region Multi-Regional IO table is used explain and demonstrate the computational disaggregation techniques. Further, to show how developing such MRIO tables can aid in performing advanced sustainability assessment, the developed MRIO table was used to quantify the multi-regional economic and energy impacts of wind energy expansion in the US.

6.2 Motivation and background

United States (US) is going through an energy transition like many other countries around the world and adoption of renewable energy options such as solar and wind energy has emerged as a competitive option over fossil fuels in several markets. In 2017, US was ranked second globally to bring new wind energy capacity in operation and added 7 gigawatts (GW) of wind energy capacity in 2017 [117]. Overall 89 GW of electricity was generated (3% of its total electricity supply mix) from wind at year end only second to China. A US Department of Energy study [118] predicts that if wind energy share continuous growing at the current pace, it will account to 35% of the total electricity supply by the year 2050. Consequently, adding renewable energy generation capacity results in local economic impacts originating from manufacturing, operations and maintenance activity along with spill-over of these impacts into other regions due to the supply chain effects and the interconnected nature of various regional economies. Quantifying such impacts has been a topic of investigation over the last two decades across the world. The scope of investigations ranged from assessing localized economic impacts in a region [119], market uncertainty analysis [120], job creation or employment effects [121], and quantifying emissions of deployment using hybrid Life Cycle Assessments (LCAs) [122] [123]. The research objective of this chapter specifically addresses this aspect of sustainability assessment using economic Multi-regional Input-Output (MRIO) analysis [74].

Since the regional economic sectors in the US actively interact with sectors in other regions, deploying wind energy infrastructure in one region can have impacts on economic sectors in other regions and these impacts can be quantified using MRIO analysis. MRIO analysis makes it possible to study the the direct and indirect economic changes at multi-regional levels in response to final demand changes of the economic outputs of specific industries in a given region under study. However, regionally disaggregate MRIO models are not readily available for the US economy. In order to perform various types of multi-regional impact assessments of renewable energy expansion, there is a need for rapid and continuous MRIO model development. In this chapter, a computational method is presented to enable rapid MRIO development for the US economy and to use the developed MRIO model for

quantifying economic and energy impacts of wind energy expansion. The method presented uses the Industrial Ecology Virtual Laboratory (IE Lab) [124] that proved to be highly effective in development of MRIO models for other countries such as Australia [125], China [126] [127], Indonesia [128], Japan [129], Taiwan [130] along with a global MRIO model [131]. IE Lab makes it possible to disaggregate a national level Input-Output (IO) table into a MRIO model using various non-survey approaches of disaggregation [74]. At its core, IE Lab uses a constrained optimization algorithm to reconcile various raw regional data it uses to constrain the national IO table. The complete methodology of IE Lab construction can be found in the work by Lenzen et al. [124]. The case study specifically attempts to answer two questions: 1) how to use computational methods to build a MRIO model for the US, and 2) how to use the developed MRIO model to calculate economic and energy impacts of wind energy expansion in the US.

Rest of the chapter is organized as follows: the details on US MRIO model construction is provided first along with various types of raw data used, it is followed by details of data collected for wind energy infrastructure deployment in ten regions of the US, and finally, details on the environmentally extended MRIO analysis performed is provided.

6.3 Methodology

The primary data needs for using the IE lab infrastructure are called raw datafeeds. Raw datafeeds constitute various regional data that are collected and formatted to start disaggregating any available aggregated data such as a national IO table. The raw datafeeds collected are shown in **table 6.1**. The 2017 national supply-use tables obtained from Bureau of Economic Analysis (BEA) were the main source for the construction of US MRIO. These national level tables when fed into IE Lab are disaggregated into sub-national or regional tables using non-survey regionalization methods [74] to get an initial estimate of the US MRIO. Of the various non-survey methods available in IE Lab [124], the Flegg Location Quotient (LQ) was selected over basic regionalized methods such as Simple LQ and Cross LQ as it performs better to estimate the inter-regional input coefficients [132]. The initial regionalization of the national supply-use tables into regional tables was done by using regional weights, which describe the economic structure of a region in comparison to the nation. To

this end, the census data available for 1058 sectors at 6-digit North American Industry Classification System (NAICS) code level [133] for 52 regions (50 states, District of Columbia, and Puerto Rico) was used as regional weights (also called "proxy") for disaggregating national supply-use table at regional level. The resulting MRIO is used as an "initial estimate" for the optimization step within the IE Lab. IE Labs then uses the initial estimate along with various regional datafeeds collected as to perform constrained optimization on different parts of the MRIO (**table 6.1**) and develop the final MRIO model. One of the primary constraints used is that all MRIO elements must be positive with the exception of changes in inventories and subsidies. More information on the optimization solvers used and default IE Lab constrains construction can be read in the work by Lenzel et al. [124]. Once the MRIO model was developed, it was then used to perform environmentally extended MRIO analysis of wind energy expansion in the US (more about the developed MRIO model is available in results section of this chapter).

Table 6.1. Primary data used for US MRIO construction

Data	Years	Regions	Sectors	MRIO part constrained	Sources
1 National Supply-Use Tables					
a. Detail-level	2007-2017	1	402	ID, FD, VA	US Bureau of Economic Analysis
b. Summary-level	2007-2017	1	72	ID, FD, VA	
2 GDP by state	2007-2017	52	64	VA	US Bureau of Economic Analysis
3 Private consumption expenditure	1997-2017	52	15	FD	US Bureau of Economic Analysis
4 Export and import	2008-2017	52	33	Export, Import	US Dept of Commerce
5 Census	2001-2017	52	1058	Proxy for regionalization	US Bureau of Labor Statistics

(ID = Intermediate Demand, FD = Final Demand, VA = Value Added)

6.3.1 Method for collecting regionalized economic impacts of wind energy expansion

To understand the impacts of wind energy expansion in the US, a scenario of installing 500 megawatts (MW) wind energy capacity (Turbine size: 2300 kW and Number of turbines: 218) in each of the top ten wind energy producing states (**table 6.2**) in the US was modeled. These ten states accounted most of the wind energy capacity in the US (63 GW of 89 GW total, or 70% of total production). The individual contribution of all the remaining 42 states is very small when compared to the top ten states, hence only the top 10 states were focused to study the renewable energy expansion impact. Although new wind energy farms were

installed in only ten of the states, the economies of each state in the US are highly connected and dependant on each other and the IE Lab allows to quantify the cascading/ripple economic impacts across the nation. Since the IE Lab can report the economic impacts at a highly disaggregated sector level (up to 1058 economic sectors at 6-digit NAICS) it makes it possible to understand the economic impacts at finest scale of disaggregation such as 6-digit of NAICS sectors level in each of the state.

Table 6.2. Installed Wind energy capacity (MW) in top 10 States of the US (2016)

	State	Installed capacity (MW)
1	Texas	21450
2	Iowa	6974
3	Oklahoma	6645
4	California	5561
5	Kansas	5110
6	Illinois	4026
7	Minnesota	3499
8	Oregon	3213
9	Washington	3075
10	Colorado	3029

(Source: <http://www.neo.ne.gov/statshhtml/205.htm>)

To obtain multi-regional economic impacts, USLab is initially fed with the data related to direct economic disruption in terms of increased final demand that take place individually in top ten wind energy producing sates due to installing new wind energy capacity. The state wise economic disruption data was obtained from the Jobs and Economic Development Impacts (JEDI) models [134] by National Renewable Energy Laboratory (NREL) of the US. The JEDI tool provides state economic data such as direct costs of building a new wind energy farm, labor costs, material and service costs, etc. **table 6.3** shows a full list of the data provided by JEDI tool that are mapped to sectors and sub-sectors. After mapping the JEDI tool data to sub-sectors, it was further mapped and classified according to NAICS nomenclature as the IE Lab needs data mapped to the economic sectors using NAICS codes. The sectors that are directly impacted by the demand created and value added in economy due to installation of new wind capacity and their associated NAICS codes and US-MRIO sectors are shown in **Table 6.4**. The wind turbine equipment was assumed to be imported

from other countries and the cost of the equipment is assumed to be an infrastructure investment that is provided by the local governments in each of the ten states. The US-MRIO table constructed already accounts for imports in the coefficients, hence the final demand for wind turbine was used as a government final demand for creating capital in the economy.

Table 6.3. Type of JEDI data for each of the ten states.

Sector	Sub-sector
Equipment	Turbines, Blades, Towers, Transportation
Balance of Plant	Materials, Construction (concrete rebar, equip, roads and site prep) Transformer, Electrical (drop cable, wire), HV, Line extension, Labor, Foundation, Erection, Electrical, Management/supervision.
HV Sub/Interconnection	Materials, Labor, Engineering, Legal Services, Land Easements, Site Certificate
Labor Costs-Personnel	Field Salaries, Administrative, Management
Materials and Services	Vehicles, Fees, Permits, Licenses, Misc. Materials, Insurance, Fuel (motor vehicle gasoline), Tools and Misc., Supplies, Spare Parts Inventory, Materials and Services Subtotal, Sales Tax (Materials & Equipment Purchases), Other Taxes/Payments

(Source: NREL JEDI model [134])

Table 6.4. Concordance matrix of sectors related to wind energy installation and US-MRIO sectors.

NAICS code	NAICS sector name related to wind energy installation	US-MRIO sector name
221115	Wind Electric Power Generation	Wind Electric Power Generation
237130	Power and Communication Line and Related Structures Construction	Construction
238120	Structural Steel and Precast Concrete Contractors	Construction
324110	Petroleum Refineries	Manufacturing
333611	Turbine and Turbine Generator Set Units Manufacturing	Manufacturing
333612	Speed Changer, Industrial High-Speed Drive, and Gear Manufacturing	Manufacturing
334416	Capacitor, Resistor, Coil, Transformer, and Other Inductor Manufacturing	Manufacturing
335312	Motor and Generator Manufacturing	Manufacturing
336112	Light Truck and Utility Vehicle Manufacturing	Manufacturing
484230	Specialized Freight (except Used Goods) Trucking, Long-Distance	Transportation and Warehousing
524126	Direct Property and Casualty Insurance Carriers	Finance and Insurance
541110	Offices of Lawyers	Professional, Scientific, and Technical Services
541199	All Other Legal Services	Professional, Scientific, and Technical Services
541320	Landscape Architectural Services	Professional, Scientific, and Technical Services
926150	Misc. Services	Other Services (except Public Administration)
926150	Fees, Permits, Licenses	Public Administration
339999	Misc. Materials	Manufacturing
921130	Sales Tax (Materials & Equipment Purchases)	Public Administration
522292	Debt Payment (average annual)	Finance and Insurance
522292	Equity Payment - Corporate	Finance and Insurance
524126	Land Lease	Real Estate and Rental and Leasing

6.3.2 Method to quantify the multi-regional impacts using the US-MRIO table

A representative template of a 3 region MRIO table that IE Lab generates is shown below in **figure 6.1**. The methodology starts with an existing national MRIO table that IE Lab generated for the year 2017. Once the table is generated, “shocks” (data from JEDI models) were injected into the table to the gross fixed capital formation (GFCF) and consumer final demand (CFD) in the final demand block. GFCF and CFD together account for all the demand for goods and services that required to build a new wind energy project [135].

		Region 1				Region 2				Region 3				RoE	
		Ind	Com	GFCF	CFD	Ind	Com	GFCF	CFD	Ind	Com	GFCF	CFD	1	
		1 2 3	1 2 3	1	1	1 2	1 2	1	1	1 2 3 4	1 2 3 4	1	1		
Region 1	Ind	1													
		2													
		3													
	Com	1	x x x	x	x		x x	x	x			x	x		x
2		x x x	x	x		x x	x	x			x	x		x	
3		x x x	x	x		x x	x	x			x	x		x	
VA	1	x x x													
Region 2	Ind	1	x x x	x	x	x x	x	x			x	x		x	
		2	x x x	x	x	x x	x	x			x	x		x	
	Com	1													
		2													
VA	1	x x x			x x										
Region 3	Ind	1													
		2													
		3													
		4													
	Com	1	x x x	x	x		x x	x	x			x	x		x
		2	x	x	x		x x	x	x			x	x		x
		3	x x x	x	x		x x	x	x			x	x		x
		4	x	x	x		x x	x	x			x	x		x
VA	1	x x x													
RoE	1	x x x		x	x x		x			x x x x		x		x	
Employment	1	x				x					x				
Climate		x					x					x			
Water			x						x					x	
Energy				x						x				x	
Land Use					x						x				
...															
...															
...															

Figure 6.1. Representative template for MRIO table generated by IE Lab. (RoE: rest of economy), Shaded Region shows the part of economy where shocks were introduced.

In input-output analysis, installing a new wind energy project is not assumed as a value-added investment but it is rather seen as an increase in demand for goods from all the industries that make it possible to build a new wind energy project which leads to new capital formation. For example, in the case of wind energy expansion, GFCF includes spending on land improvements, turbine towers, machinery, equipment purchases, construction of roads

and industrial buildings which leads to increase in capital formation. These GFCF and CFD shock values in the final demand block are obtained from the JEDI model which provides the local economic data related to installing new wind energy infrastructure in a specific state. The JEDI model uses the project development and on-site labor data coupled with turbine manufacturing and the related local supply chain data to calculate the regional final demand change (GFCF and CFD values). With these data, USMRIO table was used to calculate the induced impacts over rest of the states in the US. After the introduction of shocks, IE Lab was run again with shock data to calculate the change in economic throughput for all the sectors in each of the states using **eq 6.1**. Import and export activities were included into the intermediate matrix, and therefore the input coefficient A captures the international effects. To measure the change of output X resulted from as a result of shocks in FD - y , the Leontief model was used as:

$$X = (I - A)^{-1}y \quad (6.1)$$

In this work, only a short term impact (1 year) was analyzed resulting from the shocks introduced. Hence it was assumed the structure of the US economy to be fixed. Long term structural change due to introduction of more renewable energy was not considered, however should result in redistribution of energy supply and demand. This is out of scope for the simulations carried out in this study.

6.3.3 Estimating manufacturing sector energy footprint due to wind energy expansion

To calculate the spatial energy footprint of installing new wind energy capacity across US, the Environmentally Extended-MRIO (EE-MRIO) approach was used. In this approach, an energy consumption column for manufacturing sector was constructed based on a US government survey data. This survey by the US-Energy Information Administration (US-EIA) provides a detailed energy consumption (it refers to all the direct energy used by a sector for non-fuel purposes) data for manufacturing sector as part of Manufacturing Energy Consumption Survey (MECS) datasets [38]. The choice of selecting manufacturing sector

was informed by a) high energy consumption by manufacturing sector and b) high economic impact of installing new wind energy capacity in manufacturing sectors across US states. However, the data for energy consumption in manufacturing sector was not available for all US states in MECS, hence a regionally aggregated (4 census region aggregation) analysis at the 3-digit NAICS aggregation level was performed. **Figure 6.2** shows the 4 census regions in the US.

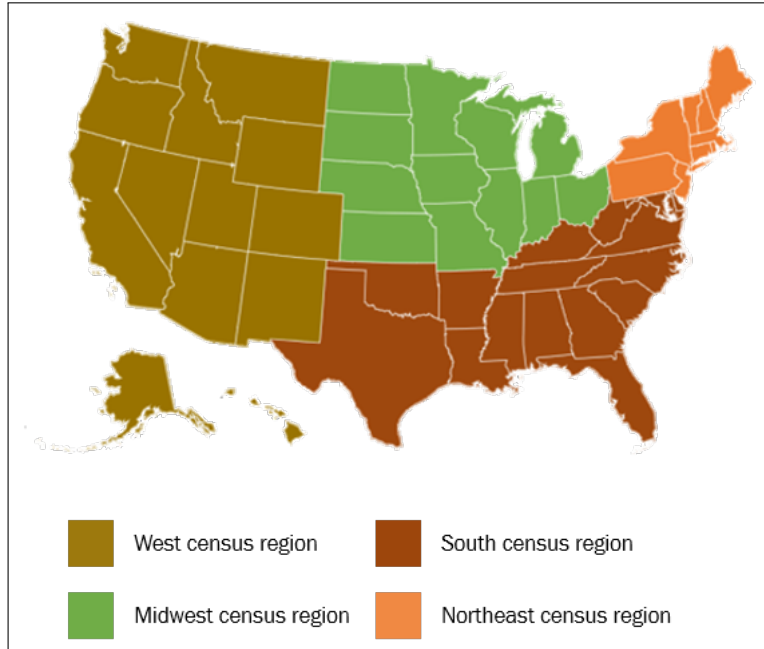


Figure 6.2. The 4-census regions of the US

The energy consumption data obtained from the EIA website for the four regions is shown in **table A.2** in the appendix(section A). The data was available in the NAICS format that was compatible with the available NAICS aggregation in the IE Lab. Energy Consumption (E) values were available for 21 manufacturing sectors at 3-digit NAICS level desegregation (311–339; discontinuous series) for 4 regions as defined by U.S Census Bureau and the unit of energy required was given in terms of trillions of British thermal units (btu). In **eq 6.2**, $E (1 \times n)$ denotes the direct energy inputs for each industry and $\Omega (1 \times n)$ denotes the direct energy intensity for each industry (R=region of interest) which was calculated as energy input per unit total throughput (X) for manufacturing sectors in each region. E_{Ri} values are from **table A.2** in appendix and X_{Ri} values are from the generated MRIO table by IE Lab.

It must be noted that each vector is an aggregation of 4 regional vectors corresponding to the 4 census regions.

$$\begin{pmatrix} \Omega_{R1} \\ \Omega_{R2} \\ \Omega_{R3} \\ \Omega_{R4} \end{pmatrix} = \begin{pmatrix} E_{R1} & 0 & 0 & 0 \\ 0 & E_{R2} & 0 & 0 \\ 0 & 0 & E_{R3} & 0 \\ 0 & 0 & 0 & E_{R4} \end{pmatrix} \begin{pmatrix} \frac{1}{X_{R1}} \\ \frac{1}{X_{R2}} \\ \frac{1}{X_{R3}} \\ \frac{1}{X_{R4}} \end{pmatrix} \quad (6.2)$$

Now to calculate the change in energy consumption, the EE-MRIO approach is invoked by using product of the energy intensity with the change in economic throughput as per **eq 6.3**. Here, X_{Ri} was obtained from **eq 6.1** for the final demand change induced by wind energy expansion.

$$\Delta E_{Ri} = \Omega_{Ri} \Delta X_{Ri} \quad (6.3)$$

6.4 Results

6.4.1 The US economic structure in the form of MRIO table

A heatmap of the 2017 US-MRIO table is shown in **figure 6.3**. The heatmap is presented only at 2-digit NAICS aggregation level (20 sectors) for simplifying the presentation, as visually representing 1058 sectors connections (6-digit NAICS level) in all regions was not feasible. The heat map allows for a visual assessment of the country's inter-regional supply-chain structure across 52 regions and 20 sectors. For example, the dark row of matrices for California indicate a high contribution of California to the national economy. California was one of the main manufacturing hubs representing a national share of 11.2%, followed by Texas (7.5%), and Ohio (5.2%). California also produced more than one fourth of agricultural output, followed by Florida (6.5%), and Washington (6.1%). The dark row of matrices of New York and Texas represent a large finance and insurance sector, and mining and quarrying sector, respectively. Texas, along with California, is also the primary host for national wind electric power generation with a combined output of more than 45% of the country's total output, again indicated by the dark row on the heat map.

The heat map in **figure 6.3** also shows inter-regional supply-chain flows, indicating the dependence of a region on the rest of regions. The regional inter-linkages demonstrate the importance of using MRIO tables for supply-chain analysis. For example, Texas has significant mining-related industries such as petroleum refineries, and oil and gas extraction. These products making the strongest inter-regional exporters of mining outputs from Texas to other regions. The MRIO table can also able to trace the flows of money and materials attached to a product that are vital for economic spill-over and footprint analysis.

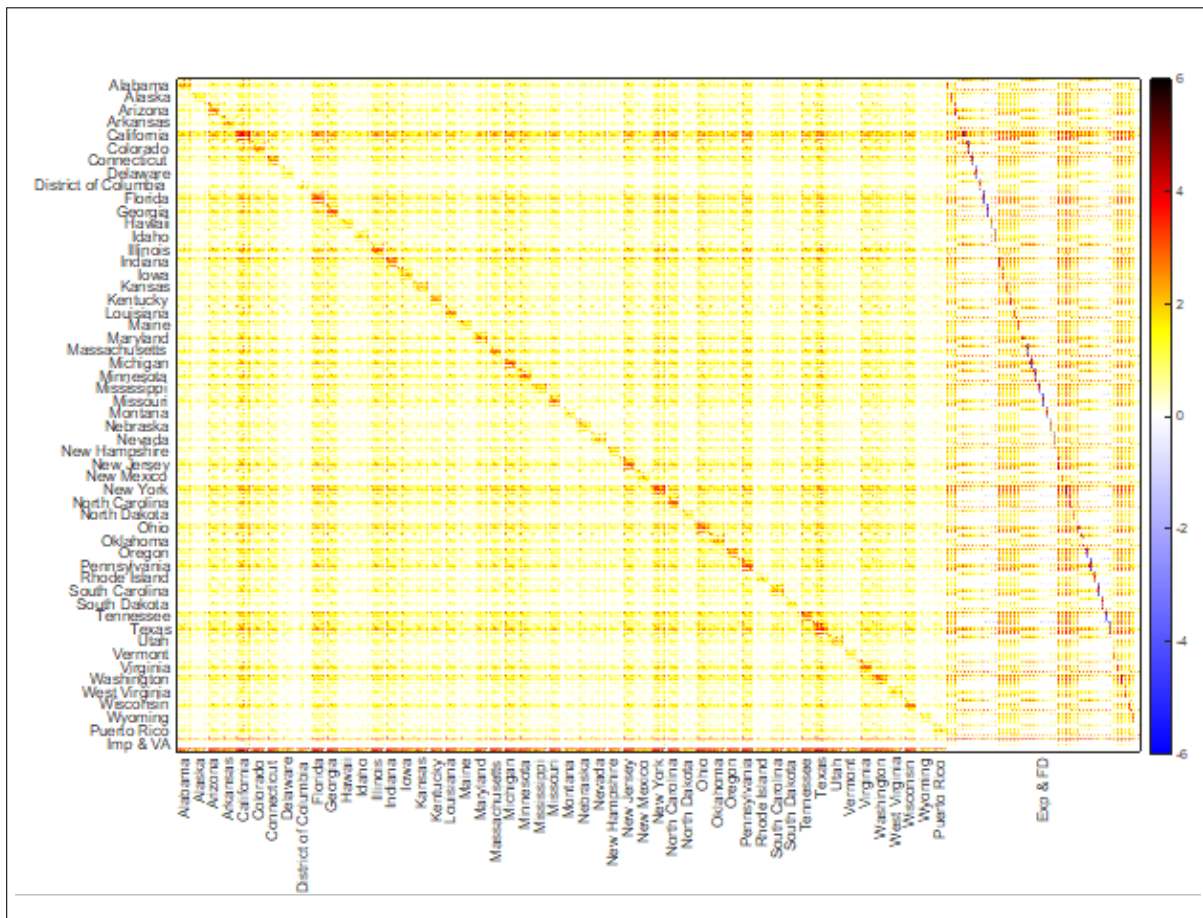


Figure 6.3. Heat Map of the US-MRIO Table for 2017

6.4.2 Multi-regional economic impacts of installing wind energy infrastructure

Installing new wind energy farms induces new economic throughputs for the whole of US. The direct impacts due to the activities related to the construction and installation of new

wind energy were introduced in the model as shocks i.e. change in final demand as ΔFD . The shocks were introduced at 3-digit disaggregation level in the US MRIO model generated at 3-digit disaggregate level for year 2017. The values of ΔFD at 3-digit disaggregate level for the NAICS sectors impacted by installation of wind infrastructure in each state are uploaded as “Shock Data”. The simulation results using **eq 6.1** show that the installation of wind energy farms in these 10 states, potentially leads to a \$26,929,083,000 (approx. \$26 billion) of total economic throughput change in the country. The calculation shows the positive short-term economic impact of introducing new renewable energy capacity in the country. This aligns with increase in labour and physical commodity demand to meet the increased economic activities. While the local impacts are directly felt in the state experiencing the increase in economic activities due to installation of new wind capacity, the positive economic effects also spill over as shown by the MRIO calculations. The state-wise change in throughput using the IE Lab is shown in **figures 6.4 and 6.5**. As one would expect, the top ten states where new wind energy capacity was installed (**figure 6.4**) show significant change in economic throughput. However, the US MRIO table built in the IE Lab made it possible to capture the economically significant multi regional impacts from the remaining states too. As shown in **figure 6.5**, these remaining states contribute to around 11% of the total economic impacts, i.e. approx. \$3 billion, a substantial amount. The nation-wide sector level distribution of change in economic throughput is shown in **figure 6.6**. **Figure 6.6** also shows that the top two sectors that contributed to the change in total throughput are Manufacturing and Construction. This is intuitive as installing new wind energy farms does involve a large amount of commodities from these two sectors, however quantification through MRIO model allows to see the spill over effect of increased activity in these sectors throughout the national economy. The statewide distribution for the top 6 sectors with the largest economic throughput change is shown in **figure 6.7**. The 6 maps in the **figure 6.7** shows the spatial distribution of economic impact spill over in different sectors. It is interesting to see that installing new wind farms in just 10 states has positive economic impact in states of Montana, Alaska, Wisconsin, North and South Dakota for sectors such as Finance and Insurance, Manufacturing etc. Such analysis can provide insights into multi-state cooperation for adoption of energy technologies that can meet both the goal

of environmentally friendly energy generation for self-reliability and economic prosperity with increase in economic opportunities, a win-win scenario.

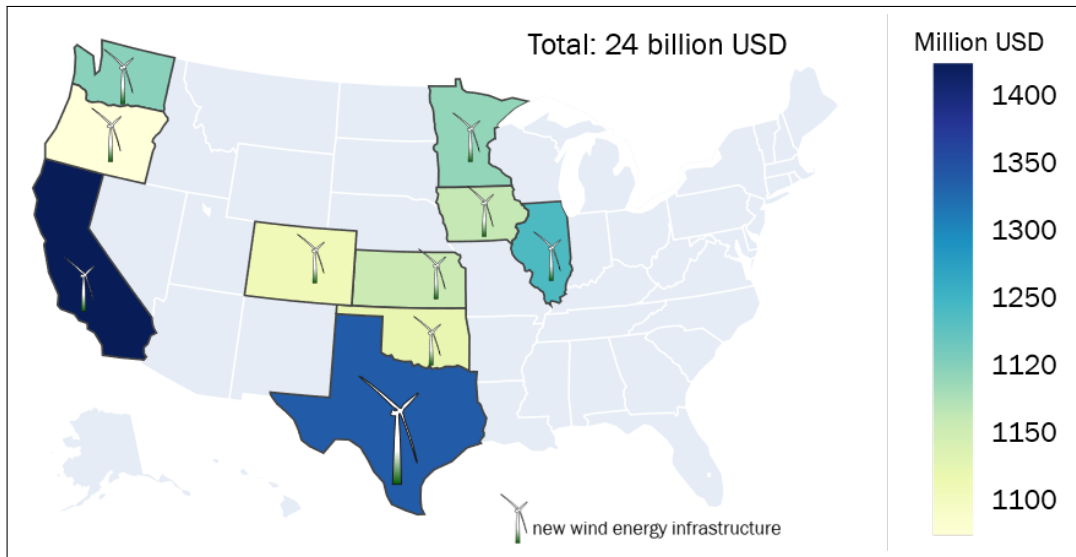


Figure 6.4. Direct multi-regional economic impacts

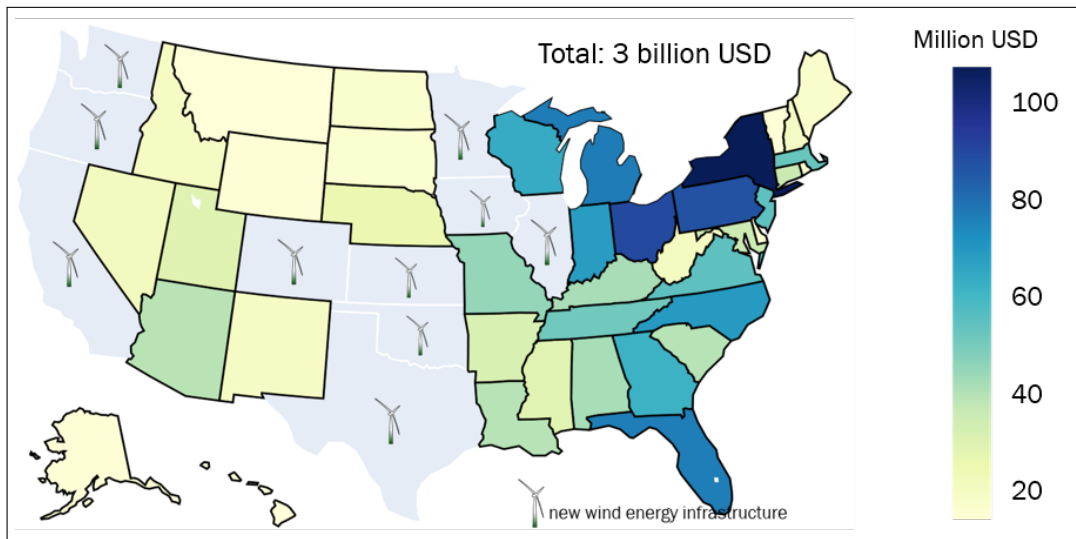


Figure 6.5. Indirect multi-regional economic impacts

6.4.3 Manufacturing sector energy analysis

The estimated energy intensity (Ω) of manufacturing sector in each of the 4-census region is shown in **table A.3** in the appendix (A). The changes in direct energy consumption using

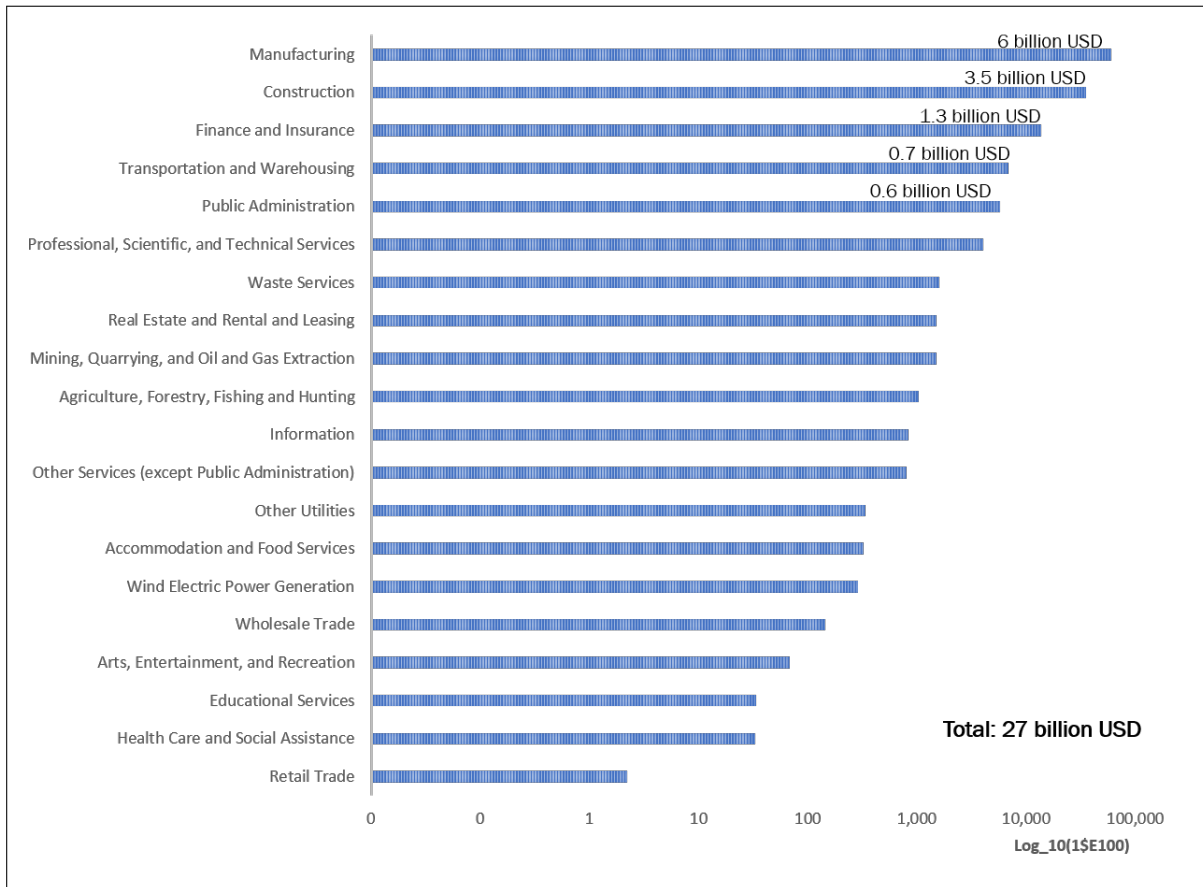


Figure 6.6. Total national economic impact by sector (log scale)

US MRIO for 4 census regions for 21 manufacturing sub-sectors was calculated and their percentage changes are shown in **figure 6.8** below. One common observation among all the 4 regions was that the change in energy consumption was the greatest for the primary metal manufacturing sector. This can be attributed to the increase in demand for more primary metals like iron, copper, aluminium, etc that are associated with installing new wind turbines. More demand implies increase in production volume and hence, increase in energy consumption. Similarly, an increase in energy consumption for the Machinery manufacturing can be attributed to the increase in demand for machinery required to install new wind turbines and both the census regions, Midwest and West have a considerable concentration of machinery manufacturing industries. The reason why some sectors showed significant increase in energy consumption and some did not can be attributed to how tightly or loosely these sectors are related to wind energy sector. The sectors such as primary metal

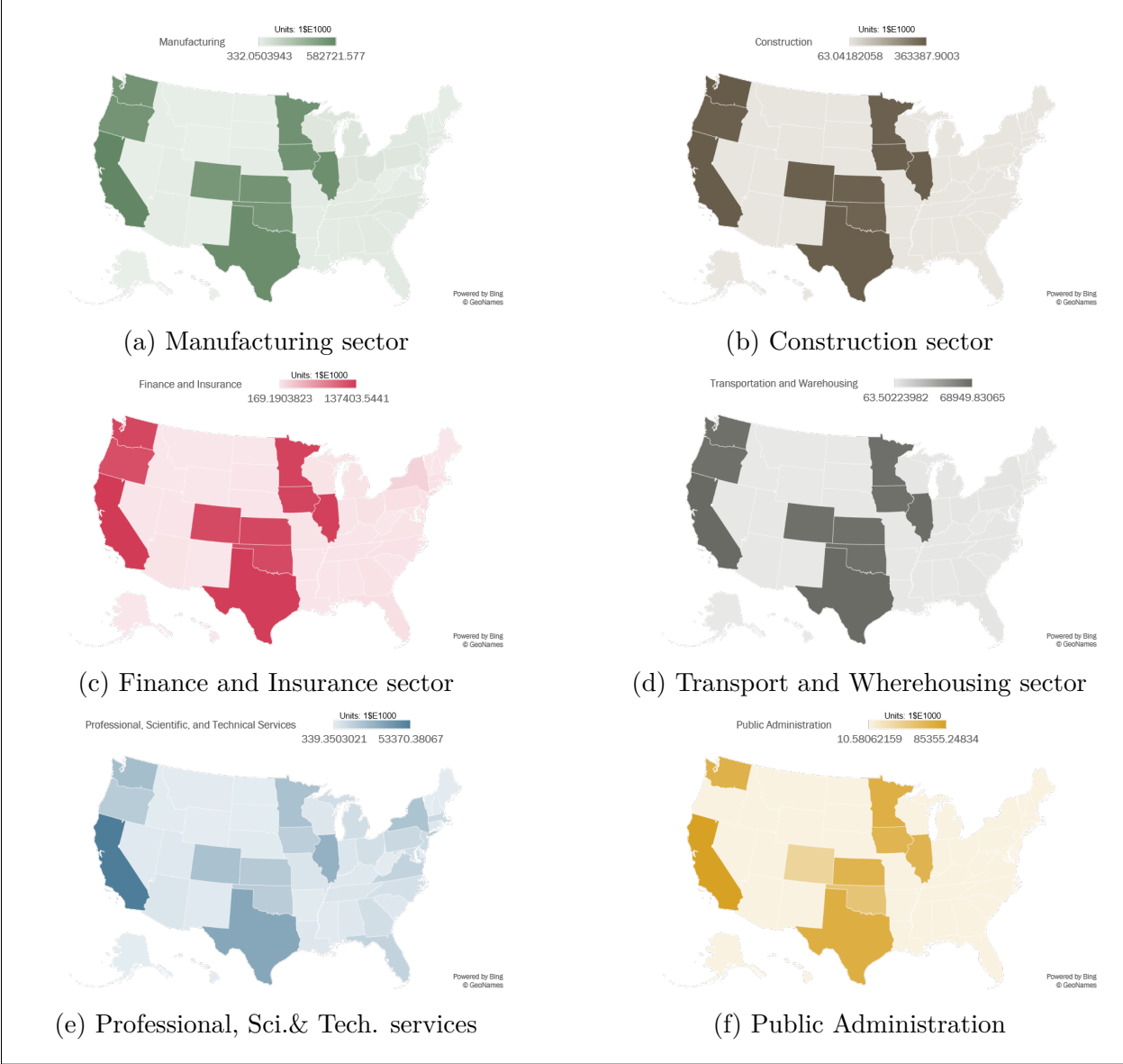


Figure 6.7. Top 6 Sector wise and state wise economic impacts in thousands of USD

and machinery manufacturing discussed before tend to be closely related to wind energy sector while other sectors such as paper, food and furniture manufacturing tend to be loosely related.

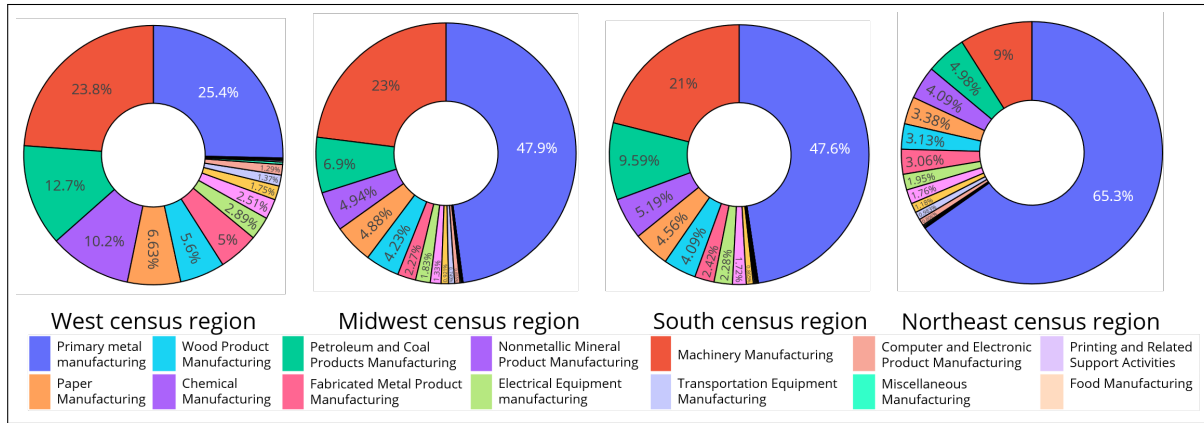


Figure 6.8. 4 census region-wise change in energy consumption (%) across the manufacturing sub-sectors

6.5 Conclusions

Creation of a US-MRIO table using the IE Lab platform has provided a very useful model to study the potential impacts of wind energy expansion in the US economy. Growing concerns of impact of greenhouse gas emissions due to rising population and increase in energy demand is leading to adoption of renewable energy technologies. While there is still a strong coal and natural gas-based generation, several federal agencies such as National Renewable Energy Laboratory (NREL) have been providing guidance on clean energy transitions and addition of new capacity because of the vast land resource that US possess. This provides ample opportunity for generation of wind and solar energy power. Through this study, it was demonstrated that adoption of wind energy only in top 10 states has a huge positive economic impact on rest of the US. Governments and citizens can equally benefit from such a boost in local and federal economy along with potential benefits of reduction in greenhouse gases providing the pollution abatement over long term. However, energy footprint of the new renewable energy capacity addition is also important to account for understanding the total increase in energy demand vs gain in additional capacity. While this increase in energy

demand is a onetime increase for the particular year, the generation capacity added will be functional for at least 25 years. Hence, overall there should be a net energy gain due to the installation of new wind farms in the US.

The results on energy consumption analysis in different regions from this study can potentially be used to calculate the energy return on investment (ERIO). These MRIO based ERIO for each region can help governments understand how introducing a new mix of renewable energy production in a region (ex: wind, solar, hydro, etc) can lead to impacts in other regions, providing a framework to establish interregional co-operation to shift towards lower environmental impacts. For example, studies were performed using I-O methodology to evaluate Chinese national level household indirect energy consumption (HIEC) and inform policymakers about the effects of using alternate energy sources on HIEC at a national level [136]. The US-MRIO table generated from this work can be used to further advance such HIEC analysis studies to calculate effects of using alternate energy sources in different regions within US. Since the IE Lab is also equipped to produce a time series of US-MRIO tables, it can also help in setting an optimal growth rate for renewable energy's share in the total energy supply mix based on given budget and environmental load constraints. Such growth studies using I-O methodology were performed in the past at national level to quantitatively analyse US energy policy [137] and more recently to understand the transformation of Turkish economy [138]. Further, US-MRIO tables can also be used by policy makers to study different scenarios such as multi regional impacts associated with achieving the target of limiting the global warming to 1.5 °C, 2 °C and 3 °C by 2100 or declining the CO₂ emissions by 20% or 30% by 2030.

7. DISSERTATION SUMMARY AND FUTURE WORK

7.1 Research gaps addressed

7.1.1 Mapping material flows at spatial resolution for LCA

Followed by the introductory chapter (**ch-1**), chapter **2** presents how material flows were quantified with the help of process modeling techniques at high spatial resolution which were then used in performing environmental sustainability assessment. Further, process models were developed to be representative of industrial production levels in the given region which made it possible to overcome the linearity challenges of LCA data-sets by taking the economies of scale into consideration. The process modeling approach described in the case study is reproducible for other regions provided the underlying mechanistic mass balances and chemical kinetics modeling is modeled accurately. Developed process models need to be sensitive to the variations in material input characteristics and production recipes of the region under study to accurately quantify material flows. For example, if the feedstock of producing biodiesel is cotton seed oil instead of soybean oil in a different region, modifications have to be made to the process model developed to accommodate the change in input material characteristics. The transesterification reactions modeled must take into account the new triglyceride compositions in cotton seed oil. By having such control over the individual unit-operations in the model, reproducibility of the approach described in this chapter can be maintained. Further expanding on the scope of the method described, process modeling approach can also be used in performing consequential environmental impact assessment. For example, a consequential LCA can be performed to calculate potential impacts of introducing cotton seed oil based biodiesel production system in Indiana. Since such an industry does not exist in Indiana, no empirical data will be available in LCA data sets to perform impact assessment and using spatially aggregated data or data from another region will not be able to accurately model the scenario. To overcome these challenges, process models can be developed to simulate cotton seed based biodiesel production in Indiana.

7.1.2 Quantifying advanced thermodynamic flows using EGA

In chapter 3, a bottom-up thermodynamic flow quantification approach was established. Using this approach, advanced thermodynamic sustainability assessments can be performed with minimal empirical data requirements. Since most of the empirical thermodynamic data available is from an energy usage standpoint, such bottom-up approaches could provide means to get a comprehensive understanding of the thermodynamic efficiencies of the various systems being studied for sustainability assessment. This thermodynamic flow accounting framework maintains all the advantages offered by the bottom-up material flow accounting from the previous chapter (2) framework and can even be appended on top of it. For example, the material flow accounting performed for the soybean biodiesel case study can be taken a step further by applying EGA to the already developed Aspen Plus process model. The energy flows from the biodiesel model can then be linked via LCA data-sets to upstream sources producing the required energy. The advancements in thermodynamic efficiencies of sub-systems of the biodiesel production can then be directly linked to reduction in impacts associated with upstream sources supplying the energy. Together with the methods from the previous chapter, both the types of physical flows (material and thermodynamic) can now be holistically quantified, thus providing a detailed understanding of physical flows and aid in reduction of overall resource usage.

7.1.3 Modeling the physical economy of a region using bottom-up approach

In chapter 4, the scope of the established bottom-up methods from previous chapters was further expanded to quantify flows at an economy-wide level. Mechanistic models that can simulate material transformation processes in various economic sectors were developed (EMs). The models outputs were then integrated with the IO framework of PSUTs and PI-OTs to provide a standardized scheme to quantify material flows at high sectoral and spatial resolution. This integrated and over-encompassing method established retains all the data resolution related to flows from each individual components (a single EM) while expanding to model a much larger system such as the physical economy of a region. This chapter also discusses the various methods that are available to model, scale, and validate different

types of material transformation processes (PCSE, Python, Aspen Plus, etc). Finally, a very detailed demonstrative case study was provided to show how the developed framework can be used. The agro-based physical economy model for Illinois was developed in the form of PSUTs and PIOTs using 11 EMs that simulated material flows across 11 different economic sectors. The PSUTs and PIOTs were interpreted to get highly useful information such as carbon and nitrogen usage in different sectors. Finally, the detailed chemical composition information available of all the material flows was then used to model potential recycling of wastes into useful commodities to increase material circularity. With a new recycling sector included, new PSUTs and PIOTs were developed to analyze changes in resource use patterns, structural changes and reduction in overall waste flows from the physical economy modeled.

7.1.4 Automated tools and cloud platform for physical economy modeling

In chapter 5, information was provided on the development of automated tools (MFDES) and collaborative cloud infrastructure (PIOTHub). Since the lead times and efforts required can be very high to develop novel EMs and construct new PSUTs and PIOTs for different regions and economic sectors, most of the model independent and standardized steps in the approach were automated. MFDES tool developed can simultaneously simulate EMs developed using different techniques, extract material flows from them, characterize the flows as various commodities and waste, and finally, construct PSUTs and PIOTs to model a physical economy. It also provides a heatmap visualization for a more qualitative interpretation of the physical economy. To increase the applications of the MFDES tool, it was implemented on a cloud-based collaborative platform called PIOTHub. Researchers across the world can upload novel EMs developed using different techniques that simulate material flows at different spatial, sectoral, and temporal resolutions. PIOTHub then simulates all the models, compiles different heterogeneous data from the simulation results, and generates PIOTs and PSUTs to model physical economies under study. The PIOTHub platform also makes it possible to share EMs and developed PIOTs with other researchers.

7.1.5 Computational tools for disaggregating national level economic data for sustainability assessment

In the final chapter 6, since bottom-up approaches may not be suitable in all scenarios, further improvements to existing allocation methods are explored, especially allocation of aggregated monetary flows. In their current stage, bottom up models such as EMs cannot directly quantify monetary flows, especially abstract flows from industries such as service sectors. While the numeric value of a physical flow (ex: kg of steel) remains the same irrespective of where and how the flow exists, monetary flow values can vary a lot. The same commodity can have different monetary values in different parts of the world and the value can even reduce to nothing when it turns into waste. Therefore, to enable a holistic integration of all existing flow accounting methods, advances have to be made in other approaches too as addressed in this chapter. A computational platform called IE Lab was used to disaggregate national level monetary flows of the US economy into multi-regional and multi-sectoral flows. Constrained optimization techniques were employed to use any available regional information as a constrain to allocate a national level flow to individual region and economic sector. Using the MRIO developed using IE lab, a case study of assessing multi-regional economic and energy impacts of wind energy expansion was performed within the EEIO framework.

7.1.6 Conclusion of objectives

With the methods demonstrated in each of the chapters of this dissertation, a mechanistic, comprehensive and integrative environmental flow accounting framework was established. Further, automated tools and collaborative cloud infrastructures were developed to reduce the lead times in flow accounting and promote cross-disciplinary collaborations. The work in this dissertation provides a template to perform mechanistic bottom-up accounting of material and thermodynamic flows. The flows can be accounted ranging from a single process at an individual industry level to modeling complete physical economy of a region, while maintaining high granularity in terms of material composition (ex: elemental level granularity). The flows accounted using the approaches presented here can be used to create highly detailed

maps of environmentally relevant flows in economies and provide highly useful information such as material consumption and emission trends, interdependencies among industries (both within and across regions), impacts of deploying new technologies, and strategies for novel environmental policy implementations. Finally, the mechanistic approaches are compatible with existing data-sets (ex: LCI databases) which make it possible to seamlessly use mechanistic model based simulated data wherever empirical data is unavailable (or not reliable) to perform sustainability assessment.

7.2 Future work

The research advancement made in this dissertation established a method to integrate multiple flow accounting methods and modeling techniques. The current MFDES and PIO-THub tools developed can simulate and handle material flows coming models built in computational environments such as Aspen Plus, Python, Excel, and can integrate the outputs with existing data built in other models environments. A modular approach was built into the tool architecture which enables adding new modules parallel to the existing ones that currently process three different computational environments. In the future, more modules can be added into the architecture to make it compatible with a wide range of modeling techniques used in multiple research areas. For example, models built in other programming languages, Aspen energy flow models, LCA software, and discreet even simulation software can be appended in MFDES to reel in more models to construct a much bigger physical economy models. Finally, while MFDES can technically process data from outputs of other top-down approaches such as the IE Lab, it was primarily built to address the need of handling heterogeneity in bottom-up modeling techniques. Integrative modules can be built and added to MFDES to bridge top down monetary flow modeling and allocation techniques with bottom-up and mechanistic physical flow techniques to greatly increase the scope of applications.

REFERENCES

- [1] “The Circularity Gap Report 2020,” Circle Economy, Tech. Rep., 2020. [Online]. Available: <https://www.circularity-gap.world/2020>.
- [2] *Climate Watch: Data for Climate Action - GHG emissions*, Washington, DC, 2018. [Online]. Available: <https://www.climatewatchdata.org/>.
- [3] S. Kaza, L. C. Yao, P. Bhada-Tata, and F. Van Woerden, *What a Waste 2.0: A Global Snapshot of Solid Waste Management to 2050*. Washington, DC: World Bank, Sep. 2018. DOI: [10.1596/978-1-4648-1329-0](https://doi.org/10.1596/978-1-4648-1329-0).
- [4] “International Energy Outlook 2019,” U.S. Energy Information Administration, Washington, DC, Tech. Rep., 2019. [Online]. Available: <https://www.eia.gov/outlooks/ieo/pdf/ieo2019.pdf>.
- [5] D. Spratt and I. Dunlop, “Existential climate-related security risk: A scenario approach,” Breakthrough National Centre for Climate Restoration, Australia, Tech. Rep., 2019. [Online]. Available: <https://www.breakthroughonline.org.au>.
- [6] V. Masson-Delmotte, P. Zhai, H.-O. Pörtner, D. Roberts, J. Skea, P. R. Shukla, A. Pirani, W. Moufouma-Okia, C. Péan, R. Pidcock, S. Connors, J. B. R. Matthews, Y. Chen, X. Zhou, M. I. Gomis, E. Lonnoy, T. Maycock, M. Tignor, and T. Waterfield, “Global warming of 1.5°C - An IPCC Special Report on the impacts of global warming of 1.5°C above pre-industrial levels and related global greenhouse gas emission pathways, in the context of strengthening the global response to the threat of climate change,” Intergovernmental Panel on Climate Change, Tech. Rep., 2018. [Online]. Available: <https://www.ipcc.ch/sr15/download/>.
- [7] Y. Xu, V. Ramanathan, and D. G. Victor, “Global warming will happen faster than we think,” *Nature*, vol. 564, no. 7734, pp. 30–32, Dec. 2018. DOI: [10.1038/d41586-018-07586-5](https://doi.org/10.1038/d41586-018-07586-5).
- [8] “Indicators of Sustainable Development: Guidelines and Methodologies, Third Edition,” United Nations, Tech. Rep., 2007. [Online]. Available: <https://sustainabledevelopment.un.org/index.php?page=view%7B%5C%7Dtype=400%7B%5C%7Dnr=107%7B%5C%7Dmenu=1515>.
- [9] A. Scerri and P. James, “Accounting for sustainability: combining qualitative and quantitative research in developing ‘indicators’ of sustainability,” *International Journal of Social Research Methodology*, vol. 13, no. 1, pp. 41–53, Feb. 2010. DOI: [10.1080/13645570902864145](https://doi.org/10.1080/13645570902864145).

- [10] I. A. Pissourios, “An interdisciplinary study on indicators: A comparative review of quality-of-life, macroeconomic, environmental, welfare and sustainability indicators,” *Ecological Indicators*, vol. 34, pp. 420–427, 2013. DOI: [10.1016/j.ecolind.2013.06.008](https://doi.org/10.1016/j.ecolind.2013.06.008).
- [11] R. Čiegis and R. Čiegis, “Laws of thermodynamics and sustainability of the economy,” *Engineering Economics*, vol. 57, no. 2, 2008. DOI: [10.5755/j01.ee.57.2.11525](https://doi.org/10.5755/j01.ee.57.2.11525).
- [12] D. P. Sekulic and J. Sankara, “Advanced thermodynamics metrics for sustainability assessments of open engineering systems,” *Thermal Science*, vol. 10, no. 1, pp. 125–140, 2006. DOI: [10.2298/TSCI0601125S](https://doi.org/10.2298/TSCI0601125S).
- [13] A. de Koning, M. Bruckner, S. Lutter, R. Wood, K. Stadler, and A. Tukker, “Effect of aggregation and disaggregation on embodied material use of products in input–output analysis,” *Ecological Economics*, vol. 116, pp. 289–299, 2015.
- [14] “U.S. Life Cycle Inventory Database,” National Renewable Energy Laboratory, Tech. Rep., 2012. [Online]. Available: <https://www.lcaccommons.gov/nrel/search>.
- [15] I. Tsiropoulos, A. P. Faaij, J. E. Seabra, L. Lundquist, U. Schenker, J. F. Briois, and M. K. Patel, “Life cycle assessment of sugarcane ethanol production in India in comparison to Brazil,” *International Journal of Life Cycle Assessment*, vol. 19, no. 5, pp. 1049–1067, 2014. DOI: [10.1007/s11367-014-0714-5](https://doi.org/10.1007/s11367-014-0714-5).
- [16] P. K. Campbell, T. Beer, and D. Batten, “Life cycle assessment of biodiesel production from microalgae in ponds,” *Bioresource technology*, vol. 102, no. 1, pp. 50–56, 2011. DOI: [10.1016/j.biortech.2010.06.048](https://doi.org/10.1016/j.biortech.2010.06.048).
- [17] S. Merciai and J. Schmidt, “Methodology for the Construction of Global Multi-Regional Hybrid Supply and Use Tables for the EXIOBASE v3 Database,” *Journal of Industrial Ecology*, vol. 22, no. 3, pp. 516–531, Jun. 2018. DOI: [10.1111/jiec.12713](https://doi.org/10.1111/jiec.12713).
- [18] M. Saidani, B. Yannou, Y. Leroy, and F. Cluzel, “Hybrid top-down and bottom-up framework to measure products’ circularity performance Hybrid top-down and bottom-up framework to measure products’ circularity performance Hybrid top-down and bottom-up framework to measure products’ circularity performance AUTHORS,” in *International Conference on Engineering Design, ICED 17*, vol. 17, Vancouver, Aug. 2017. [Online]. Available: <https://hal.archives-ouvertes.fr/hal-01571581>.
- [19] X. Zhang, Z. Li, L. Ma, C. Chong, and W. Ni, “Analyzing Carbon Emissions Embodied in Construction Services: A Dynamic Hybrid Input–Output Model with Structural Decomposition Analysis,” *Energies*, vol. 12, no. 8, p. 1456, Apr. 2019. DOI: [10.3390/en12081456](https://doi.org/10.3390/en12081456).

- [20] V. S. G. Vunnava and S. Singh, “Spatial life cycle analysis of soybean-based biodiesel production in Indiana, USA using process modeling,” *Processes*, vol. 8, no. 4, p. 392, Mar. 2020. DOI: [10.3390/PR8040392](https://doi.org/10.3390/PR8040392).
- [21] L. Nitschelm, J. Aubin, M. S. Corson, V. Viaud, and C. Walter, “Spatial differentiation in life cycle assessment lca applied to an agricultural territory: Current practices and method development,” *Journal of cleaner production*, vol. 112, pp. 2472–2484, 2016.
- [22] D. Tilman, R. Socolow, J. A. Foley, J. Hill, E. Larson, L. Lynd, S. Pacala, J. Reilly, T. Searchinger, C. Somerville, *et al.*, “Beneficial biofuels—the food, energy, and environment trilemma,” *Science*, vol. 325, no. 5938, pp. 270–271, 2009.
- [23] S. Kim and B. E. Dale, “Life cycle assessment of various cropping systems utilized for producing biofuels: Bioethanol and biodiesel,” *Biomass and Bioenergy*, vol. 29, no. 6, pp. 426–439, 2005.
- [24] Z. Qin, Q. Zhuang, X. Cai, Y. He, Y. Huang, D. Jiang, E. Lin, Y. Liu, Y. Tang, and M. Q. Wang, “Biomass and biofuels in china: Toward bioenergy resource potentials and their impacts on the environment,” *Renewable and Sustainable Energy Reviews*, vol. 82, pp. 2387–2400, 2018.
- [25] U. Kesieme, K. Pazouki, A. Murphy, and A. Chrysanthou, “Attributional life cycle assessment of biofuels for shipping: Addressing alternative geographical locations and cultivation systems,” *Journal of environmental management*, vol. 235, pp. 96–104, 2019.
- [26] J. Chen, J. Li, W. Dong, X. Zhang, R. D. Tyagi, P. Drogui, and R. Y. Surampalli, “The potential of microalgae in biodiesel production,” *Renewable and Sustainable Energy Reviews*, vol. 90, pp. 336–346, 2018.
- [27] I. Tsiropoulos, A. P. Faaij, J. E. Seabra, L. Lundquist, U. Schenker, J.-F. Briois, and M. K. Patel, “Life cycle assessment of sugarcane ethanol production in india in comparison to brazil,” *The International Journal of Life Cycle Assessment*, vol. 19, no. 5, pp. 1049–1067, 2014.
- [28] L. Reijnders and M. A. Huijbregts, “Palm oil and the emission of carbon-based greenhouse gases,” *Journal of cleaner production*, vol. 16, no. 4, pp. 477–482, 2008.
- [29] É. G. Castanheira, R. Grisoli, S. Coelho, G. A. da Silva, and F. Freire, “Life-cycle assessment of soybean-based biodiesel in europe: Comparing grain, oil and biodiesel import from brazil,” *Journal of Cleaner Production*, vol. 102, pp. 188–201, 2015.

- [30] M. A. Rajaeifar, B. Ghobadian, M. Safa, and M. D. Heidari, “Energy life-cycle assessment and co2 emissions analysis of soybean-based biodiesel: A case study,” *Journal of Cleaner Production*, vol. 66, pp. 233–241, 2014.
- [31] M. Hiloidhari, D. Baruah, A. Singh, S. Katakai, K. Medhi, S. Kumari, T. Ramachandra, B. M. Jenkins, and I. S. Thakur, “Emerging role of geographical information system (gis), life cycle assessment (lca) and spatial lca (gis-lca) in sustainable bioenergy planning,” *Bioresource technology*, vol. 242, pp. 218–226, 2017.
- [32] S. M. H. Tabatabaie, H. Tahami, and G. S. Murthy, “A regional life cycle assessment and economic analysis of camelina biodiesel production in the pacific northwestern us,” *Journal of Cleaner Production*, vol. 172, pp. 2389–2400, 2018.
- [33] F. Humpenöder, R. Schaldach, Y. Cikovani, and L. Schebek, “Effects of land-use change on the carbon balance of 1st generation biofuels: An analysis for the european union combining spatial modeling and lca,” *Biomass and bioenergy*, vol. 56, pp. 166–178, 2013.
- [34] K. R. Cronin, T. M. Runge, X. Zhang, R. C. Izaurralde, D. J. Reinemann, and J. C. Sinistore, “Spatially explicit life cycle analysis of cellulosic ethanol production scenarios in southwestern michigan,” *BioEnergy Research*, vol. 10, no. 1, pp. 13–25, 2017.
- [35] I. Butnar, J. Rodrigo, C. M. Gasol, and F. Castells, “Life-cycle assessment of electricity from biomass: Case studies of two biocrops in spain,” *Biomass and Bioenergy*, vol. 34, no. 12, pp. 1780–1788, 2010.
- [36] L. Patouillard, C. Bulle, C. Querleu, D. Maxime, P. Osset, and M. Margni, “Critical review and practical recommendations to integrate the spatial dimension into life cycle assessment,” *Journal of Cleaner Production*, vol. 177, pp. 398–412, 2018.
- [37] U. NASS, “Usda/nass quickstats ad-hoc query tool,” *United States Department of Agriculture*, 2014.
- [38] U.S. Energy Information Administration, *Manufacturing Energy Consumption Survey (MECS) - Data - U.S. Energy Information Administration (EIA)*, 2017. [Online]. Available: <https://www.eia.gov/consumption/manufacturing/data/2014/%7B%5C%7Dr1> (visited on 06/25/2019).
- [39] S. R. Potter, *Model simulation of soil loss, nutrient loss, and change in soil organic carbon associated with crop production*. United States Department of Agriculture, Natural Resource Conservation Service, 2006.
- [40] *FACT SHEET: Biofuels Plants in Indiana*. 2013.

- [41] K.-W. Lee, J. H. Mei, L. Yan, Y.-W. Kim, K.-W. Chung, *et al.*, “A kinetic study on the transesterification of glyceryl monooleate and soybean used frying oil to biodiesel,” *Journal of Industrial and Engineering Chemistry*, vol. 13, no. 5, pp. 799–807, 2007.
- [42] *Soybean Production Systems: Where Do Indiana Soybean Producers Sell*. 2006.
- [43] *ISDA: Grain Licensee Listing*. [Online]. Available: <https://www.in.gov/isda/2399.htm> (visited on 11/16/2020).
- [44] V. S. G. Vunnava and S. Singh, “Entropy generation analysis of sequential Anaerobic Digester Ion-Exchange technology for Phosphorus extraction from waste,” *Journal of Cleaner Production*, vol. 221, pp. 55–62, Jun. 2019. DOI: [10.1016/J.JCLEPRO.2019.02.020](https://doi.org/10.1016/J.JCLEPRO.2019.02.020).
- [45] T. G. Gutowski, M. S. Branham, J. B. Dahmus, A. J. Jones, A. Thiriez, and D. P. Sekulic, “Thermodynamic analysis of resources used in manufacturing processes,” *Environmental science & technology*, vol. 43, no. 5, pp. 1584–1590, 2009. DOI: [10.1021/es8016655](https://doi.org/10.1021/es8016655).
- [46] G. Houillon and O. Jolliet, “Life cycle assessment of processes for the treatment of wastewater urban sludge: Energy and global warming analysis,” *Journal of Cleaner Production*, vol. 13, no. 3, pp. 287–299, 2005. DOI: [10.1016/j.jclepro.2004.02.022](https://doi.org/10.1016/j.jclepro.2004.02.022).
- [47] A. Bejan, “Fundamentals of exergy analysis, entropy generation minimization, and the generation of flow architecture,” *International Journal of Energy Research*, vol. 26, no. 7, pp. 0–43, 2002. DOI: [10.1002/er.804](https://doi.org/10.1002/er.804).
- [48] M. A. J. Huijbregts, S. Hellweg, R. Frischknecht, H. W. M. Hendriks, K. Hungerbühler, and A. J. Hendriks, “Cumulative energy demand as predictor for the environmental burden of commodity production,” *Environmental Science & Technology*, vol. 44, no. 6, pp. 2189–2196, 2010. DOI: [10.1021/es902870s](https://doi.org/10.1021/es902870s).
- [49] X. Liu, L. Chen, X. Qin, and F. Sun, “Exergy loss minimization for a blast furnace with comparative analyses for energy flows and exergy flows,” *Energy*, vol. 93, pp. 10–19, Dec. 2015. DOI: [10.1016/j.energy.2015.09.008](https://doi.org/10.1016/j.energy.2015.09.008).
- [50] S. M. Jasinski, *2015 Minerals Yearbook, Phosphate Rock [Advance release]*. U.S. Department of the Interior, U.S. Geological Survey, 2016. [Online]. Available:
- [51] D. Cordell, J. O. Drangert, and S. White, “The story of phosphorus: Global food security and food for thought,” *Global Environmental Change*, vol. 19, no. 2, pp. 292–305, 2009. DOI: [10.1016/j.gloenvcha.2008.10.009](https://doi.org/10.1016/j.gloenvcha.2008.10.009).

- [52] E. Ghane, A. Z. Ranaivoson, G. W. Feyereisen, C. J. Rosen, and J. F. Moncrief, “Comparison of contaminant transport in agricultural drainage water and urban stormwater runoff,” *PLOS ONE*, vol. 11, no. 12, pp. 1–23, Dec. 2016. DOI: [10.1371/journal.pone.0167834](https://doi.org/10.1371/journal.pone.0167834).
- [53] L. Bouwman, K. K. Goldewijk, K. W. Van Der Hoek, A. H. W. Beusen, D. P. Van Vuuren, J. Willems, M. C. Rufino, and E. Stehfest, “Exploring global changes in nitrogen and phosphorus cycles in agriculture induced by livestock production over the 1900–2050 period,” *Proceedings of the National Academy of Sciences*, vol. 110, no. 52, pp. 20 882–20 887, 2013, ISSN: 0027-8424. DOI: [10.1073/pnas.1012878108](https://doi.org/10.1073/pnas.1012878108).
- [54] M. Oliveira and A. V. Machado, “The role of phosphorus on eutrophication: a historical review and future perspectives,” *Environmental Technology Reviews*, vol. 2, no. 1, pp. 117–127, Jan. 2013. DOI: [10.1080/21622515.2013.861877](https://doi.org/10.1080/21622515.2013.861877).
- [55] C. E. Williamson, W. Dodds, T. K. Kratz, and M. A. Palmer, “Lakes and streams as sentinels of environmental change in terrestrial and atmospheric processes,” *Frontiers in Ecology and the Environment*, vol. 6, no. 5, pp. 247–254, Jun. 2008. DOI: [10.1890/070140](https://doi.org/10.1890/070140).
- [56] A. M. Michalak, E. J. Anderson, D. Beletsky, S. Boland, N. S. Bosch, T. B. Bridgeman, J. D. Chaffin, K. Cho, R. Confesor, I. Daloglu, J. V. DePinto, M. A. Evans, G. L. Fahnenstiel, L. He, J. C. Ho, L. Jenkins, T. H. Johengen, K. C. Kuo, E. LaPorte, X. Liu, M. R. McWilliams, M. R. Moore, D. J. Posselt, R. P. Richards, D. Scavia, A. L. Steiner, E. Verhamme, D. M. Wright, and M. A. Zagorski, “Record-setting algal bloom in lake erie caused by agricultural and meteorological trends consistent with expected future conditions,” *Proceedings of the National Academy of Sciences*, vol. 110, no. 16, pp. 6448–6452, 2013. DOI: [10.1073/pnas.1216006110](https://doi.org/10.1073/pnas.1216006110).
- [57] J. D. Doyle and S. A. Parsons, “Struvite formation, control and recovery,” *Water Research*, vol. 36, no. 16, pp. 3925–3940, Sep. 2002. DOI: [10.1016/S0043-1354\(02\)00126-4](https://doi.org/10.1016/S0043-1354(02)00126-4).
- [58] J. Nieminen, “Phosphorus recovery and recycling from municipal wastewater sludge,” M.S. thesis, Aalto University, Finland, 2010.
- [59] A. Laurent, S. Olsen, and M. Hauschild, “Carbon footprint as environmental performance indicator for the manufacturing industry,” *CIRP Annals*, vol. 59, no. 1, pp. 37–40, 2010. DOI: [10.1016/j.cirp.2010.03.008](https://doi.org/10.1016/j.cirp.2010.03.008).
- [60] M. Egan, “The Water Footprint Assessment Manual. Setting the Global Standard,” *Social and Environmental Accountability Journal*, vol. 31, no. 2, pp. 181–182, 2011. DOI: [10.1080/0969160X.2011.593864](https://doi.org/10.1080/0969160X.2011.593864).

- [61] M. Wackernagel, L. Onisto, P. Bello, A. C. Linares, I. S. L. Falfan, J. M. Garcia, A. I. S. Guerrero, and M. G. S. Guerrero, “National natural capital accounting with the ecological footprint concept,” *Ecological Economics*, vol. 29, no. 3, pp. 375–390, 1999, ISSN: 0921-8009. DOI: [10.1016/S0921-8009\(98\)90063-5](https://doi.org/10.1016/S0921-8009(98)90063-5).
- [62] K. Fang, R. Heijungs, and G. R. De Snoo, “Understanding the complementary linkages between environmental footprints and planetary boundaries in a footprint-boundary environmental sustainability assessment framework,” *Ecological Economics*, vol. 114, pp. 218–226, 2015. DOI: [10.1016/j.ecolecon.2015.04.008](https://doi.org/10.1016/j.ecolecon.2015.04.008).
- [63] C. He, Z. Liu, and M. Hodgins, “Using Life Cycle Assessment for Quantifying Embedded Water and Energy in a Water Treatment System,” no. February 2012, 2013. [Online]. Available: <http://www.waterrf.org/PublicReportLibrary/4443.pdf>.
- [64] L. Liberti, D. Petruzzelli, and L. De Florio, “REM NUT Ion Exchange Plus Struvite Precipitation Process,” *Environmental Technology*, vol. 22, no. 11, pp. 1313–1324, Nov. 2001. DOI: [10.1080/09593330409355443](https://doi.org/10.1080/09593330409355443).
- [65] C. Vaneeckhaute, V. Lebuf, E. Michels, E. Belia, P. A. Vanrolleghem, F. M. G. Tack, and E. Meers, “Nutrient Recovery from Digestate: Systematic Technology Review and Product Classification,” *Waste and Biomass Valorization*, vol. 8, no. 1, pp. 21–40, 2017. DOI: [10.1007/s12649-016-9642-x](https://doi.org/10.1007/s12649-016-9642-x).
- [66] L. M. Blaney, S. Cinar, and A. K. SenGupta, “Hybrid anion exchanger for trace phosphate removal from water and wastewater,” *Water Research*, vol. 41, no. 7, pp. 1603–1613, Apr. 2007. DOI: [10.1016/j.watres.2007.01.008](https://doi.org/10.1016/j.watres.2007.01.008).
- [67] D. Hellstrom and E. Karrman, “Exergy Analysis and Nutrient Flows of Various Sewerage Systems,” *Water Science and Technology*, vol. 35, no. 9, pp. 135–144, 1997. DOI: [10.1016/S0273-1223\(97\)00191-1](https://doi.org/10.1016/S0273-1223(97)00191-1).
- [68] A. Sciacovelli, V. Verda, and E. Sciubba, “Entropy generation analysis as a design tool - a review,” *Renewable and Sustainable Energy Reviews*, vol. 43, pp. 1167–1181, 2015. DOI: [10.1016/j.rser.2014.11.104](https://doi.org/10.1016/j.rser.2014.11.104).
- [69] M. Henze and E. Publishing, *Biological Wastewater Treatment: Principles, Modelling and Design*. IWA Pub., 2008, ISBN: 9781680155822. [Online]. Available: <https://books.google.com/books?id=TDifnQAACAAJ>.
- [70] R. Caspi, T. Altman, R. Billington, K. Dreher, H. Foerster, C. A. Fulcher, T. A. Holland, I. M. Keseler, A. Kothari, A. Kubo, M. Krummenacker, M. Latendresse, L. A. Mueller, Q. Ong, S. Paley, P. Subhraveti, D. S. Weaver, D. Weerasinghe, and P. D. Zhang Peifen and Karp, “The metacyc database of metabolic pathways and enzymes and the biocyc collection of pathway/genome databases,” *Nucleic Acids Research*, vol. 42, no. D1, pp. D459–D471, 2014. DOI: [10.1093/nar/gkt1103](https://doi.org/10.1093/nar/gkt1103).

- [71] R. Torres-Castillo, P. Llabres-Luengo, and J. Mata-Alvarez, “Temperature effect on anaerobic digestion of bedding straw in a one phase system at different inoculum concentration,” *Agriculture, Ecosystems and Environment*, vol. 54, no. 1, pp. 55–66, 1995. DOI: [10.1016/0167-8809\(95\)00592-G](https://doi.org/10.1016/0167-8809(95)00592-G).
- [72] A. Amini, Y. Kim, J. Zhang, T. Boyer, and Q. Zhang, “Environmental and economic sustainability of ion exchange drinking water treatment for organics removal,” *Journal of Cleaner Production*, vol. 104, pp. 413–421, 2015. DOI: <https://doi.org/10.1016/j.jclepro.2015.05.056>.
- [73] K. H. Mistry, R. K. McGovern, G. P. Thiel, E. K. Summers, S. M. Zubair, and J. H. Lienhard V, “Entropy Generation Analysis of Desalination Technologies,” *Entropy*, vol. 13, no. 12, pp. 1829–1864, Sep. 2011. DOI: [10.3390/e13101829](https://doi.org/10.3390/e13101829).
- [74] R. E. Miller and P. D. Blair, *Input-output analysis: Foundations and extensions, second edition*, 2nd ed. 2009, pp. 1–750, ISBN: 9780511626982. DOI: [10.1017/CB09780511626982](https://doi.org/10.1017/CB09780511626982). arXiv: [arXiv:1011.1669v3](https://arxiv.org/abs/1011.1669v3).
- [75] S. Singh, J. E. Compton, T. R. Hawkins, D. J. Sobota, and E. J. Cooter, “A Nitrogen Physical Input-Output Table (PIOT) model for Illinois,” *Ecological Modelling*, vol. 360, pp. 194–203, 2017. DOI: [10.1016/j.ecolmodel.2017.06.015](https://doi.org/10.1016/j.ecolmodel.2017.06.015).
- [76] H. Wang, X. Wang, J. Song, S. Wang, and X. Liu, “Uncovering regional energy and environmental benefits of urban waste utilization: A physical input-output analysis for a city case,” *Journal of Cleaner Production*, vol. 189, pp. 922–932, Jul. 2018. DOI: [10.1016/j.jclepro.2018.04.107](https://doi.org/10.1016/j.jclepro.2018.04.107).
- [77] B. Zhang, Z. M. Chen, X. H. Xia, X. Y. Xu, and Y. B. Chen, “The impact of domestic trade on China’s regional energy uses: A multi-regional input–output modeling,” *Energy Policy*, vol. 63, pp. 1169–1181, 2013.
- [78] F. Faturay, V. S. G. Vunnava, M. Lenzen, and S. Singh, “Using a new USA multi-region input output (MRIO) model for assessing economic and energy impacts of wind energy expansion in USA,” *Applied Energy*, vol. 261, no. 3, p. 114141, Mar. 2020. DOI: [10.1016/j.apenergy.2019.114141](https://doi.org/10.1016/j.apenergy.2019.114141).
- [79] L. Brand-Correa, P. Brockway, C. Copeland, T. Foxon, A. Owen, and P. Taylor, “Developing an Input-Output Based Method to Estimate a National-Level Energy Return on Investment (EROI),” *Energies*, vol. 10, no. 4, p. 534, Apr. 2017. DOI: [10.3390/en10040534](https://doi.org/10.3390/en10040534).
- [80] M. Lenzen, D. Moran, K. Kanemoto, and A. Geschke, “Building Eora: A Global Multi-Region Input–Output Database at High Country and Sector Resolution,” *Economic Systems Research*, vol. 25, 2013.

- [81] M. P. Timmer, E. Dietzenbacher, B. Los, R. Stehrer, and G. J. de Vries, “An Illustrated User Guide to the World Input-Output Database: The Case of Global Automotive Production,” *Review of International Economics*, vol. 23, no. 3, pp. 575–605, Aug. 2015. DOI: [10.1111/roie.12178](https://doi.org/10.1111/roie.12178).
- [82] R. C. Feenstra and A. Sasahara, “The ‘China shock,’ exports and U.S. employment: A global input–output analysis,” *Review of International Economics*, vol. 26, no. 5, pp. 1053–1083, Nov. 2018. DOI: [10.1111/roie.12370](https://doi.org/10.1111/roie.12370).
- [83] R. Hoekstra and J. C. van den Bergh, “Constructing physical input-output tables for environmental modeling and accounting: Framework and illustrations,” *Ecological Economics*, vol. 59, no. 3, pp. 375–393, Sep. 2006. DOI: [10.1016/j.ecolecon.2005.11.005](https://doi.org/10.1016/j.ecolecon.2005.11.005).
- [84] A. Altimiras-Martin, “Analysing the Structure of the Economy Using Physical Input–Output Tables,” *Economic Systems Research*, vol. 26, no. 4, pp. 463–485, 2014. DOI: [10.1080/09535314.2014.950637](https://doi.org/10.1080/09535314.2014.950637). [Online]. Available: <https://doi.org/10.1080/09535314.2014.950637>.
- [85] P.-C. Chen, V. Alvarado, and S.-C. Hsu, “Water energy nexus in city and hinterlands: Multi-regional physical input-output analysis for Hong Kong and South China,” *Applied Energy*, vol. 225, pp. 986–997, Sep. 2018. DOI: [10.1016/j.apenergy.2018.05.083](https://doi.org/10.1016/j.apenergy.2018.05.083).
- [86] S. Liang and T. Zhang, “Comparing urban solid waste recycling from the viewpoint of urban metabolism based on physical input–output model: A case of Suzhou in China,” *Waste Management*, vol. 32, no. 1, pp. 220–225, Jan. 2012. DOI: [10.1016/j.wasman.2011.08.018](https://doi.org/10.1016/j.wasman.2011.08.018).
- [87] P. Piñero, M. Heikkinen, I. Mäenpää, and E. Pongrácz, “Sector aggregation bias in environmentally extended input output modeling of raw material flows in Finland,” *Ecological Economics*, vol. 119, pp. 217–229, Nov. 2015. DOI: [10.1016/j.ecolecon.2015.09.002](https://doi.org/10.1016/j.ecolecon.2015.09.002).
- [88] United States Census Bureau, “North American Industry Classification System,” Tech. Rep., 2017. [Online]. Available: .
- [89] *Illinois Soybean Association*. [Online]. Available: <https://www.ilsoy.org/> (visited on 10/23/2020).
- [90] United States Department of Agriculture, *USDA - National Agricultural Statistics Service - Statistics by State*, 2018. [Online]. Available: (visited on 12/02/2019).

- [91] USGS, *State Minerals Statistics and Information*, 2015. [Online]. Available: <https://www.usgs.gov/centers/nmic/state-minerals-statistics-and-information%20http://minerals.usgs.gov/minerals/pubs/state/> (visited on 12/01/2019).
- [92] US Department of Energy, *Energy Information Administration (EIA)*, 2020. [Online]. Available: <https://www.eia.gov/>.
- [93] A. J. de Wit, *PCSE: The Python Crop Simulation Environment*, 2018. [Online]. Available: <https://pcse.readthedocs.io/en/stable/index.html>.
- [94] N. Power, *API Documentation — NASA POWER*. [Online]. Available: <https://power.larc.nasa.gov/docs/v1/>.
- [95] A. de Wit, “PCSE Documentation,” Tech. Rep., 2019. [Online]. Available: <https://buildmedia.readthedocs.org/media/pdf/pcse/latest/pcse.pdf>.
- [96] S. Merciai and J. Schmidt, “Methodology for the Construction of Global Multi-Regional Hybrid Supply and Use Tables for the EXIOBASE v3 Database,” *Journal of Industrial Ecology*, vol. 22, no. 3, pp. 516–531, Jun. 2018. DOI: [10.1111/jiec.12713](https://doi.org/10.1111/jiec.12713).
- [97] M. Bruckner, R. Wood, D. Moran, N. Kuschig, H. Wieland, V. Maus, and J. Börner, “FABIO - The Construction of the Food and Agriculture Biomass Input-Output Model,” *Environmental Science and Technology*, vol. 53, no. 19, pp. 11 302–11 312, 2019. DOI: [10.1021/acs.est.9b03554](https://doi.org/10.1021/acs.est.9b03554).
- [98] M. Lenzen, A. Geschke, T. Wiedmann, J. Lane, N. Anderson, T. Baynes, J. Boland, P. Daniels, C. Dey, J. Fry, M. Hadjikakou, S. Kenway, A. Malik, D. Moran, J. Murray, S. Nettleton, L. Poruschi, C. Reynolds, H. Rowley, J. Ugon, D. Webb, and J. West, “Compiling and using input-output frameworks through collaborative virtual laboratories,” *Science of the Total Environment*, vol. 485-486, no. 1, pp. 241–251, Jul. 2014. DOI: [10.1016/j.scitotenv.2014.03.062](https://doi.org/10.1016/j.scitotenv.2014.03.062).
- [99] R. J. Hanes and A. Carpenter, “Evaluating opportunities to improve material and energy impacts in commodity supply chains,” *Environment Systems and Decisions*, vol. 37, no. 1, pp. 6–12, 2017. DOI: [10.1007/s10669-016-9622-5](https://doi.org/10.1007/s10669-016-9622-5).
- [100] K. Stadler, *Multi-Regional Input-Output Analysis in Python*. 2019. [Online]. Available: <https://github.com/konstantinstadler/pymrio>.
- [101] S. Nazara, D. Guo, G. J. D. Hewings, and C. Dridi, “PyIO: Input-Output Analysis with Python PyIO Input-Output Analysis with Python,” University of Illinois at Urbana-Champaign, Tech. Rep., 2003. [Online]. Available: <https://econwpa.ub.uni-muenchen.de/econ-wp/urb/papers/0409/0409002.pdf>.

- [102] S. Pauliuk, G. Majeau-Bettez, K. Stadler, and C. Mutel, *pySUT: Python class for handling supply and use tables*, 2014. [Online]. Available: <https://github.com/stefanpauliuk/pySUT>.
- [103] M. Srocka, *USIO*, 2015. [Online]. Available: <https://github.com/GreenDelta/usio>.
- [104] United Nations, *UN Comtrade, International Trade Statistics Database*, 2019. [Online]. Available: <https://comtrade.un.org/>.
- [105] *2.0 LCA consultants*, 2018. [Online]. Available: <https://lca-net.com/>.
- [106] F. Faturay, M. Lenzen, and K. Nugraha, “A new sub-national multi-region input–output database for Indonesia,” *Economic Systems Research*, vol. 29, pp. 234–251, 2017.
- [107] F. Faturay, S. Y.-Y, E. Dietzenbacher, A. Malik, A. Geschke, and M. Lenzen, “Using Virtual Laboratories for Disaster Analysis – A Case Study of Taiwan,” *Economic Systems Research.*, 2018.
- [108] U.S. Department of Commerce, *U.S. Bureau of Economic Analysis (BEA)*, 2019. [Online]. Available: <https://www.bea.gov/data>.
- [109] United Nations, *Food and Agriculture Organization*, 2020. [Online]. Available: <http://www.fao.org/faostat/en>.
- [110] V. Nicolardi, “Simultaneously balancing Supply-Use Tables at Current and Constant Prices: A new procedure,” *Economic Systems Research*, vol. 25, no. 4, pp. 409–434, Dec. 2013. DOI: [10.1080/09535314.2013.808990](https://doi.org/10.1080/09535314.2013.808990).
- [111] M. C. Serpell, “Incorporating data quality improvement into supply–use table balancing,” *Economic Systems Research*, vol. 30, no. 2, pp. 271–288, Apr. 2018. DOI: [10.1080/09535314.2017.1396962](https://doi.org/10.1080/09535314.2017.1396962).
- [112] M. Stanger, “An Algorithm to Balance Supply and Use Tables,” Statistics Department, International Monetary Fund, Tech. Rep. 03, 2018. DOI: [10.5089/9781484363966.005](https://doi.org/10.5089/9781484363966.005).
- [113] Eurostat, *Eurostat Manual of Supply, Use and Input-Output Tables*. 2008, pp. 1–592, ISBN: 978-92-79-04735-0. DOI: <http://ec.europa.eu/eurostat>.
- [114] M. McLennan and R. Kennell, “Hubzero: A platform for dissemination and collaboration in computational science and engineering,” *Computing in Science & Engineering*, vol. 12, no. 2, pp. 48–53, 2010.
- [115] R. Kalyanam, L. Zhao, C. Song, L. Biehl, D. Kearney, I. L. Kim, J. Shin, N. Villoria, and V. Merwade, “Mygeohub—a sustainable and evolving geospatial science

- gateway,” *Future Generation Computer Systems*, vol. 94, pp. 820–832, 2019. DOI: [10.1016/j.future.2018.02.005](https://doi.org/10.1016/j.future.2018.02.005).
- [116] T. Kluyver, B. Ragan-Kelley, F. Pérez, B. E. Granger, M. Bussonnier, J. Frederic, K. Kelley, J. B. Hamrick, J. Grout, S. Corlay, *et al.*, “Jupyter notebooks—a publishing format for reproducible computational workflows.,” in *ELPUB*, 2016, pp. 87–90.
- [117] R. Wisser and M. Bolinger, “2017 Wind Technologies Market Report,” U.S. Department of Energy, Office of Scientific and Technical Information, Tech. Rep., 2017. [Online]. Available: <https://www.energy.gov/eere/wind/downloads/2017-wind-technologies-market-report>.
- [118] R. Wisser, E. Lantz, T. Mai, J. Zayas, E. DeMeo, E. Eugeni, J. Lin-Powers, and R. Tusing, “Wind Vision: A New Era for Wind Power in the United States,” *Electricity Journal*, vol. 28, no. 9, pp. 120–132, 2015, ISSN: 10406190. DOI: [10.1016/j.tej.2015.09.016](https://doi.org/10.1016/j.tej.2015.09.016).
- [119] M. C. Slattery, E. Lantz, and B. L. Johnson, “State and local economic impacts from wind energy projects: Texas case study,” *Energy Policy*, vol. 39, no. 12, pp. 7930–7940, 2011. DOI: [10.1016/j.enpol.2011.09.047](https://doi.org/10.1016/j.enpol.2011.09.047).
- [120] J. Blazquez, N. Nezamuddin, and T. Zamrik, “Economic policy instruments and market uncertainty: Exploring the impact on renewables adoption,” *Renewable and Sustainable Energy Reviews*, vol. 94, 2018. DOI: [10.1016/j.rser.2018.05.050](https://doi.org/10.1016/j.rser.2018.05.050).
- [121] P. Dvořák, S. Martinát, D. V. der Horst, B. Frantál, and K. Turečková, *Renewable energy investment and job creation; a cross-sectoral assessment for the Czech Republic with reference to EU benchmarks*, Mar. 2017. DOI: [10.1016/j.rser.2016.11.158](https://doi.org/10.1016/j.rser.2016.11.158).
- [122] A. Arvesen and E. G. Hertwich, “Environmental implications of large-scale adoption of wind power: a scenario-based life cycle assessment,” *Environmental Research Letters*, vol. 6, no. 4, p. 045102, Jan. 2011, ISSN: 1748-9326. DOI: [10.1088/1748-9326/6/4/045102](https://doi.org/10.1088/1748-9326/6/4/045102).
- [123] M. Noori, M. Kucukvar, and O. Tatari, “Economic input-output based sustainability analysis of onshore and offshore wind energy systems,” *International Journal of Green Energy*, vol. 12, no. 9, pp. 939–948, Sep. 2015, ISSN: 15435083. DOI: [10.1080/15435075.2014.890103](https://doi.org/10.1080/15435075.2014.890103).
- [124] M. Lenzen, A. Geschke, T. Wiedmann, J. Lane, N. Anderson, T. Baynes, J. Boland, P. Daniels, C. Dey, J. Fry, *et al.*, “Compiling and using input–output frameworks through collaborative virtual laboratories,” *Science of the Total Environment*, vol. 485, pp. 241–251, 2014. DOI: [10.1016/j.scitotenv.2014.03.062](https://doi.org/10.1016/j.scitotenv.2014.03.062).

- [125] M. Lenzen, A. Geschke, A. Malik, J. Fry, J. Lane, T. Wiedmann, S. Kenway, K. Hoang, and A. Cadogan-Cowper, “New multi-regional input–output databases for australia—enabling timely and flexible regional analysis,” *Economic Systems Research*, vol. 29, no. 2, pp. 275–295, 2017. DOI: [10.1080/09535314.2017.1315331](https://doi.org/10.1080/09535314.2017.1315331).
- [126] Y. Wang, A. Geschke, and M. Lenzen, “Constructing a time series of nested multi-region input–output tables,” *International Regional Science Review*, vol. 40, no. 5, pp. 476–499, 2017. DOI: [10.1177/0160017615603596](https://doi.org/10.1177/0160017615603596).
- [127] Y. Wang, “An industrial ecology virtual framework for policy making in china,” *Economic Systems Research*, vol. 29, no. 2, pp. 252–274, 2017. DOI: [10.1080/09535314.2017.1313199](https://doi.org/10.1080/09535314.2017.1313199).
- [128] F. Faturay, M. Lenzen, and K. Nugraha, “A new sub-national multi-region input–output database for indonesia,” *Economic Systems Research*, vol. 29, no. 2, pp. 234–251, 2017. DOI: [10.1080/09535314.2017.1304361](https://doi.org/10.1080/09535314.2017.1304361).
- [129] T. Wakiyama, M. Lenzen, A. Geschke, R. Bamba, and K. Nansai, “A flexible multi-regional input–output database for city-level sustainability footprint analysis in japan,” *Resources, Conservation and Recycling*, vol. 154, p. 104588, 2020. DOI: [10.1016/j.resconrec.2019.104588](https://doi.org/10.1016/j.resconrec.2019.104588).
- [130] F. Faturay, Y.-Y. Sun, E. Dietzenbacher, A. Malik, A. Geschke, and M. Lenzen, “Using virtual laboratories for disaster analysis—a case study of taiwan,” *Economic Systems Research*, vol. 32, no. 1, pp. 58–83, 2020. DOI: [10.1080/09535314.2019.1617677](https://doi.org/10.1080/09535314.2019.1617677).
- [131] M. Lenzen, A. Geschke, M. D. Abd Rahman, Y. Xiao, J. Fry, R. Reyes, E. Dietzenbacher, S. Inomata, K. Kanemoto, B. Los, *et al.*, “The global mrio lab—charting the world economy,” *Economic Systems Research*, vol. 29, no. 2, pp. 158–186, 2017. DOI: [10.1080/09535314.2017.1301887](https://doi.org/10.1080/09535314.2017.1301887).
- [132] A. Bonfiglio and F. Chelli, “Assessing the behaviour of non-survey methods for constructing regional input–output tables through a monte carlo simulation,” *Economic Systems Research*, vol. 20, no. 3, pp. 243–258, 2008. DOI: [10.1080/09535310802344315](https://doi.org/10.1080/09535310802344315).
- [133] United States Census Bureau, “North American Industry Classification System,” Executive office of the president of United States, Office of management and budget, Tech. Rep., 2017. [Online]. Available: .
- [134] D. O. E. National Renewable Energy Laboratory, *JEDI Wind Models — Jobs and Economic Development Impact Models — NREL*, 2017. [Online]. Available: <https://www.nrel.gov/analysis/jedi/wind.html> (visited on 06/25/2019).

- [135] OECD, “Investment (GFCF) (indicator),” Organisation for Economic Cooperation and Development, Tech. Rep., 2019. DOI: [10.1787/b6793677-en](https://doi.org/10.1787/b6793677-en).
- [136] H.-T. Liu, J.-E. Guo, D. Qian, and Y.-M. Xi, “Comprehensive evaluation of household indirect energy consumption and impacts of alternative energy policies in china by input–output analysis,” *Energy Policy*, vol. 37, no. 8, pp. 3194–3204, 2009, ISSN: 0301-4215. DOI: [10.1016/j.enpol.2009.04.016](https://doi.org/10.1016/j.enpol.2009.04.016).
- [137] E. A. Hudson and D. A. Jorgenson, “U. S. ENERGY POLICY AND ECONOMIC GROWTH, 1975-2000.,” *Bell J Econ Manage Sci*, vol. 5, no. 2, pp. 461–514, 1974, ISSN: 00058556. DOI: [10.2307/3003118](https://doi.org/10.2307/3003118).
- [138] E. Ünal, “An institutional approach and input–output analysis for explaining the transformation of the Turkish economy,” *Journal of Economic Structures*, vol. 7, no. 1, Dec. 2018. DOI: [10.1186/s40008-017-0101-z](https://doi.org/10.1186/s40008-017-0101-z).

A. APPENDIX

A.1 Scaling PSCE models (Ch-4)

The following yaml file contents describe how parameters can be changed for PCSE models to be used in other regions.

```
AgroManagement:
#YAML code block
- 2017-05-01:
  CropCalendar:
    crop_name: 'soybean'
    variety_name: 'Soybean_906'
    crop_start_date: 2017-05-01
    crop_start_type: sowing
    crop_end_date: 2017-10-31
    crop_end_type: harvest
    max_duration: 200
  TimedEvents:
    event_signal: apply_npk
    name: Timed N/P/K application table
    comment: unit - kg/ha
    events_table:
      2017-05-10: { N_amount: 24.6587,
                  P_amount: 84.0638,
                  K_amount: 124.414}
  AreaData:
    unit: acres
    value: 10500000
  LocationData:
    latitude: 40.4842,
    longitude: -88.9937
```

Figure A.1. YAML file contents

A.2 Scaling Aspen Plus models (Ch-4)

The following example code block simulates the soybean-oil to biodiesel aspen plus model using regionally specific soybeans given as input (ex: 100, 200, 300, 400, 500 tons) to the developed EM.

```
#Python code block
import os
import numpy as np
import win32com.client as win32

ASPEN = win32.Dispatch('Apwn.Document')
ASPEN.InitFromArchive2(os.path.abspath('soybean_oil.bkp'))

soybean_input = [100, 200, 300, 400, 500] #insert regional data here

for soybean in soybean_input:
    ASPEN.Tree.FindNode('Data\\Streams\\SOYBEAN\\
                        INPUT\\MASSFLOW\\').Value = soybean
    ASPEN.Engine.Run2()
```

Figure A.2. Scaling aspen plus models for other regions

A.3 Aspen Plus property methods used (Ch-4)

Table A.1. Aspen Plus properties used

NAICS code	Aspen Plus model	Property method used
325311	Urea manufacturing	SR-POLAR
311224	Soybean crushing	NRTL
325199	Soybean biodiesel	Dortmund modified UNIFAC
325193	Corn ethanol manufacturing	NRTL
325311	Ammonia manufacturing	Electrolyte NRTL

A.4 NREL JEDI data (Ch-6)

Table A.2. State level data obtained from JEDI models

NAICS code	Industry name	Northeast	Midwest	South	West
311	Food	68	472	360	213
312	Beverage and Tobacco Products	12	16	41	25
313	Textile Mills	NA	2	70	3
314	Textile Product Mills	1	NA	20	NA
315	Apparel	NA	NA	4	NA
316	Leather and Allied Products	NA	1	1	NA
321	Wood Products	62	38	206	78
322	Paper	215	273	1,393	209
323	Printing and Related Support	13	28	40	8
324	Petroleum and Coal Products	171	565	1,944	834
325	Chemicals	134	835	2,405	154
326	Plastics and Rubber Products	29	98	127	39
327	Nonmetallic Mineral Products	96	229	354	149
331	Primary Metals	194	978	428	84
332	Fabricated Metal Products	36	193	79	37
333	Machinery	20	90	43	10
334	Computer and Electronic Products	28	28	32	73
335	Electrical Equip., Appliances, and Components	14	18	32	6
336	Transportation Equipment	24	149	110	36
337	Furniture and Related Products	4	14	15	4
339	Miscellaneous	13	15	22	8

(units: trillions of btu, NA: data not available from EIA)

Table A.3. Energy intensity (Ω) calculated using EIA data [38]

Industry	NAICS code	North East	Mid West	South	West
Food Manufacturing	311	0.000583116	0.00181635	0.00127221	0.00121331
Beverage and Tobacco Product Manufacturing	312	0.000497471	0.000377224	0.000525558	0.00040122
Textile Mills	313	–	0.000736844	0.00282679	0.000769023
Textile Product Mills	314	0.000169234	–	0.00106396	–
Apparel Manufacturing	315	–	–	0.0003933	–
Leather and Allied Product Manufacturing	316	–	0.000193356	0.000173328	–
Wood Product Manufacturing	321	0.00546519	0.00153828	0.00492586	0.00389057
Paper Manufacturing	322	0.00508736	0.00421134	–	0.00769425
Printing and Related Support Activities	323	0.000772912	0.000919893	0.00163856	0.000544709
Petroleum and Coal Products Manufacturing	324	0.00152013	0.00295213	–	0.00388171
Chemical Manufacturing	325	0.000655978	0.0031344	–	0.00099441
Plastics and Rubber Products Manufacturing	326	0.000680356	0.0010015	0.00132194	0.00113219
Nonmetallic Mineral Product Manufacturing	327	0.00481122	0.00659544	0.00683479	0.00615514
Primary Metal Manufacturing	331	0.00387278	0.00748617	0.00445002	0.00224592
Fabricated Metal Product Manufacturing	332	0.000528459	0.00137666	0.000623642	0.00057652
Machinery Manufacturing	333	0.000282959	0.000473533	0.000267088	0.000162782
Computer and Electronic Product Manufacturing	334	0.000319879	0.000366641	0.000266612	0.000363404
Electrical Equipment, Appliance, and Component ...	335	0.000406049	0.000314312	0.000495699	0.000249206
Transportation Equipment Manufacturing	336	0.000267506	0.000432323	0.00032901	0.000193093
Furniture and Related Product Manufacturing	337	0.000289326	0.000473192	0.000404329	0.000215003
Miscellaneous Manufacturing	339	0.000251328	0.000240088	0.000359855	0.000129004